UNIVERSITÀ
DEGLI STUDI
DI PADOVA

Sede Amministrativa: Università degli Studi di Padova

Dipartimento di MEDICINA MOLECOLARE

CORSO DI DOTTORATO DI RICERCA IN: MEDICINA MOLECOLARE
CURRICOLO: MEDICINA RIGENERATIVA
CICLO XXXI

EPIGENETIC CONTROL OF YAP/TAZ-MEDIATED TRANSCRIPTION

Tesi redatta con il contributo finanziario della Fondazione della Cassa di Risparmio di Padova e Rovigo

Coordinatore: Ch.mo Prof. Stefano Piccolo
Supervisore: Ch.mo Prof. Stefano Piccolo
Co-Supervisore: Dott.sa Francesca Zanconato

Dottorando: Letizia Filippi

LEFT BLANK

INDEX

The work presented in this thesis was ideated and coordinated by Prof. Stefano Piccolo Prof. Michelangelo Cordenonsi and Dr. Francesca Zanconato.
I performed experiments under their supervision, together with Dr. Giusy Battilana and Erika Giorgia Quaranta and Dr. Daniele Di Biagio.

Important contributions to our work were given by our collaborators: Prof. Silvio Bicciato and Dr. Mattia Forcato for bioinformatics, Dr. Bernard Haendler and Pascale Lejeune from Bayer and Dr. Vincenza Guzzardo for histological analysis.

ABSTRACT

An emerging paradigm in cancer biology relates to the concept of "transcriptional addiction" where transformed cells set high demand of general transcriptional regulators, chromatin modifiers and even the basal transcriptional machinery to sustain a dysregulated gene expression program. The mechanism and the players below these dependencies remained elusive. Identifying the most sensitive nodes of these regulations offers the potential of defining new targets and therapeutics with selective antitumor effects. Here we demonstrate that the two closely related transcriptional co-activator YAP and TAZ mediate transcriptional dependencies in different cellular contexts.

They are known to be aberrantly activated in different tumours where they have causative roles in initiation, progression and metastasis. They can control a huge gene expression program by binding mainly to distal enhancers that can reach their target promoters through chromatin looping. In this research project we established a new functional link between YAP/TAZ and a BET family member, BRD4. YAP/TAZ physically engage the general coactivator BRD4, dictating the genome-wide association of BRD4 to chromatin. By genome-wide analysis we proved that YAP/TAZ-bound enhancers mediate recruitment of BRD4 and RNA-Pol II at YAP/TAZ-regulated promoters. In so doing, the YAP/TAZ-BRD4 axis confers transcriptional advantage to a broad number of genes that are primarily involved in cell proliferation. Elevated BRD4 overload at YAP/TAZ cis-regulatory regions makes YAP/TAZ target genes extremely vulnerable to BET inhibition.

We showed that by exploiting the requirement of BRD4 for YAP/TAZ-dependent gene expression, we can blunt through BET inhibitors YAP/TAZ pro-tumorigenic activity in several cell and tissue contexts, causing regression of pre-established YAP/TAZ-addicted neoplastic lesions, and even revert drug resistance to molecular target therapy. These results present a new window of opportunity for a rational use of BET inhibitors for the treatment of YAP/TAZ addicted tumors.

ABSTRACT (ITALIANO)

Le cellule tumorali per sostenere l'elevato ritmo di crescita richiamano un maggior numero di fattori trascrizionali e modificatori della cromatina, diventando dipendenti dagli stessi, portando così ad un globale aumento della trascrizione. La "transcriptional addiction" è un tema sempre più emergente nella biologia del cancro, ma ad oggi sia il meccanismo che i fattori coinvolti rimangono sconosciuti.

Si è ipotizzato che YAP e TAZ, due cofattori trascrizionali, potessero essere ottimi candidati per mediare queste dipendenze in differenti contesti cellulari. YAP/TAZ ricoprono un ruolo fondamentale nel cancro, prendendo parte nell'iniziazione, progressione ed induzione di metastasi. In questo progetto di ricerca abbiamo identificato un legame fisico e funzionale tra YAP/TAZ e un membro della famiglia delle proteine BET, BRD4. Tramite ChIP-seq abbiamo dimostrato che il già noto legame di YAP/TAZ a siti enhancers media il reclutamento di BRD4 sugli stessi siti e sui promotori dei geni regolati da YAP/TAZ, richiamando l'RNA polimerasi II e permettendo la successiva trascrizione dei geni a valle.

La relazione YAP/TAZ-BRD4 conferisce un vantaggio trascrizionale a geni principalmente coinvolti nella proliferazione e nel ciclo cellulare; allo stesso tempo però l'accumulo di BRD4 su queste regioni di cromatina conferisce una certa sensibilità ai target di YAP/TAZ all'azione di inibitori farmacologici delle proteine BET. L'azione inibitoria di queste molecole si è rivelata efficace anche *in vivo* su modelli di tumore dipendenti da YAP/TAZ e inoltre sulla capacità di sovvertire la resistenza al Vemurafenib in linee cellulari di melanoma. Questi risultati aprono una nuova finestra di opportunità terapeutiche dove i BET-inhibitors usati da soli o in combinazione con farmaci preesistenti possono contrastare l'attività pro-tumorigenica di YAP/TAZ in diversi tessuti.

PUBLICATIONS

Zanconato, F., Battilana, G., Forcato, M., **Filippi, L**., Azzolin, L., Manfrin, A., … Piccolo, S. (2018). **Transcriptional addiction in cancer cells is mediated by YAP/TAZ through BRD4**. *Nature Medicine*, 1. https://doi.org/10.1038/s41591-018-0158-8

INTRODUCTION

YAP (Yes-associated protein) and TAZ (transcriptional co-activator with a PDZ-binding domain) are two closely related transcriptional regulators that shuttle between the cytoplasm and the nucleus, where they regulate transcription. They were first identified as the mammalian orthologs of *Yorkie*, in *Drosophila Melanogaster*, acting as downstream effector of the Hippo pathway (Huang, Wu, Barrera, Matthews, & Pan, 2005). Although many works highlighted the restriction by the Hippo cascade as the main modality through which YAP/TAZ activity is controlled, increasing evidence suggest a broader framework in which YAP/TAZ are regulated, in a Hippo-independent way (Totaro, Panciera, & Piccolo, 2018).

YAP/TAZ are involved in cell fate decision early in embryonic life, in the regulation of stem cell activity in adult tissue, and in malignancy. Many open questions about YAP/TAZ upstream regulators and downstream responses remain unsolved, placing them at the core of continually expanding research (Piccolo, Dupont, & Cordenonsi, 2014).

Signals converging on YAP/TAZ

Even though YAP/TAZ have been discovered as components of the Hippo signalling cascade, in the past decade numerous publications identified YAP and TAZ as a signalling nexus for different upstream cues and pathways such as mechanical signals, GPCRs, cell adhesion and cell polarity, extracellular factors (Wnt, TGFβ, EGF, Notch) and metabolism (Piccolo, Dupont & Cordenonsi, 2014; Totaro et al., 2018).

Hippo signalling pathway

The Hippo signalling pathway is an evolutionary conserved kinase cascade discovered by genetic screen for tissue overgrowth mutants in D. *Melanogaster* (Justice, Zilian, Woods, Noll, & Bryant, 1995; Xu, Wang, Zhang, Stewart, & Yu, 1995). As previously anticipated, the main function of the Hippo pathway is to restrain YAP/TAZ activity. In mammals the core of this pathway comprises two serine/threonine kinases, MST1/2 (Mammalian Ste20-like kinases, Hippo in *Drosophila*) and LATS1/2 (large tumor suppressor), together with the adaptor proteins Sav1 (Salvador) and MOB1 (Mps-one binder 1). Various upstream stimuli promote the activation of a phosphorylation cascade

where the MST/Sav1 complex phosphorylates and activates LATS1-2 together with MOB1 proteins, that in turn phosphorylate YAP on five serine/threonine residues, and TAZ on four of these motifs. YAP Ser127 and TAZ Ser89 are the most relevant residues phosphorylated by LATS to create a consensus sequence promoting YAP/TAZ binding to 14-3-3 proteins and subsequent YAP/TAZ sequestration in the cytoplasm or proteasomal degradation mediated by β-TRCP (β-transducin repeat-containing protein) (Gomez, Gomez, & Hergovich, 2014; Meng, Moroishi, & Guan, 2016; Moroishi, Hansen, & Guan, 2015; Ramos & Camargo, 2012; Varelas et al., 2014). Recent experimental evidence showed that YAP phosphorylation on Ser127 and its cytoplasmic translocation could be induced by a wide spectrum of signals, ranging from contact inhibition to apical cell polarity proteins and modification of the actin cytoskeleton (Q. Chen et al., 2015). Conversely, when YAP/TAZ are not phosphorylated, they can translocate in the nucleus where they regulate the transcription of target genes (Harvey, Zhang, & Thomas, 2013; Tremblay & Camargo, 2012).

YAP/TAZ as mechanosensors and mechanotransducers

Cells of a living organism perceive and answer to the complex surrounding microenvironment (physical properties of the extracellular matrix; ECM) and pulling forces from neighbouring cells, generally defined as *mechanical cues*.

Mechanical forces are instrumental for teaching, from embryonic development until adulthood, how cells shape themselves and change their fate according to the perturbations of the niche, inducing them to proliferate, heal tissues, differentiate until a proper mechanical equilibrium is attained (Panciera, Azzolin, Cordenonsi, & Piccolo, 2017). It is now well reviewed how YAP/TAZ act as transducers of these mechanical cues from external shape modifications to the activation of specific and different transcriptional programs. YAP/TAZ regulation relies on their subcellular localization, as they are nuclear in cells perceiving high mechanical tension (stiff matrices, large adhesive area, F-actin stabilization), whereas they are mainly cytoplasmic and inactive in cells experiencing low mechanical signal (soft matrices, small adhesive areas, F-actin disruption).

YAP/TAZ mediate mechanical cues in a Hippo-independent fashion, as their regulation involves Rho GTPase activity and integrity of actin cytoskeleton (Dupont et al., 2011). The common thread between cytoskeletal tension and YAP/TAZ regulation was also confirmed using specific small molecules inhibitors of Rho GTPase activity (C3) or

ROCK (Y27632), or molecules that, by disrupting filamentous actin (Latrunculin A) or by blocking non-muscle myosin (Blebbistatin), can recapitulate the effects of low-tension microenvironment and thereby inhibit YAP/TAZ (Dupont et al., 2011).

YAP and TAZ are not only regulated by cytoskeletal tensions, but represent the direct mediators of their biological effects, such as cell differentiation of mesenchymal stem cells (MSCs) into osteoblasts (on stiff ECM) or adipocytes (on soft ECM), proliferation, survival and differentiation (Halder, Dupont, & Piccolo, 2012; Panciera et al., 2017). In this light, the discovery of YAP and TAZ as mechanotransducers is finally revealing the relationship between aberrant cell mechanics and the onset of multiple diseases, including pathologies, such as muscular dystrophy and cancer (Panciera et al., 2017).

Cell adhesion and polarity signals

Epithelial cells are polarized entities that adhere one to another via junctional complexes, dictating the ordered architecture of the whole tissue. Several reports point out that junction protein complexes might directly influence YAP/TAZ localization and activity, with a partial involvement of the Hippo pathway. It is well known that contact inhibition of proliferation (CIP) is a condition in which cells stop proliferating as soon as they come into physical contact with their neighbours (Abercrombie, 1979), and this event has been linked to YAP/TAZ confinement outside the nucleus, while reactivation of YAP/TAZ allows cells to escape CIP (Aragona et al., 2013; Zhao et al., 2007). Two components of adherent and tight junctions, α-catenin and angiomotin (Amot), respectively, have been shown to interact with YAP/TAZ and to recruit them at the cell edge, thus preventing YAP/TAZ nuclear activity. Moreover, in close proximity to cell-cell junctions, Merlin/NF2 may promote the assembly of the appropriate protein scaffolds that allow LATS activation and YAP phosphorylation, acting as a potent tumor suppressor in different mouse models (Lallemand, Curto, Saotome, Giovannini, & McClatchey, 2003; Piccolo et al., 2014). Recent works highlighted how the YAP-Merlin association is dependent on Amot; interestingly, the phosphorylation state of Amot determines the localization of the complex at tight junctions (leading to YAP inhibition) or at the nucleus (Moleirinho et al., 2017).

Various proteins directly involved in cell polarity were found to regulate YAP/TAZ, such as Scribble-Dlg-Lgl basolateral complex, atypical protein kinase C and Crumbs (Varelas et al., 2014). In epithelial cells, delocalization of Scribble, an upstream regulator of the Hippo pathway, leads to TAZ nuclear localization, transcriptional

activation and acquisition of cancer cells properties (Cordenonsi et al., 2011). Conversely, apical Crumbs complex contributes to YAP/TAZ inhibition by sequestering them at cell junctions (Varelas et al., 2010).

G protein coupled receptors (GPCRs)

GPCRs are the major family of membrane receptors in eukaryotes and important regulator of YAP/TAZ activity. According to the stimulating molecules and the associated G protein receptor, the activity of YAP/TAZ can be either down-regulated or up-regulated (F. X. Yu et al., 2012), providing different layers of YAP/TAZ regulation, that can be either Hippo-dependent or independent (Hansen, Moroishi, & Guan, 2015; Totaro et al., 2018).

YAP/TAZ interplay with Wnt signalling pathway

Recent works highlighted that beside their roles as effectors of the Hippo pathway and mechanotransduction, YAP/TAZ are also mediators of a family of growth factors, Wnt ligands. Wnt pathway has a prominent role in regulating cell proliferation, stem cell expansion, regeneration and tumorigenesis (Clevers, 2006), mirroring YAP/TAZ biological effects. The core of the Wnt pathway is the regulation of its nuclear effector β-catenin by a cytoplasmic destruction complex consisting of different proteins (Axin, APC, CK1 and GSK3) and YAP/TAZ are integral part of this complex, where they are required for recruitment of β-TrCP to the complex and consequent β-catenin degradation (Azzolin et al., 2014, 2012). This YAP/TAZ-Wnt interconnection will be better described in the results.

YAP/TAZ and metabolism

YAP/TAZ in the context of cell metabolism have attracted considerable attention in the last years with fascinating novelties. Growing experimental evidences link metabolic cues (glucose, lipid, amino acid and other GPCRs ligand) to YAP/TAZ regulation and, in turn, to a YAP/TAZ-dependent modulation of gene expression (Koo & Guan, 2018).
Multiple studies revealed that cellular glucose level impact on YAP/TAZ phosphorylation, as glucose reduction in the culture medium is associated to YAP/TAZ inhibition and vice versa (Enzo et al., 2015; Santinon, Pocaterra, & Dupont, 2016). These remarks support the concept that growth and proliferation, functions linked to YAP/TAZ biology should be suppressed when the energy environment is not

favourable. High glucose availability increases O-linked β-N-acetylglucosamine (O-GlcNAc) protein modification, achieved by the hexosamine biosynthetic pathway, that has been recently associated to active YAP. This modification, indeed, suppresses LATS-dependent phosphorylation and β-TrCP-dependent ubiquitination of YAP. Generally, a boost of O-GlcNAcylation is a general trait of cancer cells (Slawson & Hart, 2011; Totaro et al., 2018; X. Zhang et al., 2017), suggesting a potential role of glucose-dependent YAP regulation in tumorigenesis, (Koo & Guan, 2018). Similarly, highly proliferative cells exhibit a strong demand for lipids and cholesterol for membrane development; moreover, *de novo* lipid synthesis is a major metabolic reprogramming important for oncogenic transformation.

Mevalonate pathway was one of the first reported links between YAP/TAZ and cell metabolism (Sorrentino et al., 2014; Z. Wang et al., 2014). Pharmacological inhibition of this pathway using statins was found to efficiently suppress YAP/TAZ nuclear translocation due to inhibition of geranylgeranylation of RhoA (a potent activator of YAP and TAZ), intimating an exciting clinical possibility for cancer treatment of YAP/TAZ addicted tumors (Feng et al., 2014; F.-X. Yu et al., 2014).

YAP/TAZ transcriptional activity

All the above mentioned stimuli converge on the regulation of YAP/TAZ nuclear localization, that is instrumental for their role as transcriptional regulators. YAP and TAZ own a strong transcriptional activator domain, but they do not possess a DNA-binding domain, that is, they can contact DNA only indirectly, through DNA-binding partners (Stein et al., 2015; Zhao et al., 2008). It is extensively reported that YAP/TAZ interact with transcription factors to form functional complexes that recognize cis-regulatory elements and activate the expression of target genes to exert their biological function. Several YAP/TAZ transcriptional partners have been proposed, such as TEAD1-4, Runx1/2, ErbB4, PPAR-g, Pax3 and T-box transcription factor 5 (TBX-5) (Pan, 2010). YAP/TAZ were also repeatedly found as binding proteins for Smads, key mediators of TGF-β and BMP signalling pathways. YAP/TAZ contribute to Smad2/3 cytoplasmic retention, even overruling high levels of TGF-β ligands (Piccolo et al., 2014). The interaction between YAP and p73 (a p53 family member) has raised particular interest, as YAP-p73 complex is formed after DNA damage, leading to

activation of a proapoptotic transcriptional program (Mo, Park, & Guan, 2014), thus highlighting a potential role of YAP/TAZ as transcriptional repressors.

Among all these YAP/TAZ transcriptional partners, TEAD/TEF family proteins emerge as the main YAP/TAZ-DNA binding platform in the regulation of gene expression. The four TEAD family members (TEAD 1-4) are widely expressed in most mammalian tissues and organs (Pan, 2010). Knockdown of TEADs or disruption of the YAP-TEAD interaction abolishes YAP/TAZ-dependent gene transcription and reduces YAP/TAZ functions in mammalian cells, such as cell proliferation and related oncogenic growth (Liu-Chittenden et al., 2012; Zanconato et al., 2015; Zhao et al., 2008). For many years, the YAP/TAZ regulated transcriptional program remained obscure (Hong & Guan, 2012): even if a number of YAP/TAZ target genes had been characterized (CTGF, CYR61, ANKRD1, BIRC5, AXL, InhA, Col8a1, etc), none of them could fully recapitulate YAP/TAZ biological effects (Piccolo et al., 2014). We have previously expanded this list by microarray analysis, defining the transcriptional program activated by YAP/TAZ in breast cancer cells (MDA-MB-231 cells). We combined gene expression and DNA binding data, obtaining a long list of direct YAP/TAZ-TEAD target genes involved in governing cell proliferation (Zanconato et al., 2015). We and others found that YAP/TAZ–TEAD complex is directly recruited to few promoter regions, whereas the majority of the associations to chromatin occur on distal enhancers (Galli et al., 2015; Stein et al., 2015; Zanconato et al., 2015) (Figure 1A, B). Distal enhancers contact their target promoters through chromatin looping. We define as YAP/TAZ direct target genes all the genes whose expression is sustained by YAP/TAZ (as assessed by RNA-seq in YAP/TAZ depleted cells) and whose promoter either contains a YAP/TAZ-binding sites, or is in contact with one or more enhancers containing YAP/TAZ-binding sites (as assessed by ChIP-seq; see Figure 1C).

YAP/TAZ ChIP-seq also revealed activator protein-1 (AP-1) as a new partner of the YAP/TAZ-TEAD complex on DNA. YAP/TAZ-TEAD co-occupy a large set of enhancers together with AP-1 factors, and this synergistic cooperation has a fundamental role in tumor proliferation, migration and invasion, and also in driving epigenetic reprogramming of cancer cells into a stably chemoresistant state (Liu et al., 2016; Shaffer et al., 2017; Totaro et al., 2018; Zanconato et al., 2015).

Recent evidences associate YAP/TAZ and epigenetics. It has been recently reported that YAP and TAZ can interact with components of the SWI/SNF chromatin remodelling complex through the recruitment of NCOA6 histone methyltransferase complex to

increase H3K4 methylation and subsequent transcription of downstream genes (Oh et al., 2013; Qing et al., 2014; Skibinski et al., 2014). YAP/TAZ-TEAD complex can also operate as transcriptional corepressors by recruiting the NuRD histone deacetylase complex (M. Kim, Kim, Johnson, & Lim, 2015). Stein and colleagues reported that YAP/TAZ–TEAD bound enhancers regulate gene transcription by inducing p300-dependent acetylation at lysine 27 of histone H3 (H3K27ac) through recruitment of the Mediator complex and induction of transcriptional elongation through RNA polymerase II pause release (Galli et al., 2015; Stein et al., 2015).

YAP/TAZ biological function

Early embryonic development

Specific YAP/TAZ compartmentalisation is crucial to regulate early embryonic development. Nuclear/cytoplasmic distribution of YAP/TAZ delineates the first cell fate decision in the mouse embryo: the choice of embryonic cells to become either trophectoderm (TE) or inner cell mass (ICM). In the blastocyst stage, YAP/TAZ accumulate in the nuclei of outer TE cells, whereas they are distributed in the cytoplasm in ICM cells. Nuclear YAP/TAZ control the activity of TEAD transcription factors to direct a TE-specific transcriptional program that includes the induction of Cdx2, the TE master gene, important to dictate apicobasal polarity and tight junctions formation (Nishioka et al., 2009). One of the first discoveries pointed that knockout of Yap and Taz in mouse embryos is incompatible with life, preventing implantation (Nishioka et al., 2009). Genetic ablation of the sole YAP (YAP -/- mice) brings to developmental arrest around embryonic stage 8.5 (E 8.5) (Morin-Kensicki et al., 2006), while TAZ -/- mice are viable, but they die soon after birth due to strong alterations in lung and kidney that recapitulate human polycystic kidney disease and pulmonary emphysema (Makita et al., 2008; Morin-Kensicki et al., 2006; Piccolo et al., 2014). Unfortunately, mechanisms controlling YAP/TAZ at these early stages of development remain incompletely understood.

Somatic Stem cells

YAP/TAZ have been widely described as “stemness factors”. During embryonic development increased expression of a YAP transgene or inhibition of the Hippo pathway kinases results in aberrant organ outgrowth, possibly by expanding the number

of somatic stem cells in those organs (Piccolo et al., 2014; Ramos & Camargo, 2012; Varelas et al., 2014). In adults, nuclear YAP/TAZ are enriched in anatomical compartments containing stem and progenitor cells, as for example the stem cell compartment of the intestinal epithelium (Camargo et al., 2007), skin and skeletal muscle, whereas their cytoplasmic retention is important for cellular quiescence and cellular differentiation. These observations suggest that the transcriptional activity of YAP/TAZ could be important in the preservation of stem cell identity in normal tissues (Ramos & Camargo, 2012). Importantly, genetic depletion of YAP and/or TAZ in several adult epithelia (intestine mammary gland, pancreas and liver) is inconsequential for normal homeostasis, but they are required for stem cell amplification in a context of tissue regeneration after injury or tumor growth (Azzolin et al., 2014; Cai et al., 2010; Q. Chen et al., 2014; Zanconato, Cordenonsi, & Piccolo, 2016; Weiying Zhang et al., 2014). Recently, a pioneer work demonstrated that the temporary expression of the sole YAP or TAZ is sufficient to convert differentiated cells into somatic stem cells of the same tissue with functional and molecular attributes of their original tissue-specific stem cells (Panciera et al., 2016), highlighting an innovative connection between YAP/ TAZ and cell plasticity.

YAP/TAZ as hallmarks of cancer

Numerous works showed that dysregulated YAP and TAZ activity is associated with tumor initiation, progression, metastasis formation and dissemination in several human cancers, arising from: prostate, lung, liver, colon, breast, oesophagus, brain, and skin (Piccolo et al., 2014; Zanconato, Cordenonsi, et al., 2016). Characterization of human tumor samples highlighted that YAP/TAZ are frequently overexpressed during tumorigenesis. Analysis of a large datasets of breast and colon cancer patients revealed that aberrant YAP and/or TAZ nuclear localization or increased expression of their target genes is associate to high histological grade tumor with poor prognosis (Piccolo et al., 2014). YAP/TAZ related oncogenic properties rely on their capacity to induce aberrant cell proliferation, increase cell survival and acquisition of an epithelia to mesenchymal transition (EMT) phenotype (Camargo et al., 2007; Mo et al., 2014). Moreover, YAP/TAZ are active in the cancer stem cell (CSC) fraction, and they are functionally involved and required for CSC expansion (Piccolo et al., 2014). Consistent with this observation, it has been reported that TAZ sustains metastatic and CSC properties in breast cancer and expression of a nuclear TAZ mutant (TAZ-S89A) is

sufficient to confer self-renewal ability of these breast CSCs (Chan et al., 2008; Cordenonsi et al., 2011). In *vivo* and in *vitro* evidence reveal that elevated YAP/TAZ induce chemoresistance to conventional cancer therapies, as paclitaxel and doxorubicin used in breast cancer treatment (Bartucci et al., 2015; Cordenonsi et al., 2011).

Even if YAP/TAZ are frequently upregulated in human tumors, no germline or somatic mutations have been identified either in YAP or TAZ, or in most of the components of the Hippo pathway. Actually, Hippo pathway mutations are extremely unusual (Harvey et al., 2013), and only few mutations in NF2, LATS1, or LATS2 are selected in specific tumor histotypes (Zanconato, Battilana, Cordenonsi, & Piccolo, 2016). The observation that YAP/TAZ activation cannot be fully explained by mutations in Hippo pathway components points out the idea that other YAP/TAZ modulations should be crucial for their activity in human cancer.

Mechanical signals represent a predominant factor in the control of YAP/TAZ activity. Indeed, mechanical inputs from the aberrant tumor microenvironment are key candidates to induce YAP and TAZ overactivity in cancer cells. These inputs comprise aberrant tissue architecture, accumulation of stromal cells, inflammation, increased compression forces and pressure, metalloproteinase-mediated ECM remodelling by cancer-associated fibroblasts (CAFs) and overall ECM stiffening (Panciera et al., 2017).

Anti YAP/TAZ therapeutic approaches

YAP and TAZ are widely activated in tumors, where they endow several attributes of cancer cells, such as regulation of cell proliferation, stem cell self-renewal, fate decision and organ growth, whereas they seem to be dispensable for normal tissue homeostasis, making them an appealing therapeutic target.

Many therapeutic strategies have been proposed to indirectly inhibit YAP/TAZ (reviewed in Zanconato et al., 2016b):

- Targeting mechanotransduction through anti-cytoskeletal drugs that act by disrupting F-actin microfilament or inhibitors of Rho and its upstream inducers (Src, FAK and integrins) that are already in clinical trial (Dupont et al., 2011);
- Targeting metabolic pathway, such as the mevalonate pathway and in particular Rho-GTPase through statins (Sorrentino et al., 2014), bisphosphonates, GGTI (inhibitors of geranylgeranyl transferase-1) or inhibitors of O-linked β-N-acetylglucosamine (O-GlcNAc) transferase;

- Targeting GPCR signalling (β-blockers) (Watkins et al., 2015);
- Turning off Wnt signalling by sustaining the activity of the destruction complex by promoting Axin stabilization (Tankyrase inhibitors) (Azzolin et al., 2012).

Unfortunately, YAP/TAZ inhibition remain challenging because cancer cells may integrate different combinations of YAP/TAZ-regulating inputs that are tumor specific and could also differ within the same lesion, overcoming the effect of these genetic drugs; moreover, several of the molecules mentioned above can lead to extensive toxicity due to their pleiotropic effects. Since all YAP/TAZ biological responses take place after their nuclear accumulation and subsequent transcription of cancer related genes, designing compounds able to interfere with YAP/TAZ at the nuclear level may represent a "universal" direct anti- YAP/TAZ strategy. Verteporfin (VP), was one of the first attempt to interfere with YAP binding on DNA. This molecule belongs to the porphyrin family and acts by inhibiting the physical interaction between YAP and TEAD. Optimistic results were initially obtained from experiments in mice, where liver overgrowth induce by a YAP transgene or by genetic ablation of Nf2/Merlin was reduced upon VP administration (Liu-Chittenden et al., 2012). Moreover, VP could reduce the growth of xenografts of prostate tumor cells bearing activated YAP (Nguyen et al., 2015). However, recent discoveries by Zhang and colleagues reported that the effect mediated by VP on the proliferation of cancer cells is YAP-independent and only due to general toxicity (H. Zhang et al., 2015).

Targeting YAP/TAZ at the transcriptional level could be a good compromise that open a lot of new therapeutic opportunities. For example, as just said YAP/TAZ control cancer cell fates, and moreover they promote acetylation of histones at enhancers, hinting to their involvement as epigenetic modifiers (Stein et al., 2015). Cancer is profoundly influenced by changes in the epigenome and many investments are already concentrated on the design of epigenetic drugs acting on chromatin reader, modifiers, erasers and remodelers, including: BET (bromodomain and extraterminal) protein inhibitors, demethylase inhibitors, methyltransferase and histone deacetylase (HDAC) inhibitors, dedicated to resetting the "cancer epigenome" (Dawson, 2017).

For this reason, dissecting the mechanisms by which nuclear YAP/TAZ control gene expression might elucidate new YAP/TAZ functions and new partners on chromatin that can be targeted by epigenetic molecules.

PRELIMINARY RESULTS

A prevailing research topic in our group is the study of YAP/TAZ, in particular their transcriptional program, with the goal of understanding the mechanism by which they drive tumorigenesis, mainly in breast cancer. We use as paradigm of YAP/TAZ biological activity MDA-MB-231 cells, a well-established model of triple negative breast cancer (TNBC), whose malignant phenotype relies on YAP/TAZ (Cordenonsi et al., 2011). To better characterize the whole set of genes regulated by YAP/TAZ in MDA-MB-231 cells, my colleagues performed total RNA extraction followed by next generation sequencing (RNA-seq) in control and YAP/TAZ-depleted cells.

Transcriptomic profiling of MDA-MB-231 cells revealed that direct YAP/TAZ targets genes were significantly more expressed than all the other genes (Figure 1D). Moreover, the biological function of several of these genes is associated with cell proliferation as determined by Gene Ontology (GO) annotation. Thus, YAP/TAZ activate an essential growth program in breast cancer cells. Silencing YAP/TAZ with siRNAs led to a global downregulation of this growth program, in line with the previous report that MDA-MB-231 cells depleted of YAP/TAZ undergo growth arrest (Zanconato et al., 2015).

AIM OF THE PROJECT

An emerging concept in cancer biology relates to the concept of "transcriptional addiction". Cancer cells rely on a high amount of general transcriptional regulators, including chromatin re-modellers and even the basal transcriptional machinery (Bradner, Hnisz, & Young, 2017; Villicaña, Cruz, & Zurita, 2014) to boost the expression of a specific set of genes. Transcriptional dependency makes cancer cells more sensitive than normal cells to inhibition by small molecules targeting general transcriptional regulators, through a yet unknown mechanism (Lovén et al., 2013; Shi et al., 2014). How this transcriptional addiction is established is still poorly defined.

Since YAP/TAZ have a prominent role in sustaining the malignant transcriptional program of breast cancer cell lines (such as MDA-MB-231 cells) and are associated to malignant transformation and progression (Cordenonsi et al., 2011; Zanconato, Cordenonsi, et al., 2016), we posited that they could be ideal candidates to mediate specific transcriptional addiction in breast cancer.

Our goal here was to define whether such dependency is due to a mechanistic connection between YAP/TAZ and some specific general transcriptional regulators.

A small part of the results that I will introduce in the next section were also present as preliminary results in a previous PhD thesis by Dr. Giusy Battilana, as we closely collaborated on this research project. In particular the results of the following experiments were anticipated in Dr. Battilana's work:

PLA assays in Figure 2A
Co-immunoprecipitation in Figure 2B
Preliminary analysis of RNA-seq data
BRD4 ChIP-qPCR in Figure 3B
Co-immunoprecipitation in Figure 7C
RNA-PolII ChIP-qPCR in Figure 8A

Results presented in this thesis were published in an original research article:
Zanconato, F., Battilana, G., Forcato, M., **Filippi, L**., Azzolin, L., Manfrin, A., … Piccolo, S. (2018). Transcriptional addiction in cancer cells is mediated by YAP/TAZ through BRD4. *Nature Medicine*, 1. https://doi.org/10.1038/s41591-018-0158-8

RESULTS

BRD4 and YAP/TAZ are part of the same nuclear complex

To study the connection between YAP/TAZ and transcriptional addiction in cancer, we used MDA-MB-231 cells, a well-established model of triple-negative breast cancer (TNBC). This form of neoplasia is classified according to the lack of expression of: estrogen receptor (ER), progesterone receptor (PR), and HER-2/Neu amplification. The disease is clinically and biologically heterogeneous, includes some of the most aggressive forms of mammary tumors. MDA-MB-231 cells bear genetic inactivation of the Hippo pathway (*NF2* null) leading to constitutive activation of YAP/TAZ (Aragona et al., 2013); moreover, the shape of these cells is almost mesenchymal as they do not express the classical cell-cell adhesion molecules and adopt a spread morphology. Thus, in addition to loss of Hippo inhibition, the activity of YAP/TAZ is further boosted in these cells by the increased mechanotransduction due to their spread cell shape. In sum, MDA-MB- 231 cells concentrate a number of features that potently sustain YAP/TAZ activity.

ChIP-Mass Spectrometry for YAP/TAZ

With this background in mind, we performed an unbiased search for YAP/TAZ nuclear partners by carrying out Chromatin Immunoprecipitation followed by Mass Spectrometry (ChIP-MS) for endogenous YAP/TAZ in MDA-MB-231 cells.

Chromatin Immunoprecipitation is a powerful and versatile method to fix interactions between proteins and genomic DNA as they occur in living cells (Kharchenko, Tolstorukov, & Park, 2008; Schmidt et al., 2009). With this procedure, cells are reversibly crosslinked by formaldehyde, leading to covalent association of transcription factors and chromatin-bound proteins to their DNA binding sites in the genome. Here we aimed at studying the composition of the native protein complexes entertained by YAP/TAZ by ChIP-MS. For this, we performed immunoprecipitations with anti-YAP or anti-TAZ antibodies from sonicated lysates of MDA-MB-231 cells. These antibodies were already well characterized in prior publication and can effectively pull-down YAP/ TAZ in ChIP-Seq experiments (Zanconato et al., 2015). In this case, proteins captured in YAP/TAZ complexes were analysed by Mass Spectrometry (Rafiee, Girardot, Sigismondo, & Krijgsveld, 2016). Samples for Mass Spectrometry were processed at

the German Cancer Research Center (DKFZ, Heidelberg), in the laboratories of Dr. Jeroen Krijgsveld.

The list of interacting proteins included some well-known nuclear partners of YAP/TAZ, including TEAD (the main YAP/TAZ DNA interacting partner) and Activator Protein 1 family members (Zanconato et al., 2015) and several subunits of the Swi/Snf complex (Skibinski et al., 2014). We noticed that YAP/TAZ-bound proteins included chromatin readers/modifiers, such as BRD4, histone acetyltransferases (p300, p400) and the histone methyltransferase KMT2D/MLL2 (Table 1). The roles of p300, SWI/SNF and the H3K4 methyltransferase complexes in the context of YAP-dependent transcription have been previously described (Oh et al., 2014; Skibinski et al., 2014; Stein et al., 2015). BRD4 instead attracted our attention, as it hinted to novel mechanisms by which YAP/TAZ control gene expression. Our interest in BRD4 was also guided by the fact that, behind the analogy to YAP/TAZ, small molecules (generally called BET-inhibitors) capable of inhibiting its function already exist; BET-inhibitors display antitumor activity in various xenograft model systems and are under clinical evaluation (Shi et al., 2014; C. Y. Wang & Filippakopoulos, 2015). In light of the availability of drugs targeting BET-proteins, which might be used to inhibit YAP/TAZ nuclear activity in cancer cells, we decide to get deeper in this interaction.

Bromodomain and extra-terminal domain family of adaptor proteins

BRD4 belongs to the bromodomain and extra-terminal domain (BET) family of adaptor proteins together with its homologous BRD2, BRD3 and BRDt. BET proteins share structural similarities, as they all contain two conserved N-terminal bromodomains (BD1 and BD2), which are chromatin interaction modules that recognize acetylated lysine residues (Dhalluin et al., 1999). The bromodomain structure consists of four α-helices separated by variable loop regions, which together form a hydrophobic cavity that recognizes acetyl-lysine, whereas the aminoacidic composition around this region provides ligand specificity (Shi et al., 2014).

BRD4 plays an important role as chromatin reader that positively regulates transcription by binding acetylated Lysine on histones tails and core components of the transcriptional apparatus (C. Y. Wang & Filippakopoulos, 2015). It interacts directly with the Mediator (Med1) complex, linking transcription factors to RNA Polymerase II (RNA-PolII) complex, and it facilitates recruitment of the positive transcription

elongation factor (P-TEFb) to paused RNA-PolII, allowing transcriptional elongation (Chiang, 2009).

It has been reported that BRD4 is strongly enriched at enhancers and in particular at super-enhancer regions (Chapuy et al., 2013). Super-enhancers are defined as large enhancer domains, containing clusters of "concatenated" enhancers with an unusually strong enrichment for the binding of transcriptional co-activators, such as Mediator (Med1), the histone acetyltransferases p300 and CBP or other chromatin factors such as cohesin, as well as BRD4 itself. Super-enhancers are occupied by master transcription factors and associated with key cell type-specific genes, implicating their control on mammalian cell identity and disease (Pott & Lieb, 2014). Indeed, in cancer cells super-enhancers are enriched at genes with known oncogenic function.

YAP/TAZ directly interact with BRD4

To confirm *in vivo* the biochemical interactions detected by mass spectrometry, we performed Proximity Ligation Assay (PLA) in HEK293T cells. This immunofluorescence-based technique allows the visualization of endogenous protein complexes in individual fixed cells while preserving their subcellular localization. The read-out of this procedure is the appearance of fluorescent dots only when the analysed proteins are extremely close to each other (40nm), indicative of a physical association.

HEK293T cells were seeded on fibronectin-coated glass chamber slides, transfected with an epitope-tagged BRD4 (FLAG or HA) and fixed in 4% PFA before performing the proximity ligation assays. As shown in Figure 2A, by using anti-HA(BRD4) and anti YAP or TAZ antibodies we found that exogenous HA-BRD4 interact with endogenous YAP and TAZ (red dots signal) in the nucleus of cells. As control of assay specificity, no dots could be detected in the nuclei of cells transfected with empty vector.

YAP/TAZ do not bind DNA directly, but they rely on an intermediate DNA binding protein, mainly TEAD family members. Thus, we performed the same assay with anti-FLAG (BRD4) and anti-TEAD1 antibodies to verify if BRD4 also interacts with TEAD. Indeed, we detected FLAG (BRD4)-TEAD complexes (Figure 2A). These data suggest that exogenous BRD4 is in close proximity to endogenous YAP, TAZ and TEAD1 in the nuclei of HEK293T.

Next, we performed co-immunoprecipitation (Co-IP) of endogenous proteins with anti-YAP1 and anti-BRD4 antibodies from nuclear lysates of MDA-MB-231 cells, in order

to evaluate the affinity between YAP/TAZ and BRD4 in the absence of crosslinking. We used pre-immune Rabbit IgGs as negative control. As shown in Figure 2B, immunoblot revealed the presence of endogenous BRD4 in YAP and TAZ immunocomplexes, together with TEAD1 (left panel). In a reciprocal experiment, we could detect endogenous YAP, TAZ and TEAD1 in BRD4 immunocomplexes (right panel). We confirm the interaction between YAP/TAZ and BRD4, verifying also the presence of TEAD factor in these immunocomplexes, the main DNA binding platform for YAP/TAZ.

To test whether the interaction between BRD4 and YAP/TAZ is direct we assayed the binding of purified, isolated proteins by GST-pull down. GST-YAP was produced in *E.coli* and immobilized on glutathione sepharose 4B beads, then the resin was incubated with full length human recombinant BRD4 (rBRD4). After extensive washing, we checked by immunoblot if recombinant BRD4 protein had been captured by GST-YAP functionalized resin. As shown in Figure 2C, rBRD4 was efficiently pulled down by the GST-YAP loaded resin compared to the negative control (GST-only resin).

Next, we aimed to map the minimal region sufficient for the interaction between BRD4 and YAP/TAZ. For this purpose, we carried out structure-function studies by GST pull-down assays using GST-TAZ; the structures of YAP/TAZ are highly similar, but TAZ contains a single WW domain, making it easier to dissect the involvement of different protein regions in the interaction with BRD4. We assayed distinct progressive C-terminal deletions of TAZ for ability to interact with recombinant BRD4. Schematic representations of all TAZ constructs are shown in Figure 2D (Azzolin et al., 2014). We immobilized wild type GST-TAZ or deletion mutants on glutathione sepharose 4B beads and we incubated the loaded resins with human recombinant BRD4 (rBRD4). As shown in Figure 2D rBRD4 could be efficiently captured by the full-length WT TAZ, by the 1-251 and 1-175 deletion, but not by shorter N-terminal protein fragments, mapping the minimal region between aa 108-175 of mouse TAZ. Notably this part of TAZ includes the WW domain, a protein-protein interaction domain, already reported to mediate YAP/TAZ association with several partners (H. I. Chen & Sudol, 1995). The WW domain binds a PPxY motif (proline-proline-amino acid-tyrosine) in partner proteins. Considering that BRD4 has a conserved PPxY motif in its sequence we hypothesized that this region could interact with the WW domain of TAZ (Alsarraj et al., 2011). To assess the requirement of this domain, we used a GST fusion protein containing a mutant TAZ where only the WW domain was deleted. We found that

removal of the sole WW domain from full-length TAZ was not sufficient to impair its ability to associate with BRD4 (Figure 2E). These results indicate that the WW domain-containing region of TAZ is sufficient to bind BRD4 in the absence of C-terminal domains; yet, it is not necessary. We conclude that at least two determinants for TAZ binding to BRD4 must exist: one is comprised between aa 108 and 175, the second one must be in the C-terminal part of TAZ, which indeed contains the Transactivation domain.

YAP/TAZ recruit BRD4 on chromatin

Considering that BRD4 and YAP/TAZ physically interact, we investigated if BRD4 might co-occupy the same chromatin regions bound by YAP/TAZ at the genome wide level. The full list of YAP/TAZ binding sites in MDA-MB-231 cells was available from previous work in the laboratory (Zanconato et al., 2015). As for BRD4, we obtained its DNA binding profile in MDA-MB-231 cells by performing chromatin immunoprecipitation assays coupled with next-generation sequencing (ChIP-seq; see Figure 3A).

We first performed trial experiments to assess the specificity of BRD4 antibodies to immunoprecipitate endogenous BRD4. We prepare sheared chromatin from control MDA-MB-231 cells (transfected with a control siRNA) and BRD4-depleted cells. We used a polyclonal antibody targeting BRD4, raised in rabbit. As negative control, we performed the immunoprecipitation with pre-immune immunoglobulins produced in rabbit, to assay the background signal. After the recovery and elution of the immunoprecipitated protein-DNA complexes, we checked the result of the immunoprecipitation step by quantitative real time PCR. The reliability of the antibody was attested by the fact that chromatin regions bound by BRD4 in ChIP of control cells were not enriched in cells transfected with BRD4 siRNA (Figure3B). These preliminary results anticipated that BRD4 can bind both active enhancers and promoters of YAP/TAZ targets.

BRD4 binds the same enhancers occupied by YAP/TAZ

After the validation of our BRD4 antibody, we performed ChIP for BRD4 followed by deep sequencing. We prepared duplicate samples of MDA-MB-231 cells for each of the following experimental conditions:

- MDA-MB-231 cells treated with DMSO (vehicle);
- MDA-MB-231 cells treated with JQ1 (1uM for 6 hours before collection);
- MDA-MB-231 cells transfected with two independent mix of YAP/TAZ siRNAs (48h), hereafter siYAP/TAZ.

We performed chromatin immunoprecipitation with anti-BRD4 polyclonal antibody and with pre-immune rabbit IgG as a negative control. ChIPed DNA samples were analysed for deep sequencing in the laboratories of IGA (Istituto di Genomica Applicata, Udine). Bioinformatic analysis was performed by our collaborators at the University of Modena (Mattia Forcato and Silvio Bicciato). Chromatin immunoprecipitation with IgG generated background signal in all samples, which was invariably lower than the specific enrichment that we observed in BRD4 ChIP-seq.

BRD4 ChIP-seq data were compared with YAP and TAZ ChIP-seq (previously obtained in our laboratory) and with published ChIP-seq data for histone modifications in MDA-MB-231 cells (Rhie et al., 2014). We first defined the entire set of active enhancers (promoter-distal H3K4me1+/H3K27ac+ regions) and promoters (H3K4me3+/H3K27ac+ regions close to the TSS of annotated genes); BRD4 was enriched both on active promoters and active enhancers. As previously reported, YAP/TAZ bind almost exclusively to enhancers (Galli et al., 2015; Stein et al., 2015; Zanconato et al., 2015), so we started our analysis from these regions. We compared BRD4 ChIP-seq signal on active enhancers regions containing YAP/TAZ peaks and in regions that did not contain YAP/TAZ peaks in control cells. This analysis reveals that BRD4 coverage in DMSO-treated cells was higher on enhancers containing YAP/TAZ binding sites when compared to active enhancer not occupied by YAP/TAZ, as showed by blue bars of the box plot in Figure 4A. This is something that could not be appreciated by ChIP-qPCR.

We then assessed whether the presence of YAP/TAZ was required for the engagement of BRD4 to chromatin, by performing BRD4 ChIP-seq in MDA-MB-231 cells depleted of YAP/TAZ. As shown by pink bars BRD4 coverage on YAP/TAZ-containing enhancers was heavily reduced upon YAP/TAZ depletion; instead, BRD4 binding to active enhancers void of YAP/TAZ was not affected (Figure 4A). BRD4 detachment from YAP/YAZ binding sites was confirmed in independent experiments (see ChIP-qPCR in figure 4B). This means that YAP/TAZ are required to maintain high amounts of BRD4 anchored to their binding sites.

We reasoned that differential BRD4 loading might correspond to differential sensitivity to JQ1. As previously anticipated JQ1 is a potent BET-inhibitor, that detach BET proteins from chromatin by occupying the amino-terminal bromodomains and impeding their binding to acetylated lysines of histones tails, in so doing restraining BRD proteins activity (Figure 4C). Thus, we compared BRD4 coverage in JQ1-treated cells and control cells. The data obtained displayed preferential loss of BRD4 from YAP/TAZ-occupied enhancers, compared to active enhancers without YAP/TAZ binding sites, as showed by light blue bars in the box plot of Figure4A. The effects of YAP/TAZ depletion and JQ1 were strikingly similar. Overall, data indicate that the presence of YAP/TAZ peaks defines enhancers enriched of BRD4 and highly sensitive to BET inhibitors on the genome-wide scale.

YAP/TAZ maintain high levels of BRD4 on the promoters of their targets

We next tested if BRD4 levels are similarly regulated on the promoters of YAP/TAZ target genes. Only few promoters of YAP/TAZ targets genes contain YAP/TAZ binding sites; most of them are controlled by YAP/TAZ from distal enhancer, which are in close proximity of the promoter itself thanks to chromatin looping (Zanconato et al., 2015). We analysed the BRD4-bound DNA fragments obtained by next-generation sequencing and we measured BRD4 occupancy on the promoters of all expressed genes, comparing genes activated by YAP/TAZ (hereafter direct YAP/TAZ targets) with genes not activated by YAP/TAZ (hereafter, not targets). Control cells treated with vehicle (DMSO) displayed higher BRD4 coverage on the TSS of YAP/TAZ targets compared to non-targets (Figure 4D), paralleling BRD4 loading on YAP/TAZ-bound and YAP/TAZ-void enhancers. Moreover, both YAP/TAZ depletion and treatment with JQ1 induced the detachment of BRD4 from the promoters of YAP/TAZ target genes, and YAP/TAZ depletion is as effective as JQ1 in detaching BRD4 from promoters. The latter result indicates that YAP/TAZ, when bound to cognate enhancers, foster BRD4 recruitment on those same enhancers but also on the promoter controlled by these enhancers, even in absence of YAP/TAZ association to those promoters. These results are illustrated in the heatmap Figure 4E (where each line represents the promoter of a YAP/TAZ target, with the TSS in the midpoint; colour intensity is proportional to BRD4 binding). Figure 4F shows the binding profile of YAP and BRD4 on a distal enhancer and the promoter of YAP/TAZ target CDCA5. The binding profile of BRD4 at the active enhancer region exhibit high accrual of the protein together with YAP

accumulation in the same genomic region; after JQ1 treatment or YAP/TAZ depletion BRD4 ChIP-seq signal in the same region is greatly reduced. CDCA5 promoter does not contain YAP/TAZ peaks, yet BRD4 levels at TSS closely reflect the dynamic of BRD4 engagement on the distant enhancer.

Instead, BRD4 binding on the promoters of not YAP/TAZ targets (exemplified by ZNF410 in Figure 4G) was lower and either minimally affected or unaffected by JQ1 treatment or YAP/TAZ depletion. This means that BRD4 accrual at enhancers and promoters of YAP/TAZ targets specifically makes these genomic loci more prone to be destabilized by JQ1.

Regulation of YAP/TAZ transcriptional activity by BRD4 and BET inhibitors

Selective effect of BRD4 inhibition on the expression of YAP/TAZ target genes

Data presented so far show that the cis-regulatory regions of YAP/TAZ target genes and those of genes not regulated by YAP/TAZ are characterized by differential BRD4 loading, as well as differential response to JQ1. Are these differences translated into differential regulation of transcript levels upon treatment with JQ1?

To answer this question, we analysed RNA-seq datasets obtained from MDA-MB-231 cells where the activity of BET proteins had been inhibited. We used two strategies to inhibit BRD proteins. First, we pharmacologically inhibited BRD4 with the small molecule inhibitor of BET proteins, JQ1. Second, to compare and confirm the effect of the drug, we knocked down BRD4 and its cognate proteins BRD2 and BRD3 with independent mixes of siRNAs; we chose to knockdown all the BRD transcripts because depletion of the sole BRD4 might induce compensatory effects by other BET proteins, thus being not effective. Two independent samples were processed and analysed for each experimental condition.

So far, we know that YAP/TAZ directly control the expression of >600 genes (Zanconato et al., 2015); 67% of these genes were downregulated by JQ1, and a similar percentage (56-57%) was also downregulated by BRD depletion with 2 independent combinations of siRNAs (showed in Figure 5A as mix A and mix B of BRD siRNA). Conversely, if we focused our attention on “all expressed genes”, we reach an overall inhibition of less than 30% of transcripts abundance by JQ1 or BRD siRNAs.

Looking at expression levels, we observed that treatment with JQ1 selectively decreased the transcript abundance of YAP/TAZ target genes, compared to all other active genes.

In Figure 5B we can appreciate that JQ1 induced a strong downregulation of YAP/TAZ direct targets, which was not observed for not-YAP/TAZ targets; indeed, there is a statistically significant difference in fold-reduction in expression of not-YAP/TAZ targets and YAP/TAZ targets. The depletion of BRD proteins with siRNAs leads to a similar result. Overall, we conclude that JQ1 displays a bias towards inhibition of YAP/TAZ target genes. These results fit with the results of ChIP-seq experiments discussed above, showing that JQ1 induces a preferential loss of BRD4 from the enhancers and promoters of YAP/TAZ targets genes.

Among JQ1-dependent YAP/TAZ direct targets we could find essential factors involved in replication licencing, DNA synthesis and repair (for example, CDC6, GINS1, MCM3, TOP2A, RAD18 and many others); transcriptional regulators of the cell cycle (E2F2, E2F3, MYBL1 and others); cyclins and their activators (CCNA2 and CDC25A); and factors required for mitosis (KIF23, CENPF, CENPV, CDCA5, CDCA8 and others). We verified the requirement of BET proteins for the expression of a selection of these genes in an independent experiment by RT-qPCR in MDA-MB-231 cells, confirming the results of RNA-seq. Moreover, we evaluated the effect of the depletion of BRD4, and we found that silencing of the sole BRD4 was in fact sufficient to downregulate YAP/TAZ target genes (Figure 5C).

Collectively, the data indicate that BRD4 not only interacts with YAP/TAZ, but it is a required cofactor for their transcriptional activity. This confers to YAP/TAZ target genes a disproportional vulnerability to BET inhibitors, validating previous ChIP-seq data and confirming the requirement of BRD4/YAP/TAZ axis genome wide.

BRD4 acts downstream of YAP/TAZ

Data presented so far establish a correlation between the activities of YAP/TAZ and BRD4, but they do not allow us to draw any conclusion on the epistatic relationship between the two players.

In order clarify this aspect, we performed some experiments in MCF10A mammary epithelial cells, which display low YAP/TAZ activity. We transduced these cells with activated version of YAP, named YAP5SA. This activated form lacks all LATS phosphorylation sites, causing increased YAP nuclear localization. This set up allows to appreciate gene responses exclusively induced by YAP, rather than, as done so far, the effects of endogenous YAP/TAZ inactivation in MDA-MB-231 cells. It must be noted that these experiments were performed by culturing cells at high density (75000

cells/cm^2, for 48 hours), in order to inhibit endogenous YAP/TAZ and uncover the activity of overexpressed YAP5SA.

We asked whether YAP overexpression induced BRD4 accumulation on YAP/TAZ-binding sites on chromatin. As YAP/TAZ-occupied enhancers were identified in a different cell line (MDA-MB-231 cells) we first verified by ChIP that, upon overexpression, YAP was recruited on the same enhancers in MCF10A cells (Figure 6A). We then evaluated the effect of YAP overexpression on BRD4 binding at the same enhancers sites and their associated promoters by performing ChIP for endogenous BRD4. As shown in Figure 6B, BRD4 binding on YAP/TAZ-occupied enhancers and on the promoters they control increased upon YAP5SA overexpression in MCF10A cells; thus, YAP recruits BRD4 to chromatin. JQ1 (1μM, 6h) prevented YAP-induced accumulation of BRD4 on chromatin.

YAP overexpression was sufficient to stimulate the transcription of target genes, as shown in figure 6C. Depletion of BET proteins (with two independent combinations of siRNAs) or treatment with JQ1 (1μM, 24h) prevented the upregulation of YAP transcriptional targets, overall indicating that BRD4 operates downstream of YAP/TAZ.

To further corroborate this conclusion, we forced BRD4 expression in YAP/TAZ depleted MDA-MB-231 cells (Figure 6D). We transduced MDA-MB-231 cells with a viral vector encoding siRNA-insensitive human BRD4. To assess the functionality of this exogenous BRD4, we transfected cells with BRD4 siRNA, so that the only BRD4 present in cells was the exogenous one; exogenous BRD4 could in fact substitute for the endogenous protein, as genes whose expression was downregulated by BRD4 siRNA in control cells (transfected with empty vector) were unaffected in cells transduced with exogenous BRD4. Upon depletion of YAP/TAZ, their target genes were downregulated, and even exogenous BRD4 was not able to rescue their expression, supporting the previous conclusion that BRD4 acts downstream of YAP/TAZ to promote the expression of their target genes.

Mechanism of inhibition of YAP/TAZ target genes by JQ1

We have delineated a model whereby a physical interaction between YAP/TAZ and BRD4 (and TEAD in the same immunocomplex) exists and it's functional to mediate the activation of YAP/TAZ target genes; JQ1 blocks these events.

We next performed some experiments to investigate how JQ1 impairs the expression of YAP/TAZ target genes. First, we verified by immunofluorescence that YAP/TAZ

remained nuclear upon treatment of MDA-MB-231 cells with JQ1 (Figure 7A), excluding the possibility that the compounds would indirectly cause YAP/TAZ cytoplasmic relocalization.

We then assessed whether JQ1 affected the interaction between BRD4 and YAP/TAZ. Indeed, BRD4 was reported to bind some acetylated TFs through the bromodomain (Shi et al., 2014). We performed a GST-pull down assay. We incubated a GST-YAP resin with protein extracts of HEK293T cells containing wild type FLAG-BRD4, in the presence or absence of JQ1, or a mutant FLAG-BRD4 that cannot bind acetylated histones due to mutations in both bromodomains. We found that the biochemical association between GST-YAP and FLAG-BRD4 is not affected by the presence of JQ1 or by mutations in the bromodomains (Figure 7B). Similar results were obtained by immunoprecipitation of endogenous BRD4 from lysates of MDA-MB-231 cells treated with 1μM JQ1 for 6h: YAP and TEAD1 co-precipitated with BRD4 also in the presence of JQ1 (Figure 7C), excluding the possibility that JQ1 directly changes the affinity between BRD4 and YAP (and TEAD1).

Another possible explanation for the effect of JQ1 on YAP/TAZ target genes is that JQ1 (while not affecting the capacity of BRD4 to interact with TEAD and YAP/TAZ per se), might lead to the detachment of the whole complex from chromatin. Thus, we performed ChIP experiments with anti-YAP and anti- TAZ antibodies in MDA-MB-231 cells treated with 1μM JQ1 for 6h, followed by quantitative RT-PCR. Both YAP and TAZ bound their well-known enhancers with the same strength in DMSO and in JQ1-treated cells (Figure 7D).

Thus, in the presence of JQ1 YAP/TAZ are still bound to chromatin, and they in principle can interact with BRD4; however, ChIP-seq data clearly showed that BRD4 is removed from YAP/TAZ binding sites in the presence of JQ1. We conclude that interaction of BRD4 with YAP/TAZ (in a bromodomain-independent manner) and with histones (in a bromodomain-dependent manner) are both required to keep BRD4 anchored to a large set of YAP/TAZ-bound enhancers.

Mechanism of transcriptional addiction

YAP/TAZ and BRD4 recruit RNA-Polymerase II at the TSS of YAP/TAZ target genes

So far, we have delineated the dynamic of YAP/TAZ interaction with BRD4 on chromatin, and the influence that this interaction has at the transcriptional level. We

next tried to shed light on the mechanism through which BRD4 regulates transcription at YAP/TAZ-target promoters. It has been reported that transcriptional activation is mediated by BRD4 through the recruitment of the positive transcriptional elongation factor B (P-TEFb) (Moon et al., 2005). Moreover, BRD4 was reported to contain an intrinsic kinase activity that - by phosphorylating RNA-phosphorylate Pol II at serine-2 - allows subsequent elongation in vitro, suggesting additional mechanisms through which BRD4 might regulate RNA-PolII elongation (Devaiah et al., 2012; Weishi Zhang et al., 2012). If BRD4 promotes elongation, we should expect that upon YAP/TAZ depletion or JQ1 treatment RNA-PolII should remain paused and accumulate on the promoters of YAP/TAZ targets. To verify this hypothesis, we performed ChIP-qPCR experiments for RNA Pol II in MDA-MB-231 cells in these experimental conditions:

1. Control cells treated with vehicle, DMSO;
2. Cells depleted of endogenous YAP/TAZ (siYAP/TAZ);
3. Cells treated with JQ1 (1μM, 24 hours).

RNA-Pol II was enriched at YAP/TAZ regulated promoters, but in contrast to expectation this binding decreased after depletion of YAP/TAZ or treatment with JQ1 (Figure 8A). As negative control we looked at GAPDH promoter, which represents a non-YAP/TAZ target; we did not observe any decrease in RNA-Pol II loading on GAPDH promoter in YAP/TAZ-depleted cells or JQ1 treated cells, suggesting that it might be specific for YAP/TAZ target genes. To verify this hypothesis, we analysed ChIP'd DNA by deep sequencing, so that we could assess RNA-PolII levels on promoters genome wide.

By analysing sequencing data we found that RNA-Pol II coverage on the TSSs of YAP/TAZ target genes was on average higher compared to all other expressed genes (Figure 8B): this is in agreement with RNA-seq data showing that YAP/TAZ target genes are expressed at higher levels. Pol II loading selectively decreased on the promoters of YAP/TAZ targets in YAP/TAZ-depleted cells, whereas no significant changes occurred on NOT YAP/TAZ targets (Figure 8B), as anticipated by ChIP-qPCR. Similarly, Pol II occupancy on the TSS of YAP/TAZ targets gene selectively decreased upon JQ1 administration (1μM, 24 hours) compared to promoters of genes not activated by YAP/TAZ (Figure 8C). These results exclude that YAP/TAZ promote transcript elongation; instead, data imply that YAP/TAZ promote the recruitment of RNA Pol II on the TSS of their target genes, and that this event is mediated by BRD4. Indeed, we detected an association between YAP and Pol II in endogenous complexes by Co-IP in MDA-MB-

231 cells (Figure 8D); intriguingly, this interaction was lost after experimental depletion of BRD4 (compare to pre-immune rabbit IgG), confirming the essential role of BRD4 in connecting YAP/TAZ-bound cis-regulatory elements with the transcriptional apparatus assembled on cognate promoters.

BRD4 acetyltransferase activity is required for activation of YAP/TAZ target genes

Since we found that high expression, as well as high JQ1 sensitivity, of YAP/TAZ targets is associated to high Pol II recruitment, rather than increased elongation, we reasoned that BRD4 must entail additional mechanisms to regulate YAP/TAZ-dependent gene expression. BRD4 has been recently reported to display an intrinsic acetyltransferase (HAT) activity, different from those of other known acetyltransferases. BRD4 acetylates lysine K122 in the globular domain of H3 where the histone-DNA interaction is strongest (Devaiah et al., 2016). H3K122 acetylation is associated with Pol II loading on promoters and transcriptional activation (Tropberger et al., 2013). BRD4, by depositing acetyl residues on H3K122, promotes nucleosomal disassembly and chromatin decompaction to allow the arrival of transcriptional machinery and subsequent expression of downstream gene (Devaiah et al., 2016). The acetyltransferase activity of BRD4 resides in a catalytic domain (located in the C terminus of the protein) and on two putative acetyl-CoA binding sites (one in mouse BRD4) (Devaiah et al., 2016).

With this background in mind, we assessed the relevance of BRD4 acetyltransferase activity for the expression of YAP/TAZ target genes. We transduced MDA-MB-231 cells with a viral vector encoding a HAT-defective form of mouse-BRD4 (ΔHAT, bearing a deletion of the catalytic domain and point mutations in the acetyl-CoA binding site), or with wild type mouse BRD4. As shown in Figure 9A, upon depletion of endogenous human BRD4, exogenous wild-type mouse BRD4 could rescue the expression of YAP/TAZ target genes, whereas the mutant BRD4 deficient in HAT activity could not. Thus, the HAT domain of BRD4 is crucial to sustain the expression of YAP/TAZ target genes.

This finding predicts that H3K122ac levels on the promoters of YAP/TAZ target genes are regulated by YAP/TAZ and BRD4. Thus, we measured the levels of H3K122ac by ChIP-qPCR in MDA-MB-231 cells treated with vehicle (DMSO), with JQ1 1μM (24 hours) or depleted of YAP/TAZ (by siRNA for 48h). We observed a robust loss in H3K122 acetylation close to the TSS of YAP/TAZ targets upon YAP/TAZ depletion or

treatment with JQ1 (Figure 9B). To extend these results to the genome-wide level, we performed a ChIP-seq experiment with anti-H3K122ac antibodies in control, YAP/TAZ-depleted or JQ1-treated cells. Strikingly, in control cells H3K122ac levels were significantly higher on the promoters of YAP/TAZ target genes in comparison with not-YAP/TAZ targets (Figure 9C). Moreover, the average signal of H3K122Ac (showed as the typical bimodal curve of histone modifications) was markedly decrease upon YAP/TAZ depletion or JQ1 treatment on the TSS of YAP/TAZ direct targets (Figure 9D). These results were in line with the higher coverage of BRD4 and RNA-Pol II, and with transcriptional activation. We thus propose a mechanism whereby YAP/TAZ promote transcriptional activation of their target genes by favouring BRD4 overload on their promoters; in turn, BRD4 allows Pol II recruitment through H3K122 acetylation.

Relevance of the YAP/TAZ-BRD4 axis for YAP/TAZ protumorigenic functions

Addiction to YAP/TAZ is associated with sensitivity to BET inhibitors in TNBC cells in vitro

To expand on the generality of the YAP/TAZ-BRD4 connection, we then asked whether YAP/TAZ transcriptional activity is especially sensitive to BET inhibitors in Triple Negative Breast Cancer Cell Lines (TNBC) other than MDA-MB-231. For this purpose, we measured the effects of YAP/TAZ depletion and treatment with BET inhibitors on the expression level of a set of YAP/TAZ target genes. For these experiments, we used both JQ1, and an analogous BET-inhibitor, OTX015. Quantitative RT-PCR on a panel of well-known YAP/TAZ target genes (shown in Figure 10A) demonstrated that dependency on YAP/TAZ is correlated with sensitivity to BET inhibitors: indeed, gene expression is either impaired both by YAP/TAZ depletion and pharmacological BET inhibition, or unaffected by both treatments.

Secondly, we performed viability assay on a panel of TNBC cells, to assess if addiction to YAP/TAZ and sensitivity to BET inhibitors are also functionally correlated. We either transfected cells with two independent combinations of YAP/TAZ siRNAs, or treated them with increasing doses of JQ1 (from 1nM to 10μM). At the end of the assay, we evaluated cell viability by staining with Crystal Violet. Cells whose proliferation was inhibited by YAP/TAZ depletion also decreased their growth rate in the presence of

JQ1, in a dose dependent manner; instead, cells that kept proliferating in spite of YAP/TAZ depletion were insensitive to JQ1 (Figure 10B).
Overall, most cell lines were addicted to YAP/TAZ, and also sensitive to JQ1; we only found one cell line, BT20, that is not YAP/TAZ-addicted and is resistant to BET inhibitors.

YAP/TAZ-BRD4 activity in human breast tumors

Beyond transcriptional and mechanistic data presented above, some functional in vitro assays not reported in this thesis support the relevance of BRD4 for YAP/TAZ biological activity in breast cancer cells. Thus, we evaluated whether the YAP/TAZ-BRD4 axis is relevant for the malignant phenotype of breast tumors in human patients, by testing the prognostic capacity of common YAP/TAZ-BRD4 target genes.
We used the RNA-seq data in MDA-MB-231 cells to generate three gene signatures: 1) "all BET target genes", listing all genes that were downregulated by treatment with JQ1; 2) "YAP/TAZ-dependent BET target genes", comprising genes downregulated both by BRD inhibition and YAP/TAZ downregulation; 3) "YAP/TAZ-independent BET target genes", containing genes that were downregulated by BRD inhibition but are not YAP/TAZ target genes. We calculated the expression level of these signatures in a large dataset of human breast cancer patients containing transcriptome profiling and clinical annotations of >3600 tumors, and we tried to assess whether expression of each signature was associated with longer or shorter metastasis-free survival (Cordenonsi et al., 2011; Enzo et al., 2015).
We found that patients with a higher expression of the "all BET target genes" signature had a worse prognosis, as expected from the known oncogenic functions of BRD4 (Figure 10C box 1). Remarkably, when we split the list of BET target genes into YAP/TAZ-dependent and independent signatures, we found that only common YAP/TAZ/BET target genes retained predictive value, with higher expression of the signature associated with reduced metastasis-free survival (Figure 10C box 2); instead, BET targets that were YAP/TAZ-independent had no prognostic value (Figure 10C box 3).
The results of this analysis imply that BRD4 oncogenic properties substantially rest upon YAP/TAZ transcriptional responses, and they suggest that in the future the expression level of "YAP/TAZ-dependent BET target genes" could be used as a

biomarker to identify cancer patients with a high activity of the YAP/TAZ/BRD4 axis, who could benefit of a therapy with BET inhibitors.

BET inhibitors block the growth of YAP/TAZ-dependent mammary tumors in mice

Extending the translational significance of these *in vitro* and *in silico* findings, we assayed whether inhibition of BET proteins could arrest the growth of established tumors in mice. As a model of YAP/TAZ-addicted tumor, we used TNBC-like tumors that develop in the mammary gland of mice upon activation of the Wnt signalling cascade, due to the loss of a key component, Adenomatous Polyposis Coli (*APC*).

Activation of Wnt/β-catenin signalling pathway has a widespread role in development, tissue homeostasis and cancer (Zhan, Rindtorff, & Boutros, 2016). Briefly, from a mechanistic point of view, the core of the Wnt pathway is the regulation of its nuclear transducer β-catenin by a cytoplasmic destruction complex, consisting of a central scaffold protein, Axin, that interacts with other factors, such as the tumor suppressor *APC*, CK1, and glycogen synthase kinase-3 (GSK3). In absence of Wnt ligands (Wnt OFF state), the destruction complex targets β-catenin to proteasomal degradation through phosphorylation by GSK3 and ubiquitination by β-TrCP. Conversely, the presence of Wnt ligands (Wnt ON) causes functional inactivation of the destruction complex, thus allowing β-catenin release, stabilization and formation of nuclear complexes with the DNA-binding partners TCF/Lef, finally resulting in downstream gene expression (Clevers, 2006).

Our lab discovered that YAP and TAZ are trapped in the β-catenin destruction complex in the absence of Wnt ligands, whereas Wnt signalling triggers YAP/TAZ escape from the destruction complex, their nuclear localization and activation of their transcriptional target genes (Azzolin et al., 2014). It has been reported that *APC* is the main intestinal tumor suppressor, being inactivated in the large majority of hereditary and sporadic forms of human colorectal cancers (Clevers, 2006). In mouse models bearing conditional knockout of *APC* alleles, acute activation of the Wnt cascade in the intestinal epithelium causes massive hyperplasia with altered differentiation (Sansom et al., 2004). Indeed, loss or mutations in *APC* contribute to both YAP/TAZ and β-catenin nuclear accumulation in intestinal crypts (Azzolin et al., 2014).

Like in the intestine, Wnt activation was reported to induce the formation of TNBC-like tumors in mouse models (Kuraguchi, Ohene-Baah, Sonkin, Bronson, & Kucherlapati,

2009; Li, Hively, & Varmus, 2000) and importantly, epigenetic silencing of APC is a frequent event in human TNBC (Swellam et al., 2015). With this background in mind, we carried out conditional knockout of *APC* in the mammary gland by using Cre-loxP technology, where the Cre recombinase catalyses the deletion of a DNA fragment between two directly orientated loxP sites ("floxed"). We crossed mice bearing floxed *APC* alleles ($Apc^{fl/fl}$) with mice carrying a MMTV-Cre, a constitutive Cre recombinase whose expression is under the control of the mouse mammary tumor virus (MMTV) long terminal repeat (LTR), in order to recombine *APC* alleles predominantly in the mammary epithelium (K.-U. Wagner et al., 2001).

Our first aim was to verify whether knockout of *APC* was sufficient to induce malignant transformation in the mouse mammary gland, and if this process entailed YAP/TAZ activation. 8-weeks-old $MMTV\text{-}Cre;Apc^{fl/fl}$ female mice displayed overgrowth of the mammary epithelium, with almost complete loss of the initial ordered structure, with evident signs of panductal and panlobular atypical hyperplasia and fibrosis, a typical pre-neoplastic/early neoplastic scenario, as shown in the hematoxylin-eosin (H&E) staining in Figure 11A. Staining for luminal and basal keratins (Keratin8 and Keratin14, respectively) revealed expansion of the luminal layer with large discontinuities in the basal/myoepithelial layer, confirming the abnormalities noticed in the H&E. In control $MMTV\text{-}Cre;Apc^{+/+}$ mice luminal cells did not display nuclear YAP; conversely, lesions in $MMTV\text{-}Cre;Apc^{fl/fl}$ mice exhibited massive YAP accumulation in the nuclei of $K8^{+}$ mammary cells, indicating aberrant YAP stabilization (Figure 11B). To verify if YAP/TAZ were required for the development of these epithelial lesions, we obtained triple mutant mice bearing knockout of *APC*, YAP and TAZ ($MMTV\text{-}Cre;Apc^{fl/fl};Yap^{fl/fl};Taz^{fl/fl}$). Strikingly, the mammary gland of these mice displayed a normal morphology, confirming that neoplastic transformation in $MMTV\text{-}Cre;\ Apc^{fl/fl}$ mice indeed depends on YAP/TAZ (Figure 11A and 11B).

Since our *in vitro* data indicated that YAP/TAZ establish transcriptional dependencies that induce oncogenic growth in a manner dependent on BRD4, we next wondered whether these $MMTV\text{-}Cre;Apc^{fl/fl}$ mice with established YAP/TAZ-dependent neoplastic lesions could be treated by administration of BET inhibitors. To address this point, we treated 8-weeks-old female mice (i.e., with an overt mammary gland phenotype) with a potent BET inhibitor (BAY-1238097, 75 mg/kg/week) for 6 weeks; we used the vehicle (0.9% NaCl pH4) as a control. Strikingly, at the end of treatment, histological examination of the mammary gland showed extensive epithelial remodelling and

regression of lesions, with few remaining signs of mammary hyperplasia or fibrosis (Figure 11C). Immunofluorescence staining for K8 and K14 revealed the presence, in treated mice, of ducts with ordered distribution of luminal and basal markers to an extent that the main mammary ducts returned to a normal appearance (Figure 11C). BET-inhibitor was well-tolerated, as we did not observe body weight loss throughout the entire treatment (data not shown); moreover, as a control, treatment of *Apc*$^{fl/fl}$ siblings (i.e., lacking Cre expression) was overtly well tolerated, and inconsequential for mammary gland homeostasis, as confirmed by both haematoxylin-eosin staining and immunofluorescence for K8/K14 in Figure 11D. Thus, dependency on BRD4 defines a potential vulnerability for YAP/TAZ-driven mammary tumors, in line with the *in vitro* results obtained in human TNBC cell lines.

BET-inhibitors prevent early tumorigenic events induced by YAP in the mouse liver

We next explored the functional dependence of YAP/TAZ on BET proteins in tissues other than the mammary gland, in a context in which YAP/TAZ biological effects are remarkably known, that is, the mouse liver (Camargo et al., 2007; Dong et al., 2007). It is well known that YAP activation or overexpression in the mouse liver results in massive organ overgrowth and tumor formation (Dong et al., 2007; Yimlamai et al., 2014; N. Zhang et al., 2010). We used transgenic mice bearing a doxycycline-inducible YAP allele (+YAP^{HEP}) with the point mutation S127A, sufficient to obtain a constitutive active form of YAP that remains in the nucleus and is transcriptionally active. To obtain hepatocyte-specific YAP overexpression, we put this transgene under the control of the albumin promoter (*Albumin-Cre*^{ERT2}). This Cre^{ERT2} recombinase is fused to mutated human estrogen receptor ligand-binding domain; it is inactive, unless mice are administered tamoxifen (a synthetic estrogen analogue).

The specificity of *Albumin-Cre*^{ERT2} has been tested by lineage tracing: injection of tamoxifen into *AlbuminCre*^{ERT2}*; R26-LSL-YFP* mice drove the excision of the loxP-stop-loxP (LSL) cassette upstream of the YFP reporter allowing the expression of the marker in cells where the albumin promoter is active. By co-staining of liver section with antibodies recognizing YFP, the hepatocyte-specific marker HNF4α, and the biliary cell-specific marker KRT19, we found that YFP is expressed in hepatocytes, but not in biliary cells, as expected (Figure 12A).

Albumin-Cre^{ERT2} was combined with two alleles that allow the expression of the YAPS$_{127A}$ transgene only in the presence of doxycycline. This is a standard TetON

system: $YAPS_{127A}$ transgene is under the control of a tetracycline-responsive promoter (*tet-O-YAPS127A*), and its transcription is allowed only in the presence of the rtTA (reverse tetracycline-controlled transactivator) and doxycycline. In our mice, the rtTA gene is activated by Cre-mediated excision of a lox-stop-lox (LSL) cassette.

Albumin-Cre^{ERT2}; *R26-LSL-rtTA*; *tet-O-YAPS127A* mice received tamoxifen (2 i.p. injections on consecutive days, 3 mg/day) and then doxycycline in drinking water (for 10 days); these treatments activate the expression of YAP, as shown by the western blot in Figure 12B. YAP^{HEP} expression resulted in the appearances of "ductular reactions" around the portal area, consisting of small ("oval") cells with a scant cytoplasm infiltrating the liver parenchyma, portrayed in the hematoxylin and eosin staining in Figure 12C. Differentiated hepatocytes transdifferentiated into liver progenitors labelled by hepatocellular carcinoma markers SOX9 (a direct YAP/TAZ target in the liver) and Osteopontin1 (Spp1) (Figure 12C) (Benhamouche et al., 2010). Remarkably, treatment with BET inhibitor (BAY-1238097) concomitantly to doxycycline administration abolished this "ductular reaction" and reduced the appearance of transdifferentiating cells, captured "in transition" by the co-expression of SOX9 and HNF4a by immunofluorescence (Figure 12C). Concomitantly, Spp1 expression was strongly reduced by the treatment with BET inhibitor (Figure 12C). Of note, by comparing vehicle- and BAY-1238097-treated animals, we did not find any difference in the expression of YAP transgene (immunoblot in Figure 12B), thus confirming that the different phenotype observed in mice treated with BET inhibitor did not result from a reduced YAP expression. By RT-qPCR, we observed that the average expression of oval-cell markers Sox9 and Spp1 is induced in YAP^{HEP} transgenic livers, while it is strongly blunted by concomitant treatment with BET inhibitor (Figure 12D).

Histologically, BET inhibitor remarkably prevented the otherwise massive changes in the architecture of liver parenchyma and reduced the appearance of proliferating $Ki67^{+}$ hepatocytes that are typically observed in vehicle-treated YAP transgenic livers (Figure 12E). From a macroscopic point of view, liver overgrowth induced by YAP expression was restricted by BET inhibition. Importantly, administration of BET-inhibitor to control mice had no overt consequences on liver morphology or molecular features.

Taken together, these data confirm the requirement of BET proteins in YAP/TAZ-driven initial steps of liver tumorigenesis, to the extent that pharmacological inhibition of BET proteins is sufficient to revert the massive disorganization of the tissue induced by YAP_{S127A}.

Inhibition of BET proteins as a way to overcome YAP-induced drug resistance

Beyond controlling tumor initiation and growth, YAP/TAZ endow cancer cells with the capacity to acquire resistance to chemotherapeutics and molecularly targeted drugs (Zanconato, Cordenonsi, et al., 2016). Indeed, YAP/TAZ act as survival inputs for tumor cells, dampening the efficacy of oncogene-targeting drugs. The emblematic example of YAP/TAZ-induced drug resistance are melanoma cells bearing BRAF activating mutations, where resistance is rapidly installed after the administration of BRAF inhibitors (such as PLX4032/vemurafenib). The acquisition of resistance to vemurafenib is associated with YAP/TAZ activation by increased mechanotransduction (M. H. Kim et al., 2016; Lin et al., 2015). Two main events collaborate to induce resistance in cells exposed to BRAF inhibitors, and both of them activate YAP/TAZ:

- There is an increase in polymerization of actin stress fibres inside tumor cells (making cells highly responsive to mechanical stimulation);
- In the surrounding environment, cancer associated fibroblasts are activated and produce a collagen-rich, stiff extracellular matrix, as such increasing the level of mechanical stimulation that tumor cells receive from outside.

These events inevitably unleash YAP/TAZ, allowing their accumulation in the nucleus of melanoma cells.

We decided to verify the requirement of BET proteins also in this set up, so we asked if JQ1 could re-sensitize cells that have spontaneously acquired resistance to vemurafenib after chronic exposure. This hypothesis is supported by the fact that YAP/TAZ knockout in resistant cells is sufficient to diminish their viability and re-sensitize them to vemurafenib (M. H. Kim et al., 2016).

We performed viability assays by exposing melanoma WM3248 cells, that spontaneously acquired resistance to vemurafenib after chronic exposure, to increasing doses of BRAF inhibitor (1nM to 10μM) with or without JQ1 (1μM). The combined treatment with JQ1 sensitized resistant cells to low doses of vemurafenib, and impaired tumor cell viability to an extent that neither vemurafenib nor JQ1 could achieve when used individually (Figure 13A).

In line, YAP overexpression in vemurafenib-sensitive WM3248 (still BRAF-mutant) parental cells is sufficient to install chemoresistance (M. H. Kim et al., 2016). Integrating results obtained from Kim's lab with ours we hypothesized, also in this experimental condition, that JQ1 could be used to revert YAP-induced drug resistance in parental (vemurafenib-sensitive) WM3248 cells. We transduced WM3248 cells with

a doxy-inducible lentiviral plasmid encoding for EGFP or the constitutive active YAP5SA, and we exposed them to vemurafenib alone, or vemurafenib and JQ1. We found that the growth of YAP-overexpressing BRAF-mutant melanoma cells was strongly inhibited by the combined exposure to vemurafenib and JQ1, which was *per se* poorly active (Figure 13B).

YAP/TAZ transcriptional activity is overtly induced in vemurafenib-resistant melanoma cells compared to parental sensitive cells. We found that depletion of BRD2/3/4 (siBRD mix A and mix B) impaired the expression of a panel of YAP direct targets in YAP-overexpressing parental WM3248 cells, comparably to treatment with BET inhibitors (JQ1 and OTX015 1μM for 24 hours) (Figure 13C). These genes include AXL (Zanconato et al., 2015) coding for a tyrosine-protein kinase receptor, which has been reported to be a pillar in resistance to BRAF inhibitors (Zuo et al., 2018), and the immune checkpoint ligand PD-L1 (B. S. Lee et al., 2017). Collectively, these experiments indicate the requirement of BET proteins in maintaining YAP/TAZ-induced resistance to vemurafenib in BRAF mutant melanoma cells, suggesting that BET inhibitors might indeed prove useful to revert YAP/TAZ-dependent drug resistance in melanoma cells.

DISCUSSION

Normal cells vary their behaviour through multiple mechanisms according to differential inputs, in turn every event is translated into an established gene expression program that leads to an equilibrium and to a specific cell identity. General transcription factors encoded by the human genome are expressed in all cell type and a subset of them, normally called lineage regulators, are sufficient to protect normal cells from errors (Buganim, Faddah, & Jaenisch, 2013; Graf & Enver, 2009; T. I. Lee & Young, 2013).

Cancer cells abuse of these safeguards to obtain extra functions, defined as "hallmarks of cancer", namely the acquisition of numerous aberrant traits, including immortalization, resistance to apoptosis, improved cellular metabolism, uncontrolled proliferation and resistance to conventional chemotherapeutics. An uncontrolled transcription factors (TFs) signalling can profoundly change gene expression, due to the binding of master TFs to enhancers and newly generated super-enhancer, defined as large clusters of enhancers massively bound by transcriptional components responsible for dysregulations gene expression in cancer (Mullen et al., 2011; Trompouki et al., 2011). Nevertheless, the molecular identity of the key TFs underlying the properties of these super-enhancers elements remains mysterious (Pott & Lieb, 2014). This massive dependency of cancer cells on TFs has been rephrased as "transcriptional addiction" (Bradner et al., 2017).

The mechanisms that produce transcriptional addiction and how they can be exploited for new strategic therapies are the object of intense investigation.

In the work presented here, we have identified YAP/TAZ as a key player in the transcriptional addiction of transformed cells and established tumors. We discovered a physical association between BRD4 and YAP/TAZ in the nuclei of MDA-MB-231 cells, a triple negative breast cancer cell line. This physical association between BRD4 and YAP/TAZ retains also important functional consequences. It was previously reported that the epigenetic reader and modifier BRD4 regulates the expression of oncogenic drivers through occupying super-enhancers in multiple myeloma cells and other tumors (Lovén et al., 2013), paralleling YAP/TAZ occupancy in these large regulatory regions (Galli et al., 2015; Zanconato et al., 2015). ChIP-seq analysis in MDA-MB-231 cells showed that BRD4 co-occupy the same enhancers and promoters

of YAP/TAZ regulated genes; in fact, YAP/TAZ actively promote the recruitment of very high amounts of BRD4 to the same enhancers they occupy, and to the TSS of the genes they control. In turn, BRD4 accumulation on the promoter stimulates the recruitment of RNA-polymerase II through acetylation of H3K122 in the globular domain of H3, thus allowing chromatin decompaction and subsequent transcription of the downstream gene. In so doing, the YAP/TAZ-BRD4 axis confers transcriptional advantage to a broad number of genes that are primarily involved in cell proliferation: replication licensing, DNA synthesis and repair and many other factors required for mitosis. The functional outcome is that turning off YAP/TAZ transcriptional program (by YAP/TAZ depletion) is sufficient to induce growth arrest in MDA-MB-231 cells (Zanconato et al., 2015).

Given its well reported role in cancer, BRD4 is an attractive therapeutic target and several drugs targeting BET-proteins have been developed in the last years and now are available (Filippakopoulos & Knapp, 2014). Some of the chemical compounds targeting BRD4 are currently under pre-clinical or clinical evaluations and show promising effects in a variety of malignancies (Shi et al., 2014). Here we reported that YAP/TAZ/TEAD-dependent transcription is largely sensible to BET inhibitors. High BRD4 overload at YAP/TAZ cis-regulatory regions makes YAP/TAZ target genes extremely vulnerable to BET inhibition. JQ1 (the prototypical BET inhibitor) induced preferential loss of BRD4 from YAP/TAZ-occupied enhancers, compared to enhancers without YAP/TAZ binding sites; in line, BRD4 preferentially dropped from the promoters of YAP/TAZ target genes in the presence of JQ1; and YAP/TAZ targets displayed a higher responsiveness to JQ1, as their expression levels were more severely reduced by JQ1 than the levels of not-YAP/TAZ targets. Such susceptibility also affects YAP/TAZ-induced tumorigenic ability *in vivo,* both at the early stages of neoplastic transformation and in established tumors.

Other transcription factors have been shown to bind BRD4, in no case these could explain genome-wide recruitment of BRD4 at regulatory elements of entire groups of genes essential for cancer biology. Here, we have linked a rather elusive and wide concept, such as transcriptional addiction, to specific transcription factors. Our results offer a solution to the enigma of how a general transcriptional regulator such as BRD4 is specifically enriched at discrete chromatin sites to regulate transcription in a gene-

specific manner in transformed cells. We have found that YAP/TAZ drive BRD4 recruitment to the *cis*-regulatory elements of their own target genes; indeed, BRD4 must engage in a dual interaction with acetylated histones and with YAP/TAZ to be stably anchored to chromatin. Thus, YAP/TAZ may impart specificity to BRD4 recruitment to selected loci in the genome. These findings would also explain why general transcriptional inhibitors (such as BET-inhibitors) do not induce a global downregulation of all transcripts, but impair transcription in a gene-specific manner.

The investigation of the structure of YAP/TAZ-BRD4 complex needs further studies. We have assessed that both the WW domain and the transactivation domain of YAP/TAZ are involved in the association to BRD4. Further details could provide the ground to design new therapeutics around the BET-YAP/TAZ interaction surfaces, and the YAP/TAZ-interacting domains of BRD4, that remain here unexplored.

Our findings also advance on the mechanistic details of YAP/TAZ dependent transcription. It is well established that YAP/TAZ bind enhancers, mainly in association with TEAD transcription factors. We have added that YAP/TAZ promote the recruitment of RNA-polymerase II on the TSS of their target genes, and that this event is mediated by BRD4. It was previously reported that YAP/TAZ promote transcriptional pause release – rather than transcription initiation - by recruiting CDK9/ P-TEFb. Our ChIP-seq data for RNA-polymerase II, instead, point to a different mechanism; and other experiments performed in the lab revealed that P-TEFb inhibitors are not as selective as JQ1 in the regulation of YAP/TAZ target genes. That said, it is possible that different mechanisms act together to maximize the expression of YAP/TAZ target genes; the chromatin context, the availability of cofactors and also the presence of other transcription factors might determine which mechanism prevails.

Drugging YAP/TAZ is a challenging and ambitious goal for cancer research (Johnson & Halder, 2014). Here we have shown that targeting BET proteins could be a valuable strategy to blunt YAP/TAZ activity in tumor cells, both in vitro and in vivo.
BET inhibitors are promising anticancer drugs, although drug resistance and identification of responsive patient subpopulations remain critical open issues (Andrieu, Belkina, & Denis, 2016). Our results collectively indicate that the oncogenic effects of BET proteins are in close association to YAP/TAZ biology, and that YAP/TAZ-BRD4

common target genes identified in our study have prognostic value in human breast tumors. Thus, we hypothesize that this signature could be used to identify tumors with a high activity of the YAP/TAZ-BRD4 axis; we expect these tumors to be more responsive to BET inhibitors. Unluckily, at the moment no clinical data are available to verify this hypothesis.

One major problem in cancer treatment is the onset of resistance to chemotherapeutics and molecularly-targeted drugs. YAP/TAZ play a role in this event, thus we envision that YAP/TAZ inhibition through BET inhibitors might prove beneficial to overcome drug resistance. We have shown that – in the context of YAP-induced drug resistance in melanoma - the combinatorial treatment of resistant cells with the BRAF-inhibitor Vemurafenib and JQ1 re-sensitized them to Vemurafenib. Of note, treatment with the sole JQ1 was not sufficient to impair tumor cell viability in this context. Thus, it might be important to combine BET-inhibitors with other drugs in order to achieve the desired therapeutic effect. Indeed, ongoing clinical trials have revealed that BET-inhibitors are poorly effective as monotherapy. Moreover, emerging evidence indicate that tumor cells can develop resistance against BET inhibitors (Fong et al., 2015; Rathert et al., 2015; Shu et al., 2016), once again raising the need for the exploration of possible combinatorial therapies, for example using BET inhibitors together with compounds targeting YAP/TAZ upstream activators.

Interestingly, it was recently reported that YAP/TAZ directly control the expression of PD-L1 (Taha, Janse van Rensburg, & Yang, 2018). PD-L1 is upregulated in cancer cells, and it plays a pivotal role in inhibiting the immune response against tumor cells; PD-L1 blocking agents are successfully used to elicit the immune response in some malignancies. We have shown that JQ1 could downregulate PD-L1 expression in YAP-overexpressing melanoma cells, suggesting that BET inhibitors might be combined with PD-L1 inhibitors to simultaneously inhibit PD-L1 expression and activity.

YAP/TAZ also play important roles in regulating stem cell self-renewal and cell fate plasticity (Panciera et al., 2016). The epigenetic changes associated with YAP/TAZ activation in these contexts remain unknown. It will be interesting to assess the relevance of BRD4 for YAP/TAZ physiological activity, such as tissue regeneration.

MATHERIAL AND METODS

The methods here listed are part of the Piccolo's Lab protocol book and thus presented with minor modifications, if any, in respect to published material or others thesis works published by our Lab.

Reagents and plasmids

Doxycycline, OTX015 (SML1605), human insulin, hydrocortisone and cholera toxin were from Sigma. Human EGF was from Peprotech. Vemurafenib-PLX4032 (A3004) was from Apex Bio. JQ1 was from BPS Bioscience (27402).

pCDNA-FLAG-YAP vectors (wild-type or 5SA, siRNA insensitive) were described in (Aragona et al., 2013). FLAG-YAP 5SA and FLAG-YAP wild type were subcloned in pBABE- retroviral plasmids. pBABE-blasti retroviral vectors was generated by replacing the puromycin resistance gene with the blasticidin resistance gene in pBABE-puro (Addgene plasmid #1764, a gift of H. Land, J. Morgenstern and R. Weinberg).

pFlag-CMV2-BRD4 was from Addgene (#22304, a gift from Eric Verdin (Bisgrove, Mahmoudi, Henklein, & Verdin, 2007). BRD4 CDS with a N-ter HA tag was subcloned in CSII-CMV-MCS-IRES2-Puro lentiviral plasmid. CSII-CMV-MCS-IRES2-Puro vector was generated by replacing the blasticidin resistance gene with the puromycin resistance gene in CSII-CMV-MCS-IRES2-Bsd, kindly provided by H. Miyoshi (RIKEN BSI, #RDB04385). pcDNA5-Flag-BRD4-WT (Addgene plasmid # 90331) and pCDNA5-Flag-BRD4-BD (Addgene plasmid # 90005) were a gift from Kornelia Polyak (Shu et al., 2016).

The coding sequence of HAT-deficient mBRD4 was a gift from Dinah S. Singer (Devaiah et al., 2016). Wild-type and HAT-deficient mBRD4 were subcloned in CSII-CMV-MCS-IRES2-Bsd lentiviral plasmid. GFP from PL-SIN-EOS-C(3+)-EiP (Addgene plasmid # 21313, a gift from James Ellis (Hotta et al., 2009) and FLAG-YAP 5SA were subcloned in pCW57.1 lentiviral plasmid to establish stable cell lines. pCW57.1 was a gift from David Root (Addgene plasmid # 41393). For GST-pull down experiments WT full-length YAP was cloned in pGEX-4T-3. GST-TAZ constructs were described in (Azzolin et al., 2012). All constructs were confirmed by sequencing.

Generation of Retroviral and Lentiviral particles and infection

To generate retroviral particles we used 293GP cells, a packaging cell line that constitutively express retroviral proteins: Gag and Pol, whereas retroviral vector and the plasmid expressing Env (pmd2-Env) were transfected with TransIT-LT1 (MirusBio) on cells seeded on a 10 cm diameter dish. Culture medium containing viral particle was collected 24-48 hours after transfection and filtered to discard any cellular debris. Infection was performed by colturing cells with virus-containing medium for 24 hours. Only cells that contain the retroviral vectors encoding for antibiotic resistance can survive under selection (1μg/mL of Puromycin/Higromycin). Usually in a week all un-transduced cells should die, meaning the correct functioning of the selection agent and infection procedure.

Similar procedure has been followed for the production of lentiviral particles: lentiviral vectors were transfected in 293T cells in combination with Gag-Pol (psPAX2) and Env (pmd2-VSVG) coding plasmids.

Cell lines, treatments and transfections

MDA-MB-231 cells were from ICLC. MDA-MB-231 cells were cultured in DMEM/F12 (Life Technologies) supplemented with 10% FBS, glutamine and antibiotics. For BRD4 overexpression, cells were transduced with CSII-CMV-MCS-IRES2-Puro-HA-hBRD4, or CSII-CMV-MCS-IRES2-Bst-FLAG-mBRD4 WT or HAT-deficient (or empty vector as control). After infection with doxycycline-inducible vectors, MDA-MB-231 cells were maintained in media supplemented with Tet-approved FBS (Clontech), to reduce background expression of the transgene in the absence of doxycycline.

MCF10A cells (from ATCC) were cultured in DMEM/F12 (Life Technologies) with 5% horse serum, glutamine and antibiotics, freshly supplemented with insulin, human EGF, hydrocortisone, and cholera toxin. For gene expression and ChIP experiments, MCF10A cells were seeded at high density (75.000 cells/cm^2) and harvested after 48 hours. For YAP overexpression, cells were transduced with pBABE-blasti-FLAG-YAP5SA (or empty vector as control). HEK293T cells (from ATCC) were maintained in DMEM supplemented with 10% FBS (Life Technologies), glutamine and antibiotics. MDA-MB-231, MCF10A and HEK293T were authenticated by DSMZ service.

BT-20 cells were obtained from the ATCC (HTB-19) and cultured in DMEM supplemented with 10%FBS (Life Technologies), glutamine and antibiotics. SUM149T

and SUM-159 were kindly provided by Dr. S. Ethier and cultured in F12 with 5%FBS (Life Technologies), glutamine and antibiotics, freshly supplemented with 5μg/ml Insulin and 1μg/ml hydrocortisone. Hs578T cells were obtained from ICLC and maintained in DMEM with 10%FBS (Life Technologies), glutamine and antibiotics, freshly supplemented with 10μg/ml Insulin.

WM3248 and WM3248-R6 cells (a gift from J.Kim, KAIST) were cultured in MCBD (Sigma), 2%FBS, 1.68mM $CaCl_2$. For YAP overexpression WM3248 cells were transduced with pCW57.1-Flag-YAP5SA (or EGFP as control) and maintained in presence of doxycycline. All cell lines were routinely tested for mycoplasma contamination and were negative. None of the cell lines used in this study is present in the database of commonly misidentified cell lines.

Drugs were resuspended in DMSO and used at a final concentration of 1μM for 24h, unless differently specified. DNA transfections were performed with TransitLT1 (Mirus Bio) according to manufacturer instructions. siRNAs were transfected with Lipofectamine RNAi-MAX (Life Technologies) in antibiotics-free medium according to manufacturer instructions. Cells were harvested 48h after transfection with YAP/TAZ siRNAs and 72h after transfection with siRNAs targeting BET-proteins.

siRNA sequences:

siRNA mix name	*siRNA sequence*
YAP/TAZ siRNA mix 1 (siYT1)	GACAUCUUCUGGUCAGAGAdTdT; ACGUUGACUUAGGAACUUUdTdT
YAP/TAZ siRNA mix 2 (siYT2)	CUGGUCAGAGAUACUUCUUdTdT; AGGUACUUCCUCAAUCACAdTdT
BRD2/3/4 siRNA mix A (siBRD A)	GUAGCAGUGUCACGCCUUAdTdT; CCUGCCGGAUUAUCAUAAAdTdT; GAGGACAAGUGCAAGCCUAdTdT
BRD2/3/4 siRNA mix B (siBRD B)	GUAGCAGUGUCACGCCUUAdTdT; GCCCGUGGACGCAAUCAAAdTdT; GCGUUUCCACGGUACCAAAdTdT

Negative control siRNA was purchased from Qiagen (cat. 1027280, AllStars Negative Control siRNA).

ChIP-MS

Cells were cross-linked with 1% formaldehyde (Sigma) in culture medium for 10min at room temperature followed by 5min treatment with 0.125M Glycine/PBS. Cells were harvested and incubated in Lysis Buffer 1 (50mM HEPES, pH7.5, 10mM NaCl, 1mM EDTA, 10% Glycerol, 0.5% NP-40, 0.25% Triton X-100, with protease inhibitors; 20 min at 4°C), then in Lysis Buffer 2 (10mM Tris-HCl pH8, 200 mM NaCl, 1mM EDTA, 0.5 mM EGTA, plus protease inhibitors; 10 min at RT); finally nuclei were resuspended in Lysis Buffer 3 (10mM Tris-HCl pH8, 200 mM NaCl, 1mM EDTA, 0.5 mM EGTA, 0.1% Na-deoxycholate, 0.5% N-lauroylsarcosine, plus protease inhibitors) and sonicated using a Branson Sonifier 4500D (5x1min pulse, duty cycle 0.5, 30% amplitude). Immunoprecipitation was performed by incubating cleared extracts (corresponding to $2x10^6$ cells) with 20 µg of antibody overnight at 4°C (anti-YAP: EP1674Y, Abcam; anti-TAZ: HPA007415, Sigma; pre-immune rabbit IgGs: I5006, Sigma). Antibody/antigen complexes were recovered with ProteinG-Dynabeads (Invitrogen, 5 µL Dynabeads/1 µg antibody) for 3h at 4°C. The precipitates were washed twice in low salt wash buffer (20mM Tris-HCl pH8, 150mM NaCl, 0.1 % SDS, 0.5% Triton X-100 and 2mM EDTA), twice in high salt wash buffer (20mM Tris-HCl pH8, 2mM EDTA, 300mM NaCl, 0.1% SDS and 0.5% TritonX), and once with 100 mM Tris-HCl. Precipitates were eluted in 7.5%SDS, 200mM DTT and incubated at 37°C for 30min to revert crosslinks. Upon alkylation with iodoacetamide (IAA), proteins were purified with SP3 beads as previously described (PMID 25358341), resuspended in 50mM ammonium bicarbonate and digested with 300 ng trypsin 16h at 37°C. Peptides were subjected to SP3 cleanup and they were eluted in 0.1% TFA. Samples were analyzed on an Orbitrap Fusion mass spectrometer (Thermo Fisher).

Co-immunoprecipitation of endogenous nuclear proteins

Cells were rinsed twice with ice-cold HBSS and incubated with ice-cold hypotonic buffer (2 x 1min, 20mM HEPES, 20% Glycerol, 10mM NaCl, 1.5mM $MgCl_2$, 0.2mM EDTA, 0.1% NP40, freshly supplemented with 1 mM DTT, and protease and phosphatase inhibitor cocktails). Nuclei were then harvested by scraping in hypertonic buffer (hypotonic buffer + 500mM NaCl, 400 µl/60 cm^2) and disrupted by sonication in a water-bath sonicator. Nuclear lysates were cleared by centrifugation and quantified by Bradford. For immunoprecipitation, extracts were diluted to 140mM NaCl and incubated 4h at 4°C with magnetic beads (Dynabeads Protein A or G, Invitrogen)

preloaded with specific primary antibodies. Immunocomplexes were then washed in binding buffer four times; finally, beads were resuspended in SDS sample buffer.
Antibodies used for immunoprecipitation: anti-BRD4 (E2A7X, CST); anti-YAP1 (13584-1-AP, Proteintech raised in rabbit); anti-WWTR1 (HPA007415, Sigma); anti-FLAG (clone M2, A8592, Sigma); normal rabbit IgG (I5006, Sigma).

GST Pull-Down

GST-YAP and GST-TAZ were produced in E.coli and immobilized on glutathione sepharose 4B (GE/Sigma). Resins were blocked in 5%BSA/PBS and then incubated with full length recombinant BRD4 (cat. RD-21-153, Cambridge Bioscience, 500ng/reaction) in binding buffer (20mM Hepes KOH, 20% glycerol, 100mM KCl, 1.5mM $MgCl_2$, 0.2mM EDTA, 0.1% NP-40, 1mM DTT) o.n. at 4°C. Resins were then washed in binding buffer (4 x 5min) and resuspended in SDS sample buffer for subsequent analysis)

Western Blot

Cells were harvested in Lysis Buffer (20 mM HEPES (pH 7.8), 100 mM NaCl, 5% Glycerol, 0.5% NP40, 5mM EDTA, 1 mM DTT, phosphatase and protease inhibitors) and lysed by sonication.
About 10mg of liver were mechanically disrupted, resuspended in 500µl of Lysis Buffer and lysed by sonication. Extracts were quantified with Bradford method. Samples were run in 4-12% Nupage-MOPS acrylamide gels (ThermoFisher) and transferred onto PVDF membranes by wet electrophoretic transfer. Blots were blocked with 0.5% non-fat dry milk and incubated overnight at 4°C with primary antibodies. Secondary antibodies were incubated 1 hour at room temperature, and then blots were developed with chemiluminescent reagents. Images were acquired with Image Quant LAS 4000 (GE healthcare). *In vitro* experiments were performed three times with similar results.
Antibodies used for Western blot: anti-YAP/TAZ (sc-101199) from Santa Cruz; anti-GAPDH (MAB347, Millipore); anti-TEF1 (clone 31, 610923, BD Biosciences); horseradish-peroxidase-conjugated anti-FLAG (clone M2, A8592) and anti-BRD4 (HPA015055) from Sigma; anti-RNA polymerase II CTD repeat YSPTSPS antibody (ab817) from Abcam.

Immunofluorescence of cultured cells

Cells were cultured on glass slides and treated with 1μM JQ1 or OTX015 for 24h. Cells were fixed 10 min at room temperature with 4% PFA in PBS, permeabilized 10 min at RT with PBS+0.3% Triton X-100, blocked in 10% Goat Serum (GS) in PBS + 0.1% Triton X-100 (PBST) for 1h, and then incubated with anti-YAP/TAZ (sc-101199; SantaCruz) primary antibody diluted in 2% GS in PBST, overnight at 4°C. After four washes in PBST, samples were incubated with secondary antibody (Alexa 488, 1:200 in 2% GS in PBST) for 2h at room temperature. Nuclei were counterstained with ProLong-DAPI (Molecular Probes, Life Technologies). Images were acquired with a Leica TCS SP5 confocal microscope equipped with a CCD camera.

In situ proximity ligation assay (PLA)

HEK293T cells were seeded on fibronectin-coated glass chamber slides and transfected with pFlag-CMV2-BRD4, pCS2-HA-BRD4 or empty pCS2+ as negative control. After 24 hours, cells were fixed in 4% PFA for 10 min at RT. *In situ* PLA was performed with DuoLink In Situ Reagents (Sigma) according to manufacturer's instructions. Primary antibodies used in the PLA are: mouse anti-HA (F-7, sc-7392, SantaCruz), mouse anti-TEF1 (610923; BD Biosciences), rabbit anti-FLAG (F-7425; Sigma), rabbit anti-YAP1 (EP1674Y, abcam), rabbit anti-WWTR1 (HPA007415, Sigma). Images were acquired with a Leica TCS SP5 confocal microscope equipped with a CCD camera; for each field, a Z-stack was acquired; images were processed using Volocity software (PerkinElmer). We verified that the fraction of nuclei with positive PLA signal corresponded to the fraction of transfected cells (determined by immunofluorescence for FLAG or HA).

Viability assays

Cells were seeded in 96-well plates (4000 cells/well) one day before treatment with drugs or transfection with siRNAs. Cells fixed after 72h with a crystal violet solution (0.05% w/v Crystal violet, 1% formaldehyde, 1% methanol in PBS) for 20 min at RT; stained cells were washed with water until a clear background was visible, and air-dried. Crystal violet was extracted with 1% SDS (w/v in ddH2O, 100 μl/well) and absorbance at λ=595 nm was measured with an Infinite F200PRO plate reader (TECAN). 8 technical replicates were analyzed for each sample; data are presented as mean + SD. Data are presented as % viability compared to control cells (treated with DMSO or

transfected with siCO), where absorbance at the beginning of treatment was set as 0%, and absorbance at the end of experiment was set as 100%. Each experiment was performed at least twice, with similar results.

Mice

Animal experiments were performed adhering to our institutional guidelines as approved by OPBA (University of Padua) and the Italian Ministry of Health. All experimental mice used in this study were mixed strains and more than 6 weeks old; for mammary gland experiments we used exclusively female mice. Transgenic lines used in the experiments were kindly provided by: Duojia Pan (N. Zhang et al., 2010) (Yap1fl/fl); Alan R. Clarke (Sansom et al., 2004) (Apcfl/fl); F. Camargo (Camargo et al., 2007) (tetO-YAPS127A); Pierre Chambon (Schuler, Dierich, Chambon, & Metzger, 2004) (Albumin-CreERT2). Tazfl/fl and double Yapfl/fl; Tazfl/fl conditional knock-out mice were as described in (Azzolin et al., 2014); MMTV-Cre (K. U. Wagner et al., 1997) (stock #003553) and R26-LSL-rtTA (Belteki et al., 2005) (stock #005670) were purchased from The Jackson Laboratory. Yap, Taz and Apc conditional knockouts were intercrossed with MMTV-Cre mice to obtain the different genotypes. Mice carrying Albumin-CreERT2, R26-LSL-rtTA and tetO-YAPS127A alleles were intercrossed to obtain Albumin-CreERT2; R26-LSL-rtTA/+; tetO-YAPS127A mice. Albumin-CreERT2; R26-LSL-rtTA/+ littermates were used as control. Animals were genotyped with standard procedures and with the recommended set of primers.

Control (Apcfl/fl, n=3) or MMTV-Cre; Apcfl/fl (n=3) mice were administered BAY-BET-inh (BAY-1238097) by intraperitoneal injection for 6 weeks, starting at 8 weeks of age (15mg/kg, 5inj/week). Control mice were injected with vehicle (0.9% NaCl, pH 4). Harvesting, processing and stainings on mammary glands were performed as in (Panciera et al., 2016). For the induction of the recombination in the liver, control (Albumin-CreERT2; R26-LSL-rtTA/+) mice and Albumin-CreERT2; R26-LSL-rtTA/+; tetO-YAPS127A mice received 1 intraperitoneal injection per day of 3 mg Tamoxifen (Sigma) dissolved in corn oil (Sigma) during 2 consecutive days. After 2 weeks, mice were administered doxycycline in drinking water for 10 days, during which they also received BAY-BETinh (15 mg/kg, 5 inj/week) or vehicle by intraperitoneal injections, as indicated in the corresponding Figures.

For validation of the Albumin-CreERT2 driver (Figure 12A), Albumin-CreERT2; R26-LSL-YFP/+ mice were injected with 3 mg Tamoxifen (Sigma) per day dissolved in corn oil (Sigma) during 5 consecutive days and were sacrificed after 2 weeks.

Immunostainings and immunofluorescences of liver tissue

Immunohistochemical staining was performed on formalin-fixed, paraffin-embedded tissue sections as described in (Cordenonsi et al., 2011). Primary anti-Ki67 polyclonal antibody (clone SP6; M3062, Spring Bioscience) was from Spring Bioscience.

Immunofluorescences on PFA-fixed paraffin embedded tissue slices was performed as (Cordenonsi et al., 2011). Slides were permeabilized 10 min at RT with PBS 0.3% Triton X-100, and processed for immunofluorescence (IF) according to the following conditions: blocking in 10% BSA or Goat Serum (GS) in PBST for 1 hr followed by incubation with primary antibody (diluted in 2% BSA or GS in PBST) for 16 hr at 4°C, four washes in PBST and incubation with secondary antibodies (diluted in 2% BSA or GS in PBST) for 1.5 hr at room temperature. Primary antibodies were anti-cytokeratin (wide spectrum screening, ZO622; Dako), anti-HNF4α (sc-6556; Santa Cruz Biotechnology), anti-SOX9 (AB5535; Millipore) and anti-GFP (ab13970; abcam). Samples were counterstained with ProLong-DAPI (Molecular Probes, Life Technologies) to label cell nuclei. Confocal images were obtained with a Leica TCS SP5 equipped with a CCD camera. Bright field images were obtained with a Nanozoomer Scanner 2.0RS (Hamamatsu).

RNA in situ hybridization

Tissue sections (formalin-fixed paraffin-embedded) were processed for RNA in situ detection using the RNAscope Duplex Detection Kit (Chromogenic) according to the manufacturer's instructions (Advanced Cell Diagnostics). RNAscope probe used was Spp1 (Osteopontin; NM_001204201.1, region 2-1079), which was detected using the Fast-Red detection reagent.

RT-qPCR

Total RNA extraction from cells and tissue was performed with NucleoSpin 8 RNA Core Kit (Macherey-Nagel, REF.740465.4) using an automated system (Freedom EVO, Tecan). Contaminant DNA was removed by rDNase Set (Macherey-Nagel, REF.740963).

Gene expression analyses by quantitative real-time PCR (RT-qPCR) were carried out with QuantStudio 5 thermal cycler (ThermoFisher). Experiments were performed at least three times. Expression levels are calculated relative to GAPDH.

Human primer pairs are:

Primers	Forward	Reverse
AURKA	GCCCTCTGGGTAAAGGAAAG	GCCGAAGGTGGGACTGTAT
AXL	CACCAGCAAGAGCGATGTGT	CGGTCCTGGGGATTTAGCTC
BRD4	GAGGCAGACCAACCAACTGC	CAGGGAGGTTCAGCTTGACG
CCNA2	TTTGATAGATGCTGACCCATACC	ATGCTGTGGTGCTTTGAGGT
CDC6	CGCAAAGCACTGGATGTTT	CAACCCTCTTGGGAATCAGA
CDCA5	CCTGAAATCTGGCCGAAGAC	CTCCTGCGAGGTGATTGGAC
E2F3	GAACAAGGCAGCAGAAGTGC	CCCCCATCCTCAGACAGACT
FST1	CCGGTGTTCCCTCTGTGATG	TCCTCTTCCTCGGTGTCTTCC
GAPDH	CTCCTGCACCACCAACTGCT	GGGCCATCCACAGTCTTCTG
GINS1	TCAACGAGGATGGACTCAGA	AAGCAAGCGGTCATACAGGT
KIF23	AGTTCAGGCTCCCTTGGATG	TCTGTTCCCTTCTGCTCTGGTC
MCM3	TGGGTTGTGCCGAGAGAGTT	CCAACATTCCTCGCCTTCAG
PD-L1	GGTGCCGACTACAAGCGAAT	GGTGACTGGATCCACAACCAA
PLAU	CGCCACACACTGCTTCATT	CAAACTTCATCTCCCCTTGC
RRM2	TGGCTCAAGAAACGAGGACTG	TGAACATCAGGCAAGCAAAATC
TOP2A	CGCCGCAAAAGGAAGCCATC	TTTTGCCCGAGGAGCCACAG
TUBB1	GTGGCCTCAAGATGGCAGTC	TCTCAGCCTCGGTGAACTCC

Mouse primer pairs are:

Primers	Forward	Reverse
Gapdh	ATCCTGCACCACCAACTGCT	GGGCCATCCACAGTCTTCTG
Sox9	AGGCCACGGAACAGACTCAC	CCCCTCTCGCTTCAGATCAA
Spp1	CTGGTGCCTGACCCATCTCA	TCATCCGAGTCCACAGAATCC

RNA-seq

Cells were harvested by RNeasy Mini Kit (Qiagen) for total RNA extraction and contaminant DNA was removed by RNase-Free DNase Set (Qiagen).

RNA-seq libraries for deep-sequencing were prepared with the Illumina TruSeq Standard Total RNA with Ribo-Zero GOLD kit, and sequencing was performed with Illumina HiSeq2500. About 40M reads/sample were obtained. Raw reads were aligned using TopHat59 (version 2.0.5) to build version hg19 of the human genome. Counts for UCSC annotated genes were calculated from the aligned reads using HTSeq60 (version 0.6.0). Normalization and differential analysis were carried out using edgeR package61 and R (version 3.0.0). Raw counts were normalized to obtain Counts Per Million

mapped reads (CPM) and Reads Per Kilobase per Million mapped reads (RPKM). Only genes with a RPKM greater than 1 in at least 2 samples were retained for differential analysis. Genes were considered differentially expressed with a Benjamini-Hochberg FDR less than or equal to 1% and a fold change equal or lower than 0.75. The 10th percentile, first quartile, median, third quartile and 90th percentile are plotted in box and whiskers graphs. Fold changes were calculated as the ratio of RPKM.

ChIP-seq and ChIP-qPCR

ChIP was performed as previously described13. Briefly, cells were crosslinked with 1% formaldehyde (Sigma) in culture medium for 10 min at room temperature, and chromatin from lysed nuclei was sheared to 200–600 bp fragments using a Branson Sonifier 4500D.

For ChIP-seq, ~200 µg of chromatin were incubated with 10 µg of antibody overnight at 4°C (anti-BRD4: A301-985A, Bethyl-Lab; anti-PolII: ab817, abcam; normal rabbit IgG: Sigma; normal mouse IgG: Santa Cruz). For ChIP-seq of H3K122ac, ~50 µg of chromatin were incubated with 10 µg of anti-Histone H3 (acetyl K122) (ab33309, abcam). Antibody/antigen complexes were recovered with ProteinA-Dynabeads (Invitrogen, 5 µl Dynabeads/1 µg antibody) for 2h at 4°C (1h for anti-H3K122ac). The precipitates were washed and eluted in 50mM Tris-HCl pH 8, 1%SDS, 1mM EDTA for 20 min at 65°C. Chromatin was decrosslinked, treated with RNaseA and Proteinase K and DNA was purified by QIAquick PCR Purification Kit (Qiagen, 28106). Enrichment of target sequences was checked by qPCR, then libraries were generated with the Ovation Ultra Low Library Prep Kit (NuGEN) according to manufacturer's instructions. Sequencing was performed on an Illumina HiSeq 2500 platform.

For ChIP-qPCR, 100 µg of sheared chromatin and 3–5 µg of antibody were used.

For ChIPs of YAP, anti-YAP1 (ab52771) from Abcam was used. For ChIPs of H3K122ac, at least 10 µg of chromatin were incubated with 2 µg of antibody. Quantitative real-time PCR was carried out with QuantStudio 5 thermal cycler (ThermoFisher); each sample was analysed in triplicate and was presented as mean + SD. The amount of immunoprecipitated DNA in each sample was determined as the fraction of the input [amplification efficiency ^ (Ct INPUT - Ct ChIP)] and normalized to IgG control.

Duplicate experiments were performed at least twice with similar results.

ChIP primers pairs are:

Primers	Forward	Reverse
ANKRD1	AAAAAGGGCAGTGATGTGGTG	GAAGAGGGAGGGGAGGACAA
CCNA2 Enh	ACAGAAGGGGAGCGACTGG	CCCACCGTTTTCACTTTTTC
CDC6 Enh	GCTGGGCATCACAGTCTTGG	GGCATGGCTGGGTGACTC
CDC6 TSS	CAAGGCGAAAGGCTCTGTGA	CAAGCCCCTGAACAAACTGC
CDCA5 Enh	AGTGCTGCTCCCCCACACTA	CCTGCAAGGAAAGAGCTGGA
CDCA5 TSS	GCGTTCGCCTCCCAGACATA	TTCCGCTTCCTTTCCCGCAG
CYR61	CACACACAAAGGTGCAATGGAG	CCGGAGCCCGCCTTTTATAC
ETS1 Enh	CCCTTGTCCCAACACACACA	AAAACTGTCTCCACCTCCTAATGC
E2F3 TSS	GCGTAAACCGTATCCCTTCA	CAAAAATAATCGGGGCTCTGG
FOSL1 TSS	TACACGGCTGCTGGGTTC	GGTGGAGCCTGGAGGTGAC
GAPDH TSS	TCGCTCTCTGCTCCTCCTGT	GTTTCTCTCCGCCCGTCTTC
GINS1 Enh	CCCCAAAAGTGTCCATGACC	CAGGATCACCCCCATCTCAA
GINS1 TSS	GCCGAGAGCCCAGATACCAT	CGTTGAAGGCAGGCAGTAG
HBB	GCTTCTGACACAACTGTGTTCACT AGC	CACCAACTTCATCCACGTTCACC
KIF23 TSS	TTGGCCCGTTTGAAATGCGC	ACGTTAGGACCGGCAGCAAG
MCM3 Enh	AGTTGGGATAGGCGGAGACC	GCAGGTGGGGCTTGTTTAGG
MCM3 TSS	TCCCGCCACCAAAGGTTAC	AGCGGAAAACCCGAAGAAGA
PLAU Enh	GCTGGCTTCACCCTTCACAC	ATGGGGCAGACGGACTCTTC
PLAU TSS	CCTCAGTCCAGACGCTGTTG	CTCCCTCCCCTGTCTTGCAG
RRM2 Enh	AGGGCTGTTGCTCACCTCTTG	GCATTCTTCCTGGCTCTTTGTG
RRM2 TSS	TTAAAGGCTGCTGGAGTGAGG	CGGAGGGAGAGCATAGTGGA
TMEM200B TSS	AAAGGGAGGGCGAGGGAGAA	CAGCGCGGTGGTTCTTTAGGA
TOP2A Enh	CCCCACCCAGACAGGAAA	TGAGGCAGGGCAGTTTAGAA
TUBB Enh	ACTGGCTTCGGCTGTGTCTT	AATAAAGGATGTGGGGAGCA
TUBB TSS	TTCTTGGCAGGCACATTTTG	GACCGTTTCCGCATCTCTCT

Analysis of ChIP-seq data

Raw reads were aligned using Bowtie64 (version 0.12.7) to build version hg19 of the human genome retaining only uniquely mapped reads. Redundant reads were removed using SAMtools.

The lists of H3K4me1-, H3K4me3-, YAP- and TAZ-enriched regions (peaks) in MDA-MB-231 cells were already described in (Zanconato et al., 2015).

The overlap of peaks from different ChIP-seq experiments was determined using the BEDTools2 suite 65.

Definition of promoters and enhancers

To define promoter regions in the genome of MDA-MB-231 cells, we first defined a list of 2 kb-wide regions centered on each transcription start site (TSS) mapped in the build

version hg19 of the human genome (downloaded from the UCSC genome browser, Ref. 66). We then obtained a list of promoter regions by including only the TSSs overlapping with H3K4me3-enriched regions.

Active enhancers were defined as non-promoter regions displaying enrichment for H3K4me1 (and H3K27ac, data not shown in this thesis). For this, we first defined a list of enhancers based on H3K4me1 peaks, purged of those overlapping with promoter regions. The width of each enhancer was set to the same of the corresponding H3K4me1 peak. From this list we generated a list of active enhancers, by including only the enhancer elements overlapping with peaks for H3K27ac (data not shown).

Annotation of active enhancers to target genes

Active enhancers were annotated using the chromatin interactions reported in Supplementary data 2 of Jin et al. 201367, derived from a high-resolution Hi-C experiment; the data sheets report the genomic locations of all target peaks interacting with more than 10,000 anchors located at gene promoters. Active enhancers overlapping with these target peaks were assigned to the corresponding interacting promoter region.

Annotation of YAP/TAZ binding regions to enhancers and target gene promoters

YAP/TAZ-bound enhancers were defined as active enhancers overlapping with both YAP and TAZ peaks. Similarly, YAP/TAZ-bound promoters were defined as promoter regions (as defined above) overlapping with both YAP and TAZ peaks. Gene promoters associated with YAP/TAZ-bound enhancers through DNA looping were defined as promoter regions associated with at least one YAP/TAZ-bound enhancer on the bases of Hi-C data (Zanconato et al., 2015). YAP/TAZ direct target genes were defined as those whose promoters are associated with YAP/TAZ-bound enhancers or are directly binding YAP/TAZ.

Calculating normalized read count and density at enhancers and promoters

ChIP-Seq reads aligning to each cis-regulatory region (active enhancers and promoters for BRD4 ChIP-seq experiments and promoters only for PolII and H3K122ac ChIP-seq experiments) were calculated using the BEDTools2 suite 65. Total number of reads was normalized to the total number of million mapped reads, producing normalized read counts in units of reads per million mapped reads (RPM). Normalized read density in units of reads per kilobase per million mapped reads (RPKM) was determined by dividing the total RPM count by the width of each cis-regulatory region in kilobases.

Relative occupancy was calculated as the ratio of RPKM. The 5th percentile, first quartile, median, third quartile and 95th percentile are plotted in box and whiskers graphs.

ChIP-seq heatmaps and average profiles

Heatmaps and average signal profiles were generated using a custom R script which considers a 1-kb window centered on TAZ peak summits falling on active enhancers or a 1.5 kb window centered on TSS of YAP/TAZ target genes. Normalized read density (reads per million, rpm) was calculated from pooled replicates using MACS69 (version 2.0.10) callpeak function with appropriate control samples (IgG for BRD4 and Input DNA for PolII and H3K122ac) and displayed using Integrative Genomics Viewer (IGV). Normalized reads density was calculated with a resolution of 50 bp. Each row in the heatmap represents a genomic region around a peak summit or TSS and rows are ranked according to TAZ or DMSO_BRD4 ChIP-seq signal intensity, respectively.

Generation of the signatures of BET-dependent genes

For analysis of the breast cancer dataset, we used the data generated for this study to identify a list of BET-dependent genes, defined as those whose expression was significantly downregulated (fold change equal or lower than 0.75; FDR less than or equal to 0.01) in both JQ1-treated and siBRD2/3/4-transfected MDA-MB-231 cells compared to control cells. Starting from this list, we then defined a list of common YAP/TAZ/BRD target genes, defined as BET-dependent genes that are also YAP/TAZ direct target genes whose expression is robustly downregulated (fold change less than or equal to 0.67) upon transfection with both YAP/TAZ siRNA mixes. We also defined a list of BRD-dependent but YAP/TAZ-independent genes in BC cells, composed by genes that are not downregulated (fold changes greater than 0.75) after transfection with either YAP/TAZ siRNA mixes. These two lists are of similar size, being the YAP/TAZ/ BRD signature composed by 220 genes, and the BRD-dependent/ YAP/TAZ-independent signature composed by 228 genes.

Collection and processing of gene expression data

Breast cancer gene expression data were generated, normalized, and annotated as described in (Enzo et al., 2015). Briefly, starting from a collection of 4,640 samples from 27 major data sets comprising microarray data and clinical information, we derived a compendium (meta-data set) comprising gene expression levels and clinical outcome for 3,661 unique samples from 25 independent cohorts. All microarray data analyses have been performed in R version 3.4.2 with the annotation packages of Bioconductor packages of Release 3.5.

Average signature expression and signature scores

Signature scores have been obtained summarizing the standardized expression levels of signature genes into a combined score with zero mean. Average signature expression has been calculated as the standardized average expression of all signature genes in all samples and plotted as mean ± standard error of the mean (SEM).

Kaplan–Meier survival analysis

To identify two groups of tumors with either high or low signature, we used the classification rule described in (Adorno et al., 2009). Briefly, tumors were classified as 'Low' if the combined signature score was negative and as 'High' if the combined signature score was positive. This classification was applied to expression values of the breast cancer meta-dataset. To evaluate the prognostic value of the BRD-dependent signatures, we estimated the probabilities that patients would remain free of metastases/ survive using the Kaplan–Meier method. To confirm these findings, the Kaplan–Meier curves were compared using the log-rank (Mantel–Cox) test. P-values were calculated according to the standard normal asymptotic distribution. Survival analysis was performed in GraphPad Prism.

REFERENCES

Abercrombie, M. (1979). Contact inhibition and malignancy. *Nature*, *281*(5729), 259–262. https://doi.org/10.1038/281259a0

Adorno, M., Cordenonsi, M., Montagner, M., Dupont, S., Wong, C., Hann, B., … Piccolo, S. (2009). A Mutant-p53/Smad Complex Opposes p63 to Empower TGFβ-Induced Metastasis. *Cell*, *137*(1), 87–98. https://doi.org/10.1016/j.cell.2009.01.039

Alsarraj, J., Walker, R. C., Webster, J. D., Geiger, T. R., Crawford, N. P. S., Simpson, R. M., … Hunter, K. W. (2011). Deletion of the Proline-Rich Region of the Murine Metastasis Susceptibility Gene Brd4 Promotes Epithelial-to-Mesenchymal Transition- and Stem Cell-Like Conversion. *Cancer Research*. Retrieved from http://cancerres.aacrjournals.org/content/early/2011/03/09/0008-5472.CAN-10-4417.abstract

Andrieu, G., Belkina, A. C., & Denis, G. V. (2016). Clinical trials for BET inhibitors run ahead of the science. *Drug Discovery Today. Technologies*, *19*, 45–50. https://doi.org/10.1016/j.ddtec.2016.06.004

Aragona, M., Panciera, T., Manfrin, A., Giulitti, S., Michielin, F., Elvassore, N., … Piccolo, S. (2013). A mechanical checkpoint controls multicellular growth through YAP/TAZ regulation by actin-processing factors. *Cell*, *154*(5), 1047–1059. https://doi.org/10.1016/j.cell.2013.07.042

Azzolin, L., Panciera, T., Soligo, S., Enzo, E., Bicciato, S., Dupont, S., … Piccolo, S. (2014). No Title. *Cell*, *158*(1), 157–170. Retrieved from http://www.ncbi.nlm.nih.gov/pubmed/24976009

Azzolin, L., Zanconato, F., Bresolin, S., Forcato, M., Basso, G., Bicciato, S., … Piccolo, S. (2012). Role of TAZ as mediator of Wnt signaling. *Cell*, *151*(7), 1443–1456. https://doi.org/10.1016/j.cell.2012.11.027

Bartucci, M., Dattilo, R., Moriconi, C., Pagliuca, A., Mottolese, M., Federici, G., … De Maria, R. (2015). TAZ is required for metastatic activity and chemoresistance of breast cancer stem cells. *Oncogene*, *34*(6), 681–690. https://doi.org/10.1038/onc.2014.5

Belteki, G., Haigh, J., Kabacs, N., Haigh, K., Sison, K., Costantini, F., … Nagy, A. (2005). Conditional and inducible transgene expression in mice through the combinatorial use of Cre-mediated recombination and tetracycline induction.

Nucleic Acids Research, *33*(5), e51–e51. https://doi.org/10.1093/nar/gni051

Benhamouche, S., Curto, M., Saotome, I., Gladden, A. B., Liu, C. H., Giovannini, M., & McClatchey, A. I. (2010). Nf2/Merlin controls progenitor homeostasis and tumorigenesis in the liver. *Genes and Development*, *24*(16), 1718–1730. https://doi.org/10.1101/gad.1938710

Bisgrove, D. A., Mahmoudi, T., Henklein, P., & Verdin, E. (2007). Conserved P-TEFb-interacting domain of BRD4 inhibits HIV transcription. *Proceedings of the National Academy of Sciences of the United States of America*, *104*(34), 13690–13695. https://doi.org/10.1073/pnas.0705053104

Bradner, J. E., Hnisz, D., & Young, R. A. (2017). Transcriptional Addiction in Cancer. *Cell*, *168*(4), 629–643. https://doi.org/10.1016/J.CELL.2016.12.013

Buganim, Y., Faddah, D. A., & Jaenisch, R. (2013). Mechanisms and models of somatic cell reprogramming. *Nature Reviews. Genetics*, *14*(6), 427–439. https://doi.org/10.1038/nrg3473

Cai, J., Zhang, N., Zheng, Y., de Wilde, R. F., Maitra, A., & Pan, D. (2010). The Hippo signaling pathway restricts the oncogenic potential of an intestinal regeneration program. *Genes & Development*, *24*(21), 2383–2388. https://doi.org/10.1101/gad.1978810

Camargo, F. D., Gokhale, S., Johnnidis, J. B., Fu, D., Bell, G. W., Jaenisch, R., & Brummelkamp, T. R. (2007). YAP1 increases organ size and expands undifferentiated progenitor cells. *Current Biology: CB*, *17*(23), 2054–2060. https://doi.org/10.1016/j.cub.2007.10.039

Chan, S. W., Lim, C. J., Guo, K., Ng, C. P., Lee, I., Hunziker, W., … Hong, W. (2008). A Role for TAZ in Migration, Invasion, and Tumorigenesis of Breast Cancer Cells. *Cancer Research*, *68*(8), 2592 LP-2598. Retrieved from http://cancerres.aacrjournals.org/content/68/8/2592.abstract

Chapuy, B., McKeown, M. R., Lin, C. Y., Monti, S., Roemer, M. G. M., Qi, J., … Bradner, J. E. (2013). Discovery and Characterization of Super-Enhancer-Associated Dependencies in Diffuse Large B Cell Lymphoma. *Cancer Cell*, *24*(6), 777–790. https://doi.org/10.1016/j.ccr.2013.11.003

Chen, H. I., & Sudol, M. (1995). The WW domain of Yes-associated protein binds a proline-rich ligand that differs from the consensus established for Src homology 3-binding modules. *Proceedings of the National Academy of Sciences of the United States of America*, *92*(17), 7819–7823. https://doi.org/10.1073/PNAS.92.17.7819

Chen, Q., Zhang, N., Gray, R. S., Li, H., Ewald, A. J., Zahnow, C. A., & Pan, D. (2014). A temporal requirement for Hippo signaling in mammary gland differentiation, growth, and tumorigenesis. *Genes & Development*, *28*(5), 432–437. https://doi.org/10.1101/gad.233676.113

Chen, Q., Zhang, N., Xie, R., Wang, W., Cai, J., Choi, K.-S., … Pan, D. (2015). Homeostatic control of Hippo signaling activity revealed by an endogenous activating mutation in YAP. *Genes & Development*, *29*(12), 1285–1297. https://doi.org/10.1101/gad.264234.115

Chiang, C.-M. (2009). Brd4 engagement from chromatin targeting to transcriptional regulation: selective contact with acetylated histone H3 and H4. *F1000 Biology Reports*, *1*(98), 98. https://doi.org/10.3410/B1-98

Clevers, H. (2006). Wnt/β-Catenin Signaling in Development and Disease. *Cell*, *127*(3), 469–480. https://doi.org/10.1016/j.cell.2006.10.018

Cordenonsi, M., Zanconato, F., Azzolin, L., Forcato, M., Rosato, A., Frasson, C., … Piccolo, S. (2011). The Hippo transducer TAZ confers cancer stem cell-related traits on breast cancer cells. *Cell*, *147*(4), 759–772. https://doi.org/10.1016/j.cell.2011.09.048

Dawson, M. A. (2017). The cancer epigenome: Concepts, challenges, and therapeutic opportunities. *Science (New York, N.Y.)*, *355*(6330), 1147–1152. https://doi.org/10.1126/science.aam7304

Devaiah, B. N., Case-Borden, C., Gegonne, A., Hsu, C. H., Chen, Q., Meerzaman, D., … Singer, D. S. (2016). BRD4 is a histone acetyltransferase that evicts nucleosomes from chromatin. *Nature Structural & Molecular Biology*, *23*(August 2015), 1–12. https://doi.org/10.1038/nsmb.3228

Devaiah, B. N., Lewis, B. A., Cherman, N., Hewitt, M. C., Albrecht, B. K., Robey, P. G., … Singer, D. S. (2012). BRD4 is an atypical kinase that phosphorylates Serine2 of the RNA Polymerase II carboxy-terminal domain. *Proceedings of the National Academy of Sciences of the United States of America*, *109*(18), 6927–6932. https://doi.org/10.1073/pnas.1120422109

Dhalluin, C., Carlson, J. E., Zeng, L., He, C., Aggarwal, A. K., Zhou, M.-M., & Zhou, M.-M. (1999). Structure and ligand of a histone acetyltransferase bromodomain. *Nature*, *399*, 491. Retrieved from http://dx.doi.org/10.1038/20974

Dong, J., Feldmann, G., Huang, J., Wu, S., Zhang, N., Comerford, S. A., … Pan, D. (2007). Elucidation of a Universal Size-Control Mechanism in Drosophila and

Mammals. *Cell*, *130*(6), 1120–1133. https://doi.org/10.1016/J.CELL.2007.07.019

Dupont, S., Morsut, L., Aragona, M., Enzo, E., Giulitti, S., Cordenonsi, M., … Piccolo, S. (2011). Role of YAP/TAZ in mechanotransduction. *Nature*, *474*(7350), 179–183. https://doi.org/10.1038/nature10137

Enzo, E., Santinon, G., Pocaterra, A., Aragona, M., Bresolin, S., Forcato, M., … Dupont, S. (2015). Aerobic glycolysis tunes YAP/TAZ transcriptional activity. *The EMBO Journal*, *34*(10), 1349–1370. https://doi.org/10.15252/embj.201490379

Feng, X., Degese, M. S., Iglesias-Bartolome, R., Vaque, J. P., Molinolo, A. A., Rodrigues, M., … Gutkind, J. S. (2014). Hippo-independent activation of YAP by the GNAQ uveal melanoma oncogene through a Trio-regulated Rho GTPase Signaling Circuitry. *Cancer Cell*, *25*(6), 831–845. https://doi.org/10.1016/j.ccr.2014.04.016

Filippakopoulos, P., & Knapp, S. (2014). Targeting bromodomains: epigenetic readers of lysine acetylation. *Nature Reviews Drug Discovery*, *13*(5), 337–356. https://doi.org/10.1038/nrd4286

Fong, C. Y., Gilan, O., Lam, E. Y. N., Rubin, A. F., Ftouni, S., Tyler, D., … Dawson, M. A. (2015). BET inhibitor resistance emerges from leukaemia stem cells. *Nature*, *525*(7570), 538–+. https://doi.org/10.1038/nature14888

Galli, G. G., Carrara, M., Yuan, W.-C. C., Valdes-Quezada, C., Gurung, B., Pepe-Mooney, B., … Camargo, F. D. (2015). YAP Drives Growth by Controlling Transcriptional Pause Release from Dynamic Enhancers. *Molecular Cell*, *60*(2), 328–337. https://doi.org/10.1016/j.molcel.2015.09.001

Gomez, M., Gomez, V., & Hergovich, A. (2014). The Hippo pathway in disease and therapy: cancer and beyond. *Clinical and Translational Medicine*, *3*(Figure 1), 22. https://doi.org/10.1186/2001-1326-3-22

Graf, T., & Enver, T. (2009). Forcing cells to change lineages. *Nature*, *462*, 587. Retrieved from http://dx.doi.org/10.1038/nature08533

Halder, G., Dupont, S., & Piccolo, S. (2012). Transduction of mechanical and cytoskeletal cues by YAP and TAZ. *Nature Publishing Group*, *13*(9), 591–600. https://doi.org/10.1038/nrm3416

Hansen, C. G., Moroishi, T., & Guan, K.-L. L. (2015). YAP and TAZ: A nexus for Hippo signaling and beyond. *Trends in Cell Biology*, *25*(9), 499–513. https://doi.org/10.1016/j.tcb.2015.05.002

Harvey, K. F., Zhang, X., & Thomas, D. M. (2013). The Hippo pathway and human

cancer. *Nature Reviews. Cancer*, *13*(4), 246–257. https://doi.org/10.1038/nrc3458

Hong, W., & Guan, K.-L. L. (2012). The YAP and TAZ transcription co-activators: Key downstream effectors of the mammalian Hippo pathway. *Seminars in Cell and Developmental Biology*, *23*(7), 785–793. https://doi.org/10.1016/j.semcdb.2012.05.004

Hotta, A., Cheung, A. Y. L., Farra, N., Vijayaragavan, K., Séguin, C. A., Draper, J. S., … Ellis, J. (2009). Isolation of human iPS cells using EOS lentiviral vectors to select for pluripotency. *Nature Methods*, *6*, 370. Retrieved from http://dx.doi.org/10.1038/nmeth.1325

Huang, J., Wu, S., Barrera, J., Matthews, K., & Pan, D. (2005). The Hippo signaling pathway coordinately regulates cell proliferation and apoptosis by inactivating Yorkie, the Drosophila homolog of YAP. *Cell*, *122*(3), 421–434. https://doi.org/10.1016/j.cell.2005.06.007

Johnson, R., & Halder, G. (2014). The two faces of Hippo: targeting the Hippo pathway for regenerative medicine and cancer treatment. *Nature Reviews. Drug Discovery*, *13*(1), 63–79. https://doi.org/10.1038/nrd4161

Justice, R. W., Zilian, O., Woods, D. F., Noll, M., & Bryant, P. J. (1995). The Drosophila Tumor-Suppressor Gene Warts Encodes a Homolog of Human Myotonic-Dystrophy Kinase and Is Required for the Control of Cell-Shape and Proliferation. *Genes & Development*, *9*(5), 534–546. https://doi.org/Doi 10.1101/Gad.9.5.534

Kharchenko, P. V, Tolstorukov, M. Y., & Park, P. J. (2008). Design and analysis of ChIP-seq experiments for DNA-binding proteins. *Nature Biotechnology*, *26*(12), 1351–1359. https://doi.org/10.1038/nbt.1508

Kim, M. H., Kim, J., Hong, H., Lee, S.-H., Lee, J.-K., Jung, E., & Kim, J. (2016). Actin remodeling confers BRAF inhibitor resistance to melanoma cells through YAP/TAZ activation. *The EMBO Journal*, *35*(5), 462–478. https://doi.org/10.15252/embj.201592081

Kim, M., Kim, T., Johnson, R. L., & Lim, D. S. (2015). Transcriptional co-repressor function of the hippo pathway transducers YAP and TAZ. *Cell Reports*, *11*(2), 270–282. https://doi.org/10.1016/j.celrep.2015.03.015

Koo, J. H., & Guan, K.-L. (2018). Interplay between YAP/TAZ and Metabolism. *Cell Metabolism*, *28*(2), 196–206. https://doi.org/10.1016/J.CMET.2018.07.010

Kuraguchi, M., Ohene-Baah, N. Y., Sonkin, D., Bronson, R. T., & Kucherlapati, R.

(2009). Genetic mechanisms in Apc-mediated mammary tumorigenesis. *PLoS Genetics*, *5*(2), e1000367. https://doi.org/10.1371/journal.pgen.1000367

Lallemand, D., Curto, M., Saotome, I., Giovannini, M., & McClatchey, A. I. (2003). NF2 deficiency promotes tumorigenesis and metastasis by destabilizing adherens junctions. *Genes and Development*, *17*(9), 1090–1100. https://doi.org/10.1101/gad.1054603

Lee, B. S., Park, D. Il, Lee, D. H., Lee, J. E., Yeo, M. kyung, Park, Y. H., … Chung, C. (2017). Hippo effector YAP directly regulates the expression of PD-L1 transcripts in EGFR-TKI-resistant lung adenocarcinoma. *Biochemical and Biophysical Research Communications*, *491*(2), 493–499. https://doi.org/10.1016/j.bbrc.2017.07.007

Lee, T. I., & Young, R. A. (2013). Transcriptional regulation and its misregulation in disease. *Cell*, *152*(6), 1237–1251. https://doi.org/10.1016/j.cell.2013.02.014

Li, Y., Hively, W. P., & Varmus, H. E. (2000). Use of MMTV-Wnt-1 transgenic mice for studying the genetic basis of breast cancer. *Oncogene*, *19*(8), 1002–1009. https://doi.org/10.1038/sj.onc.1203273

Lin, L., Sabnis, A. J., Chan, E., Olivas, V., Cade, L., Pazarentzos, E., … Bivona, T. G. (2015). The Hippo effector YAP promotes resistance to RAF- and MEK-targeted cancer therapies. *Nature Genetics*, *47*(3), 250–256. https://doi.org/10.1038/ng.3218

Liu-Chittenden, Y., Huang, B., Shim, J. S., Chen, Q., Lee, S.-J., Anders, R. A., … Pan, D. (2012). Genetic and pharmacological disruption of the TEAD-YAP complex suppresses the oncogenic activity of YAP. *Genes & Development*, *26*(12), 1300–1305. https://doi.org/10.1101/gad.192856.112

Liu, X., Li, H., Rajurkar, M., Li, Q., Cotton, J. L., Ou, J., … Mao, J. (2016). Tead and AP1 Coordinate Transcription and Motility. *Cell Reports*, *14*(5), 1169–1180. https://doi.org/10.1016/j.celrep.2015.12.104

Lovén, J., Hoke, H. A., Lin, C. Y., Lau, A., Orlando, D. A., Vakoc, C. R., … Young, R. A. (2013). Selective inhibition of tumor oncogenes by disruption of super-enhancers. *Cell*, *153*(2), 320–334. https://doi.org/10.1016/j.cell.2013.03.036

Makita, R., Uchijima, Y., Nishiyama, K., Amano, T., Chen, Q., Takeuchi, T., … Kurihara, H. (2008). Multiple renal cysts, urinary concentration defects, and pulmonary emphysematous changes in mice lacking TAZ. *AJP: Renal Physiology*, *294*(3), F542–F553. https://doi.org/10.1152/ajprenal.00201.2007

Meng, Z., Moroishi, T., & Guan, K. (2016). Mechanisms of Hippo pathway regulation.

Genes and Development, *30*(1), 1–17. https://doi.org/10.1101/gad.274027.115.1/2

Mo, J.-S., Park, H. W., & Guan, K.-L. (2014). The Hippo signaling pathway in stem cell biology and cancer. *EMBO Reports*, *15*(6), 642–656. https://doi.org/10.15252/embr.201438638

Moleirinho, S., Hoxha, S., Mandati, V., Curtale, G., Troutman, S., Ehmer, U., & Kissil, J. L. (2017). Regulation of localization and function of the transcriptional co-activator YAP by angiomotin. *ELife*, *6*, e23966. https://doi.org/10.7554/eLife.23966

Moon, K. J., Mochizuki, K., Zhou, M., Jeong, H. S., Brady, J. N., & Ozato, K. (2005). The bromodomain protein Brd4 is a positive regulatory component of P-TEFb and stimulates RNA polymerase II-dependent transcription. *Molecular Cell*, *19*(4), 523–534. https://doi.org/10.1016/j.molcel.2005.06.027

Morin-Kensicki, E. M., Boone, B. N., Howell, M., Stonebraker, J. R., Teed, J., Alb, J. G., … Milgram, S. L. (2006). Defects in yolk sac vasculogenesis, chorioallantoic fusion, and embryonic axis elongation in mice with targeted disruption of Yap65. *Molecular and Cellular Biology*, *26*(1), 77–87. https://doi.org/10.1128/MCB.26.1.77-87.2006

Moroishi, T., Hansen, C. G., & Guan, K.-L. (2015). The emerging roles of YAP and TAZ in cancer. *Nature Reviews. Cancer*, *15*(2), 73–79. https://doi.org/10.1038/nrc3876

Mullen, A. C., Orlando, D. A., Newman, J. J., Lovén, J., Kumar, R. M., Bilodeau, S., … Young, R. A. (2011). Master Transcription Factors Determine Cell-Type-Specific Responses to TGF-β Signaling. *Cell*, *147*(3), 565–576. https://doi.org/10.1016/j.cell.2011.08.050

Nguyen, L. T., Tretiakova, M. S., Silvis, M. R., Lucas, J., Klezovitch, O., Coleman, I., … Vasioukhin, V. (2015). ERG Activates the YAP1 Transcriptional Program and Induces the Development of Age-Related Prostate Tumors. *Cancer Cell*, *27*(6), 797–808. https://doi.org/10.1016/j.ccell.2015.05.005

Nishioka, N., Inoue, K., Adachi, K., Kiyonari, H., Ota, M., Ralston, A., … Sasaki, H. (2009). The Hippo signaling pathway components Lats and Yap pattern Tead4 activity to distinguish mouse trophectoderm from inner cell mass. *Developmental Cell*, *16*(3), 398–410. https://doi.org/10.1016/j.devcel.2009.02.003

Oh, H., Slattery, M., Ma, L., Crofts, A., White, K. P., Mann, R. S., & Irvine, K. D. (2013). Genome-wide Association of Yorkie with Chromatin and Chromatin-

Remodeling Complexes. *Cell Reports*, *3*(2), 309–318. https://doi.org/10.1016/j.celrep.2013.01.008

Oh, H., Slattery, M., Ma, L., White, K. P., Mann, R. S., & Irvine, K. D. (2014). Yorkie Promotes Transcription by Recruiting a Histone Methyltransferase Complex. *Cell Reports*, *8*(2), 449–459. https://doi.org/10.1016/j.celrep.2014.06.017

Pan, D. (2010). The hippo signaling pathway in development and cancer. *Developmental Cell*, *19*(4), 491–505. https://doi.org/10.1016/j.devcel.2010.09.011

Panciera, T., Azzolin, L., Cordenonsi, M., & Piccolo, S. (2017). Mechanobiology of YAP and TAZ in physiology and disease. *Nature Reviews Molecular Cell Biology*, *18*(12), 758–770. https://doi.org/10.1038/nrm.2017.87

Panciera, T., Azzolin, L., Fujimura, A., Di Biagio, D., Frasson, C., Bresolin, S., … Piccolo, S. (2016). Induction of Expandable Tissue-Specific Stem/Progenitor Cells through Transient Expression of YAP/TAZ. *Cell Stem Cell*, 1–13. https://doi.org/10.1016/j.stem.2016.08.009

Piccolo, S., Dupont, S., & Cordenonsi, M. (2014). The biology of YAP/TAZ: hippo signaling and beyond. *Physiological Reviews*, *94*(4), 1287–1312. https://doi.org/10.1152/physrev.00005.2014

Pott, S., & Lieb, J. D. (2014). What are super-enhancers? *Nature Genetics*, *47*, 8. Retrieved from http://dx.doi.org/10.1038/ng.3167

Qing, Y., Yin, F., Wang, W., Zheng, Y., Guo, P., Schozer, F., … Pan, D. (2014). The Hippo effector Yorkie activates transcription by interacting with a histone methyltransferase complex through Ncoa6. *ELife*, *3*. https://doi.org/10.7554/eLife.02564

Rafiee, M.-R., Girardot, C., Sigismondo, G., & Krijgsveld, J. (2016). Expanding the Circuitry of Pluripotency by Selective Isolation of Chromatin-Associated Proteins. *Molecular Cell*, *64*(3), 624–635. https://doi.org/10.1016/j.molcel.2016.09.019

Ramos, A., & Camargo, F. D. (2012). The Hippo signaling pathway and stem cell biology. *Trends in Cell Biology*, *22*(7), 339–346. https://doi.org/10.1016/j.tcb.2012.04.006

Rathert, P., Roth, M., Neumann, T., Muerdter, F., Roe, J.-S. J.-S., Muhar, M., … Zuber, J. (2015). Transcriptional plasticity promotes primary and acquired resistance to BET inhibition. *Nature*, *525*(7570), 543–547. https://doi.org/10.1038/nature14898

Rhie, S. K., Hazelett, D. J., Coetzee, S. G., Yan, C., Noushmehr, H., & Coetzee, G. A. (2014). Nucleosome positioning and histone modifications define relationships

between regulatory elements and nearby gene expression in breast epithelial cells. *BMC Genomics*, *15*(1), 331. https://doi.org/10.1186/1471-2164-15-331

Sansom, O. J., Reed, K. R., Hayes, A. J., Ireland, H., Brinkmann, H., Newton, I. P., … Winton, D. J. (2004). Loss of Apc in vivo immediately perturbs Wnt signaling, differentiation, and migration. *Genes & Development*, *18*(12), 1385–1390. https://doi.org/10.1101/gad.287404

Santinon, G., Pocaterra, A., & Dupont, S. (2016). Control of YAP/TAZ Activity by Metabolic and Nutrient-Sensing Pathways. *Trends in Cell Biology*, *26*(4), 289–299. https://doi.org/10.1016/j.tcb.2015.11.004

Schmidt, D., Wilson, M. D., Spyrou, C., Brown, G. D., Hadfield, J., & Odom, D. T. (2009). ChIP-seq: using high-throughput sequencing to discover protein-DNA interactions. *Methods (San Diego, Calif.)*, *48*(3), 240–248. https://doi.org/10.1016/j.ymeth.2009.03.001

Schuler, M., Dierich, A., Chambon, P., & Metzger, D. (2004). Efficient temporally controlled targeted somatic mutagenesis in hepatocytes of the mouse. *Genesis*, *39*(3), 167–172. https://doi.org/10.1002/gene.20039

Shaffer, S. M., Dunagin, M. C., Torborg, S. R., Torre, E. A., Emert, B., Krepler, C., … Raj, A. (2017). Rare cell variability and drug-induced reprogramming as a mode of cancer drug resistance. *Nature*, *546*, 431. Retrieved from http://dx.doi.org/10.1038/nature22794

Shi, J., Vakoc, C. R., Junwei, S., Vakoc, C. R., Shi, J., & Vakoc, C. R. (2014). The mechanisms behind the therapeutic activity of BET bromodomain inhibition. *Molecular Cell*, *54*(5), 728–736. https://doi.org/10.1016/j.molcel.2014.05.016

Shu, S., Lin, C. Y., He, H. H., Witwicki, R. M., Tabassum, D. P., Roberts, J. M., … Polyak, K. (2016). Response and resistance to BET bromodomain inhibitors in triple-negative breast cancer. *Nature*, *529*(7586), 1–24. https://doi.org/10.1038/nature16508

Skibinski, A., Breindel, J. L., Prat, A., Galván, P., Smith, E., Rolfs, A., … Kuperwasser, C. (2014). The Hippo Transducer TAZ Interacts with the SWI/SNF Complex to Regulate Breast Epithelial Lineage Commitment. *Cell Reports*, *6*(6), 1059–1072. https://doi.org/10.1016/j.celrep.2014.02.038

Slawson, C., & Hart, G. W. (2011). O-GlcNAc signalling: Implications for cancer cell biology. *Nature Reviews Cancer*, *11*(9), 678–684. https://doi.org/10.1038/nrc3114

Sorrentino, G., Ruggeri, N., Specchia, V., Cordenonsi, M., Mano, M., Dupont, S., …

Del Sal, G. (2014). Metabolic control of YAP and TAZ by the mevalonate pathway. *Nature Cell Biology*, *16*(4), 357–366. https://doi.org/10.1038/ncb2936

Stein, C., Bardet, A. F., Roma, G., Bergling, S., Clay, I., Ruchti, A., … Bauer, A. (2015). YAP1 Exerts Its Transcriptional Control via TEAD-Mediated Activation of Enhancers. *PLOS Genetics*, *11*(8), e1005465. https://doi.org/10.1371/journal.pgen.1005465

Swellam, M., Abdelmaksoud, M. D. E., Sayed Mahmoud, M., Ramadan, A., Abdel-Moneem, W., & Hefny, M. M. (2015). Aberrant methylation of APC and RARβ2 genes in breast cancer patients. *IUBMB Life*, *67*(1), 61–68. https://doi.org/10.1002/iub.1346

Taha, Z., Janse van Rensburg, H. J., & Yang, X. (2018). The hippo pathway: Immunity and cancer. *Cancers*, *10*(4), 1–20. https://doi.org/10.3390/cancers10040094

Totaro, A., Panciera, T., & Piccolo, S. (2018). YAP/TAZ upstream signals and downstream responses. *Nature Cell Biology*, *20*(8), 888–899. https://doi.org/10.1038/s41556-018-0142-z

Tremblay, A. M., & Camargo, F. D. (2012). Hippo signaling in mammalian stem cells. *Seminars in Cell & Developmental Biology*, *23*(7), 818–826. https://doi.org/10.1016/j.semcdb.2012.08.001

Trompouki, E., Bowman, T. V., Lawton, L. N., Fan, Z. P., Wu, D.-C., DiBiase, A., … Zon, L. I. (2011). Lineage Regulators Direct BMP and Wnt Pathways to Cell-Specific Programs during Differentiation and Regeneration. *Cell*, *147*(3), 577–589. https://doi.org/10.1016/j.cell.2011.09.044

Tropberger, P., Pott, S., Keller, C., Kamieniarz-Gdula, K., Caron, M., Richter, F., … Schneider, R. (2013). Regulation of transcription through acetylation of H3K122 on the lateral surface of the histone octamer. *Cell*, *152*(4), 859–872. https://doi.org/10.1016/j.cell.2013.01.032

Varelas, X., Abercrombie, M., Alarcön, C., Zaromytidou, A.-I., Xi, Q., Gao, S., … Yang, X. (2014). The Hippo pathway effectors TAZ and YAP in development, homeostasis and disease. *Development (Cambridge, England)*, *141*(8), 1614–1626. https://doi.org/10.1242/dev.102376

Varelas, X., Samavarchi-Tehrani, P., Narimatsu, M., Weiss, A., Cockburn, K., Larsen, B. G., … Wrana, J. L. (2010). The Crumbs complex couples cell density sensing to Hippo-dependent control of the TGF-β-SMAD pathway. *Developmental Cell*, *19*(6), 831–844. https://doi.org/10.1016/j.devcel.2010.11.012

Villicaña, C., Cruz, G., & Zurita, M. (2014). The basal transcription machinery as a target for cancer therapy. *Cancer Cell International*, *14*, 18. https://doi.org/10.1186/1475-2867-14-18

Wagner, K.-U., Mcallister, K., Ward, T., Davis, B., Wiseman, R., & Hennighausen, L. (2001). Spatial and temporal expression of the Cre gene under the control of the MMTV-LTR in different lines of transgenic mice. *Transgenic Research*, *10*, 545–553. Retrieved from https://link.springer.com/content/pdf/10.1023%2FA%3A1013063514007.pdf

Wagner, K. U., Wall, R. J., St-Onge, L., Gruss, P., Wynshaw-Boris, A., Garrett, L., … Hennighausen, L. (1997). Cre-mediated gene deletion in the mammary gland. *Nucleic Acids Research*, *25*(21), 4323–4330. Retrieved from http://www.ncbi.nlm.nih.gov/pubmed/9336464

Wang, C. Y., & Filippakopoulos, P. (2015). Beating the odds: BETs in disease. *Trends in Biochemical Sciences*, *40*(8), 468–479. https://doi.org/10.1016/j.tibs.2015.06.002

Wang, Z., Wu, Y., Wang, H., Zhang, Y., Mei, L., Fang, X., … Huang, L. (2014). Interplay of mevalonate and Hippo pathways regulates RHAMM transcription via YAP to modulate breast cancer cell motility. *Proceedings of the National Academy of Sciences of the United States of America*, *111*(1), E89–E98. https://doi.org/10.1073/pnas.1319190110

Watkins, J. L., Thaker, P. H., Nick, A. M., Ramondetta, L. M., Kumar, S., Urbauer, D. L., … Sood, A. K. (2015). Clinical impact of selective and nonselective beta-blockers on survival in patients with ovarian cancer. *Cancer*, *121*(19), 3444–3451. https://doi.org/10.1002/cncr.29392

Xu, T., Wang, W., Zhang, S., Stewart, R. A., & Yu, W. (1995). Identifying tumor suppressors in genetic mosaics: the Drosophila lats gene encodes a putative protein kinase. *Development*, *121*(4), 1053–1063. https://doi.org/10.1101/gad.3.9.1273

Yimlamai, D., Christodoulou, C., Galli, G. G., Yanger, K., Pepe-Mooney, B., Gurung, B., … Camargo, F. D. (2014). Hippo Pathway Activity Influences Liver Cell Fate. *Cell*, *157*(6), 1324–1338. https://doi.org/10.1016/j.cell.2014.03.060

Yu, F.-X., Luo, J., Mo, J.-S., Liu, G., Kim, Y. C., Meng, Z., … Guan, K.-L. (2014). Mutant Gq/11 Promote Uveal Melanoma Tumorigenesis by Activating YAP. *Cancer Cell*, *25*(6), 822–830. https://doi.org/10.1016/j.ccr.2014.04.017

Yu, F. X., Zhao, B., Panupinthu, N., Jewell, J. L., Lian, I., Wang, L. H., … Guan, K. L.

(2012). Regulation of the Hippo-YAP pathway by G-protein-coupled receptor signaling. *Cell*, *150*(4), 780–791. https://doi.org/10.1016/j.cell.2012.06.037

Zanconato, F., Battilana, G., Cordenonsi, M., & Piccolo, S. (2016). YAP/TAZ as therapeutic targets in cancer. *Current Opinion in Pharmacology*, *29*, 26–33. https://doi.org/10.1016/j.coph.2016.05.002

Zanconato, F., Cordenonsi, M., & Piccolo, S. (2016). YAP/TAZ at the Roots of Cancer. *Cancer Cell*, *29*(6), 783–803. https://doi.org/10.1016/j.ccell.2016.05.005

Zanconato, F., Forcato, M., Battilana, G., Azzolin, L., Quaranta, E., Bodega, B., … Piccolo, S. (2015). Genome-wide association between YAP/TAZ/TEAD and AP-1 at enhancers drives oncogenic growth. *Nature Cell Biology*, *17*(9), 1218–1227. https://doi.org/10.1038/ncb3216

Zhan, T., Rindtorff, N., & Boutros, M. (2016). Wnt signaling in cancer. *Oncogene*, *36*, 1461. Retrieved from http://dx.doi.org/10.1038/onc.2016.304

Zhang, H., Ramakrishnan, S. K., Triner, D., Centofanti, B., Maitra, D., Győrffy, B., … Shah, Y. M. (2015). Tumor-selective proteotoxicity of verteporfin inhibits colon cancer progression independently of YAP1. *Science Signaling*, *8*(397), ra98. https://doi.org/10.1126/scisignal.aac5418

Zhang, N., Bai, H., David, K. K., Dong, J., Zheng, Y., Cai, J., … Pan, D. (2010). The Merlin/NF2 Tumor Suppressor Functions through the YAP Oncoprotein to Regulate Tissue Homeostasis in Mammals. *Developmental Cell*, *19*(1), 27–38. https://doi.org/10.1016/j.devcel.2010.06.015

Zhang, W., Nandakumar, N., Shi, Y., Manzano, M., Smith, A., Graham, G., … Yi, C. (2014). Downstream of mutant KRAS, the transcription regulator YAP is essential for neoplastic progression to pancreatic ductal adenocarcinoma. *Science Signaling*, *7*(324), ra42. https://doi.org/10.1126/scisignal.2005049

Zhang, W., Prakash, C., Sum, C., Gong, Y., Li, Y., Kwok, J. J. T., … Chin, K. C. (2012). Bromodomain-containing protein 4 (BRD4) regulates RNA polymerase II serine 2 phosphorylation in human CD4+ T cells. *Journal of Biological Chemistry*, *287*(51), 43137–43155. https://doi.org/10.1074/jbc.M112.413047

Zhang, X., Qiao, Y., Wu, Q., Chen, Y., Zou, S., Liu, X., … Sun, F. (2017). The essential role of YAP O-GlcNAcylation in high-glucose-stimulated liver tumorigenesis. *Nature Communications*, *8*(May). https://doi.org/10.1038/ncomms15280

Zhao, B., Wei, X., Li, W., Udan, R. S., Yang, Q., Kim, J., … Guan, K.-L. (2007).

Inactivation of YAP oncoprotein by the Hippo pathway is involved in cell contact inhibition and tissue growth control. *Genes & Development*, *21*(21), 2747–2761. https://doi.org/10.1101/gad.1602907

Zhao, B., Ye, X., Yu, J., Li, L., Li, W., Li, S., … Lin, J. D. (2008). TEAD mediates YAP-dependent gene induction and growth control TEAD mediates YAP-dependent gene induction and growth control. *Genes & Development*, 1962–1971. https://doi.org/10.1101/gad.1664408

Zuo, Q., Liu, J., Huang, L., Qin, Y., Hawley, T., Seo, C., … Yu, Y. (2018). AXL/AKT axis mediated-resistance to BRAF inhibitor depends on PTEN status in melanoma. *Oncogene*, *37*(24), 3275–3289. https://doi.org/10.1038/s41388-018-0205-4

TABLE & FIGURES

Table 1

ChIP-MS for YAP/TAZ

Protein IDs	Gene names	Protein names	Unique peptides			LFQ value		
			IP: YAP	IP: TAZ	IP: IgG	IP: YAP	IP: TAZ	IP: IgG
Q9GZV5	WWTR1; TAZ	WW domain-containing transcription regulator protein 1	7	13	0	9.00E+07	3.00E+09	0
P46937	YAP1	Yes-associated protein 1	3	3	0	2.00E+10	8.00E+09	4.00E+06
P28347	TEAD1;TEAD4	TEF-1, TEF3	2	1	0	1.00E+07	8.00E+07	0
P05412	JUN	Transcription factor AP-1	2	2	0	7.00E+06	5.00E+06	0
Q53GM9	FOSL1	Fos-related antigen 1	1	1	0	2.00E+06	3.00E+06	0
F8VZ70	SMARCD1; SMARCD3	SWI/SNF complex subunit	1	1	0	2.00E+06	3.00E+06	0
O60264	SMARCA5	SWI/SNF complex subunit	2	3	0	4.00E+06	3.00E+06	0
P51532	SMARCA4	Transcription activator BRG1	5	2	0	7.00E+06	2.00E+07	0
Q05BW5	SMARCC1	SWI/SNF complex subunit	3	1	0	3.00E+07	2.00E+07	0
Q59FG6	KMT2D	Histone-lysine N-methyltransferase 2D	1	1	0	1.00E+06	9.00E+06	0
Q96L91	EP400	E1A-binding protein p400	1	2	0	1.00E+06	2.00E+06	0
Q9Y265	RUVBL1	RuvB-like 1	3	2	0	1.00E+07	8.00E+06	0
Q09472	EP300	Histone acetyltransferase p300	2	1	0	6.00E+06	3.00E+06	0
O00422	SAP18	Histone deacetylase complex subunit SAP18	3	2	0	5.00E+07	1.00E+07	0
O60885	BRD4	Bromodomain-containing protein 4	10	2	0	8.00E+07	1.00E+07	0

Figure 1

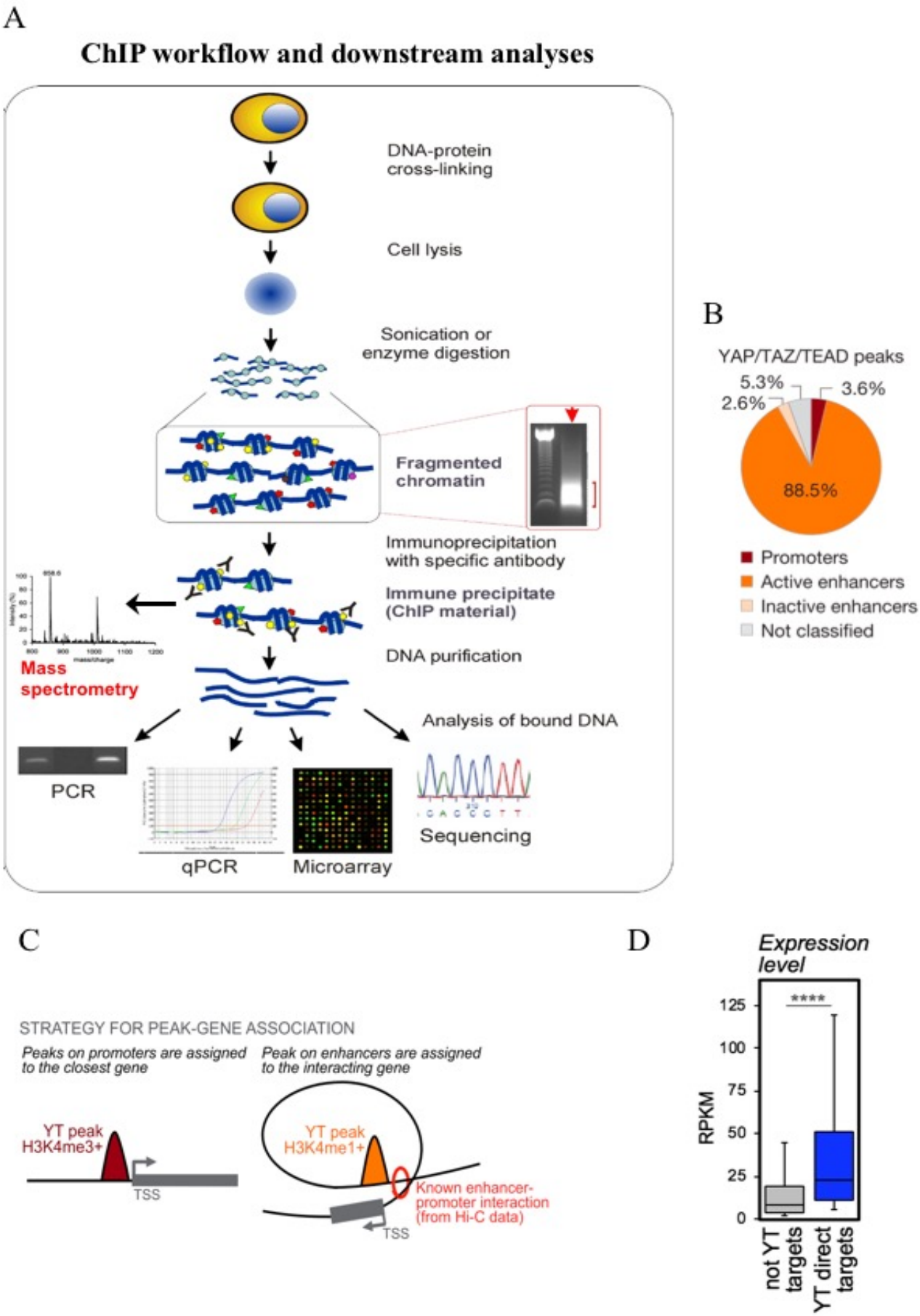
A
ChIP workflow and downstream analyses
DNA-protein cross-linking
Cell lysis
Sonication or enzyme digestion
Fragmented chromatin
Immunoprecipitation with specific antibody
Immune precipitate (ChIP material)
DNA purification
Mass spectrometry
Analysis of bound DNA
PCR
qPCR
Microarray
Sequencing
B
YAP/TAZ/TEAD peaks
5.3%
2.6%
3.6%
88.5%
Promoters
Active enhancers
Inactive enhancers
Not classified
C
STRATEGY FOR PEAK-GENE ASSOCIATION
Peaks on promoters are assigned to the closest gene
Peak on enhancers are assigned to the interacting gene
YT peak H3K4me3+
TSS
YT peak H3K4me1+
Known enhancer-promoter interaction (from Hi-C data)
TSS
D
Expression level
****
RPKM
125
100
75
50
25
0
not YT targets
YT direct targets

Figure 1

a. Schematic representation of Chromatin ImmunoPrecipitation (ChIP) and downstream analyses. Generally speaking Chromatin Immunoprecipitation is a powerful and versatile method to detect interactions between proteins and genomic DNA. Living cells are reversibly crosslinked by formaldehyde, sticking, for example, transcription factors to their DNA binding sites in the genome. Cells are chemically lysed to isolate cells nuclei and these nuclei are then sonicated, in order to obtain chromatin fragments sized from 200 to 600 base pairs through high-frequency sound waves. Specific antibodies are used to immunoprecipitate the protein of interest together with bound DNA fragments. These protein-DNA complexes are then isolated with protein A or G-functionalized magnetic beads (according to the isotype of the antibody of interest). From this step on there are many possibilities: we can purify proteins and identify them by mass spectrometry, in order to find new partners of the bait protein; or we can enrich for DNA fragments and analyse them by qPCR (ChIP-qPCR) or deep sequencing (ChIP-seq), in order to identify the DNA regions bound by the protein of interest. Image modified from: "*Chop it, ChIP it, check it: the current status of chromatin immunoprecipitation." Front. Bioscience 2008 Jan 1;13:929-43. Collas P., Dahl JA.;*
b. Almost 90% of YAP/TAZ binding sites are localized on enhancers in MDA-MB-231 cells; less than 4% of YAP/TAZ binding sites are in close proximity of a promoter (*Zanconato, F., et al. 2015*);
c. Schematic representation of the procedure used to associate YAP/TAZ/TEAD binding sites to their target genes: peaks located on promoters control the transcription of the downstream gene; peaks located on enhancers control the promoters that are in close proximity to the enhancers in the three-dimensional organization of chromatin, due to chromatin looping;
d. Box plot of expression values of YAP/TAZ direct targets (n=616) vs. genes not activated by YAP/TAZ (not YT targets, n=771) in MDA-MB-231 cells. The group of not YT targets represents genes not significantly affected by YAP/TAZ depletion (FDR>0.05) in our RNA-seq dataset. **** p<10-10 (one-tailed Mann-Whitney U test).

Figure 2

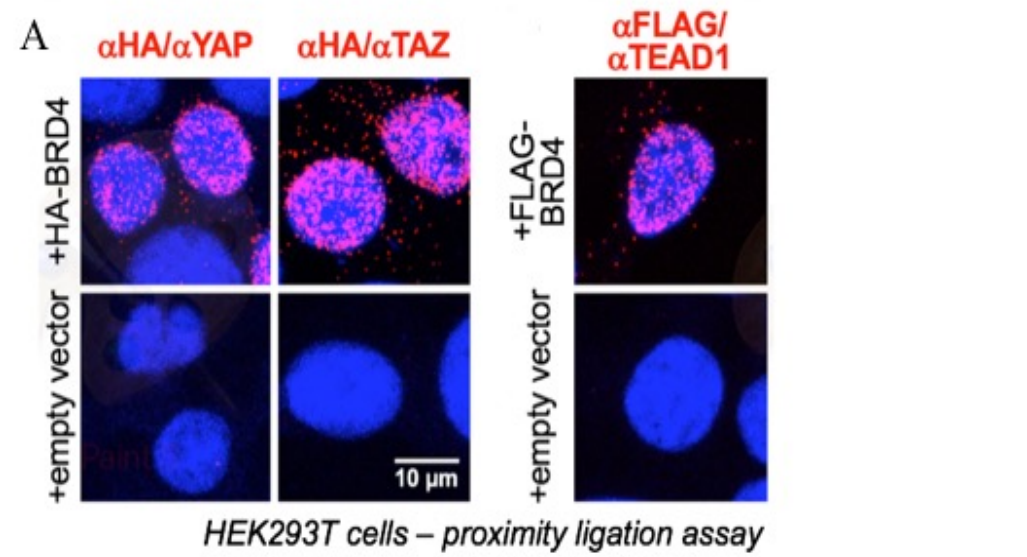
A
αHA/αYAP
αHA/αTAZ
αFLAG/
αTEAD1
+HA-BRD4
+empty vector
+FLAG-
BRD4
+empty vector
10 μm
HEK293T cells – proximity ligation assay

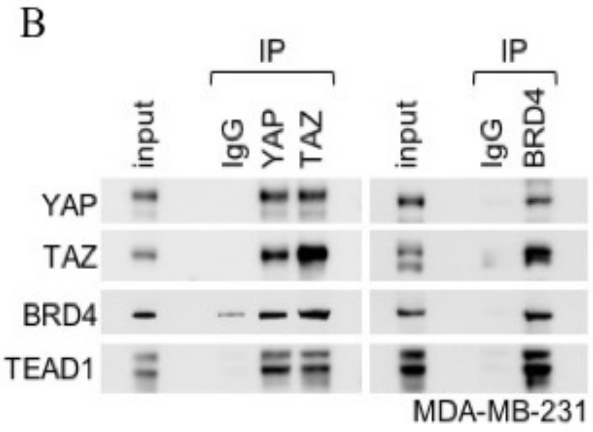
B
IP
IP
input
IgG
YAP
TAZ
input
IgG
BRD4
YAP
TAZ
BRD4
TEAD1
MDA-MB-231

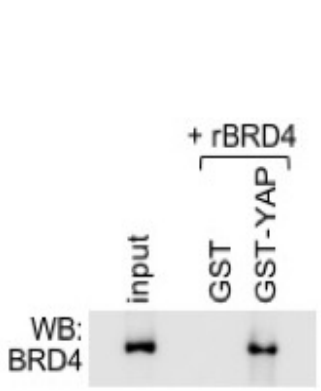
C
+ rBRD4
input
GST
GST-YAP
WB:
BRD4

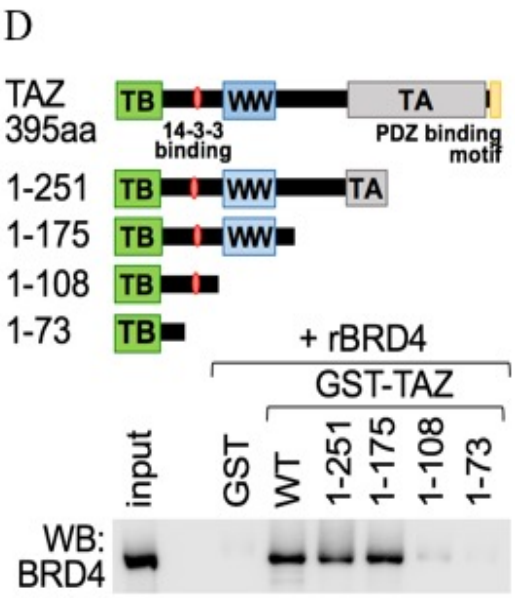
D
TAZ
395aa
TB
WW
TA
14-3-3
binding
PDZ binding
motif
1-251
1-175
1-108
1-73
+ rBRD4
GST-TAZ
input
GST
WT
1-251
1-175
1-108
1-73
WB:
BRD4

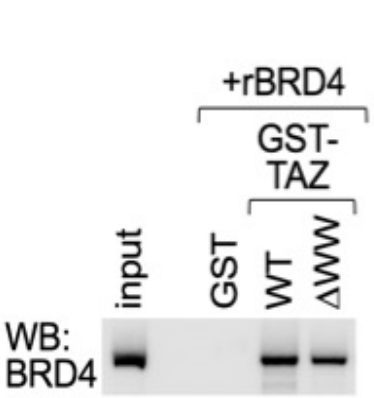
E
+rBRD4
GST-
TAZ
input
GST
WT
ΔWW
WB:
BRD4

Figure 2

a. In situ Proximity ligation assay (PLA) detect the interactions between endogenous YAP, TAZ or TEAD1 and exogenous FLAG- or HA-BRD4 in HEK293T cells. The detected dimers are represented by fluorescent dots (red). Nuclei are counterstained with DAPI (blue). No dots could be detected in the nuclei of cells transfected with empty vector, confirming the specificity of interactions;
b. Immunoprecipitation experiment showing the interaction of endogenous YAP/TAZ, TEAD1 and BRD4 in MDA-MB-231 cells;
c. Western blot showing recombinant BRD4 (rBRD4) pulled-down by GST-YAP fusion protein;
d. Schematic representation of the TAZ constructs here used, and immunoblot of recombinant BRD4 pulled-down by the indicated GST-TAZ constructs. TB: TEAD binding domain; TA: Transcriptional Activation domain; WW: WW protein domain.
e. Recombinant BRD4 is pulled-down by GST-TAZ even after deletion of the WW domain (△WW).

Figure 3

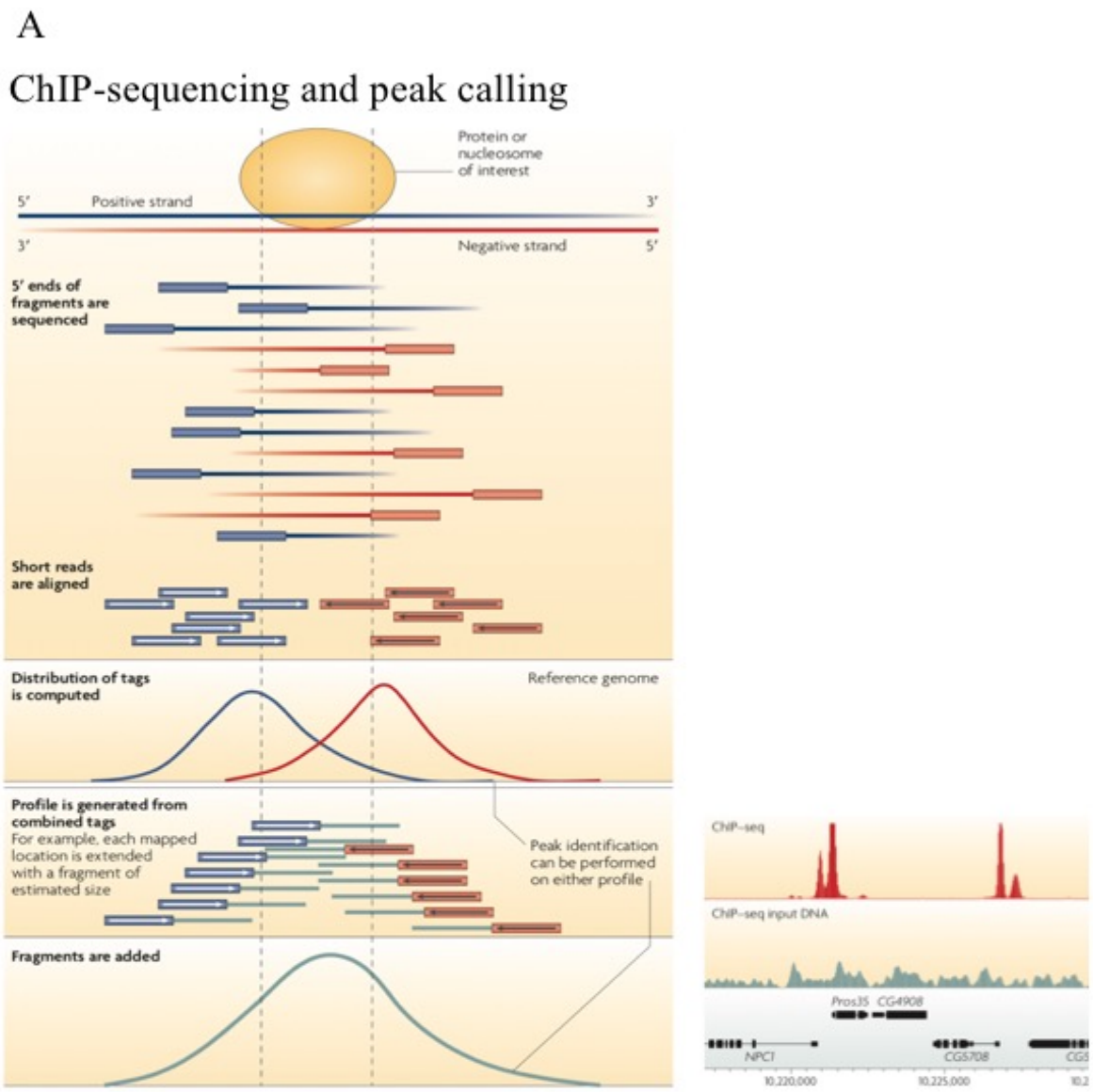
A
ChIP-sequencing and peak calling
Protein or nucleosome of interest
5′
Positive strand
3′
3′
Negative strand
5′
5′ ends of fragments are sequenced
Short reads are aligned
Distribution of tags is computed
Reference genome
Profile is generated from combined tags
For example, each mapped location is extended with a fragment of estimated size
Peak identification can be performed on either profile
Fragments are added
ChIP–seq
ChIP–seq input DNA
Pros35
CG4908
NPC1
CG5708
10,220,000
10,225,000

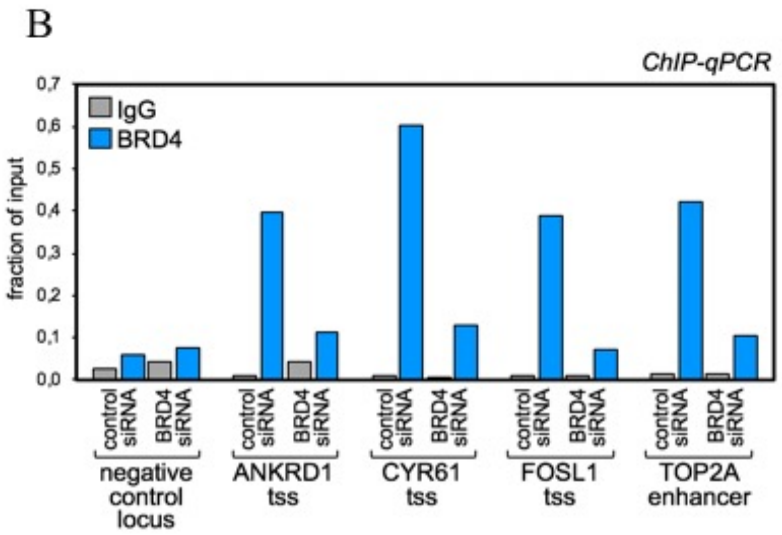
B
ChIP-qPCR
IgG
BRD4
fraction of input
0,7
0,6
0,5
0,4
0,3
0,2
0,1
0,0
control siRNA
BRD4 siRNA
negative control locus
ANKRD1 tss
CYR61 tss
FOSL1 tss
TOP2A enhancer

Figure 3

a. Schematic representation of ChIP-sequencing steps, peak calling and an example of a resulting peak from*: Park, P. J. (2009). ChIP–seq: advantages and challenges of a maturing technology. Nature Reviews Genetics, 10(10), 669–680;* Purified DNA fragments, derived from the immunoprecipitation with a candidate antibody, are processed to generate a sequencing library, ligation of "adapter sequences", amplification and size selection. Then, the DNA library is hybridized to the sequencing flowcell and amplified by bridge PCR to generate the template for sequencing. Short reads (50 base pairs) from one end of the fragments are generated. The recommended sequencing depth is ~20 mln uniquely mapping reads/sample; an increased depth of coverage allows the detection of more sites that have lower levels of enrichment over the genomic background. Uniquely mapping sequences are then aligned to the entire reference genome and the alignment of sequenced tags to the genome results in two peaks (one for the positive and one for the negative DNA strands) flanking the point where the protein of interest is bound. These two strand-specific peaks of tags are combined to generate an approximate profile of fragment distribution. Then, a "peak caller" algorithm scans the genome to identify regions that are significantly enriched in the ChIP sample compared to the experimental control. The final outcome consists in a list of genome locations that represent likely binding sites of the protein of interest. Image from: *Schmidt, D., et al., 2009. ChIP-seq: using high-throughput sequencing to discover protein-DNA interactions. 48(3), 240–248;*
b. ChIP-qPCR showing the specificity of anti-BRD4 antibody, performed in control (control siRNA) or BRD4 depleted (BRD4 siRNA) MDA-MB-231 cells. ChIP with pre-immune IgG displayed background signal. DNA enrichment was calculated as fraction of input.

Figure 4

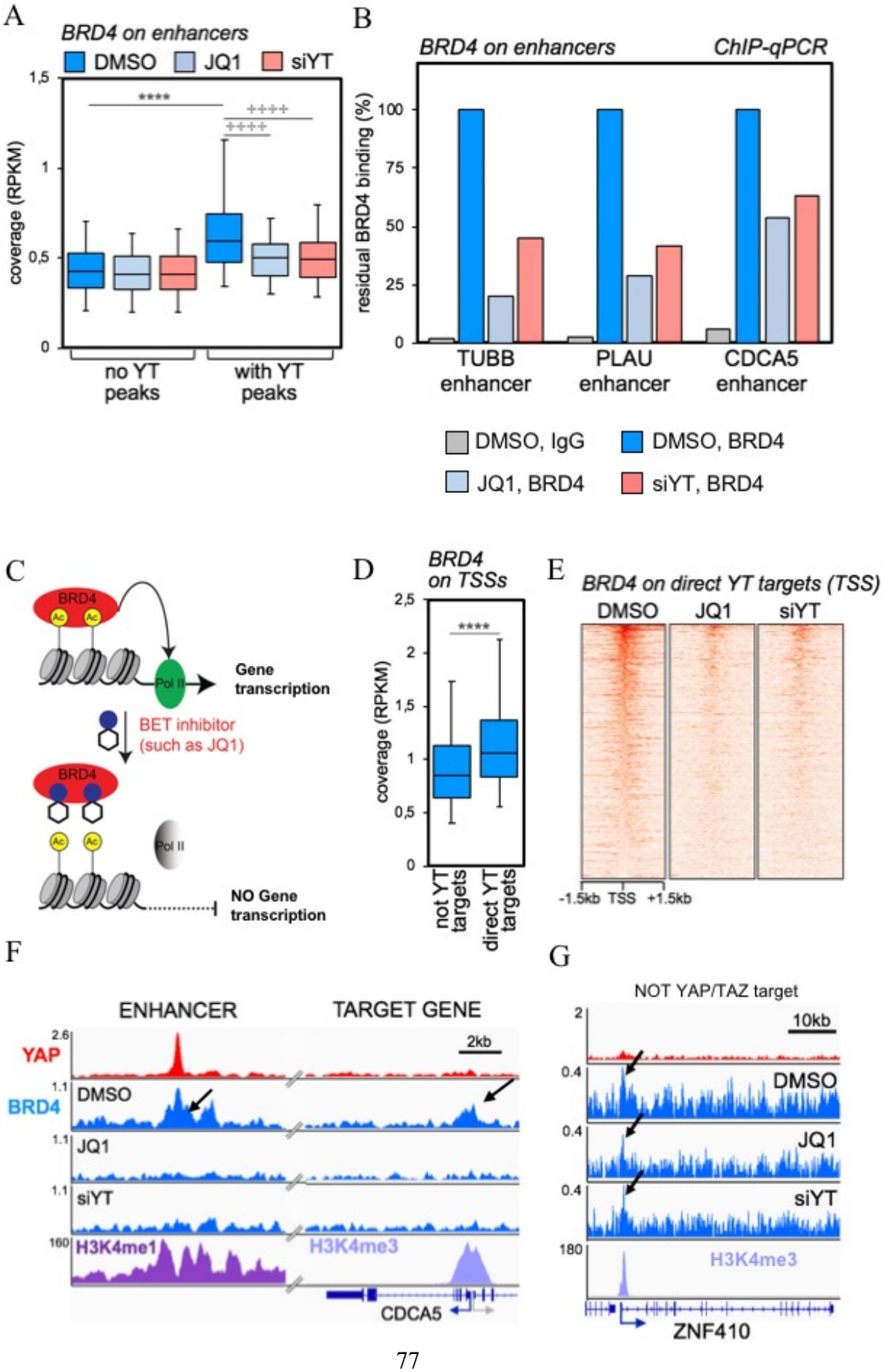
A
BRD4 on enhancers
DMSO
JQ1
siYT
coverage (RPKM)
no YT peaks
with YT peaks
B
BRD4 on enhancers
ChIP-qPCR
residual BRD4 binding (%)
TUBB enhancer
PLAU enhancer
CDCA5 enhancer
DMSO, IgG
DMSO, BRD4
JQ1, BRD4
siYT, BRD4
C
BRD4
Pol II
Gene transcription
BET inhibitor (such as JQ1)
NO Gene transcription
D
BRD4 on TSSs
coverage (RPKM)
not YT targets
direct YT targets
E
BRD4 on direct YT targets (TSS)
DMSO
JQ1
siYT
-1.5kb TSS +1.5kb
F
ENHANCER
TARGET GENE
YAP
BRD4
DMSO
JQ1
siYT
H3K4me1
H3K4me3
CDCA5
2kb
G
NOT YAP/TAZ target
10kb
DMSO
JQ1
siYT
H3K4me3
ZNF410

Figure 4

a. Box plot showing the distribution of BRD4 ChIP-seq signal (expressed as normalized read density, RPKM) comparing active enhancers with or without YAP/TAZ peaks in MDA-MB-231 cells treated with DMSO or JQ1 (1μM, 6h), or transfected with YAP/TAZ siRNAs (48h). **** p<10-10 (one-tailed Mann-Whitney U test); ++++ p<10-10 (one-tailed Wilcoxon matched-pairs signed rank test);
b. Validation by ChIP-qPCR of BRD4 detachment from enhancers containing YAP/TAZ peaks in MDA-MB-231 cells upon treatment with JQ1 or YAP/TAZ depletion. ChIP with pre-immune IgG displayed only background signal, which was comparable throughout samples and is shown for control cells only (DMSO). DNA enrichment was calculated as fraction of input and is presented as % of BRD4 binding in control cells (DMSO);
c. Cartoon showing the mechanism by which JQ1 detach BRD4 from chromatin preventing downstream gene transcription, modified from: *Zhu, H., et al,. (2016). BET Bromodomain Inhibition Promotes Anti-tumor Immunity by Suppressing PD-L1 Expression. Cell Reports, 16(11), 2829–2837.*
d. Box plot showing the distribution of BRD4 ChIP-seq signal (RPKM) comparing promoters of genes not activated by YAP/TAZ vs. YAP/TAZ target genes (YT targets) in MDA-MB-231 cells (treated with DMSO). **** p<10-10 (one-tailed Mann-Whitney U test);
e. Heatmap showing BRD4 binding on promoters of YAP/TAZ targets in MDA-MB-231 cells, treated with DMSO, JQ1 (1μM, 6h), or transfected with YAP/TAZ siRNAs (48h), in a window of ±1.5kb centred on the transcription start site (TSS);
f. Individual gene tracks of YAP, BRD4 and H3K4me1/H3K4me3 binding profiles on a distal enhancer and on CDCA5 promoter. JQ1 (1μM, 6h) and siYAP/TAZ (48h) induce a strong decrease in BRD4 binding both on the enhancer, containing YAP/TAZ peak, and on TSS of CDCA5.
g. Individual gene track of YAP, BRD4 and H3K4me3 binding profiles on ZNF410 (Not YAP/TAZ target) promoter. JQ1 (1μM, 6h) and siYAP/TAZ (48h) do not alter BRD4 binding on TSS of ZNF410.

Figure 5

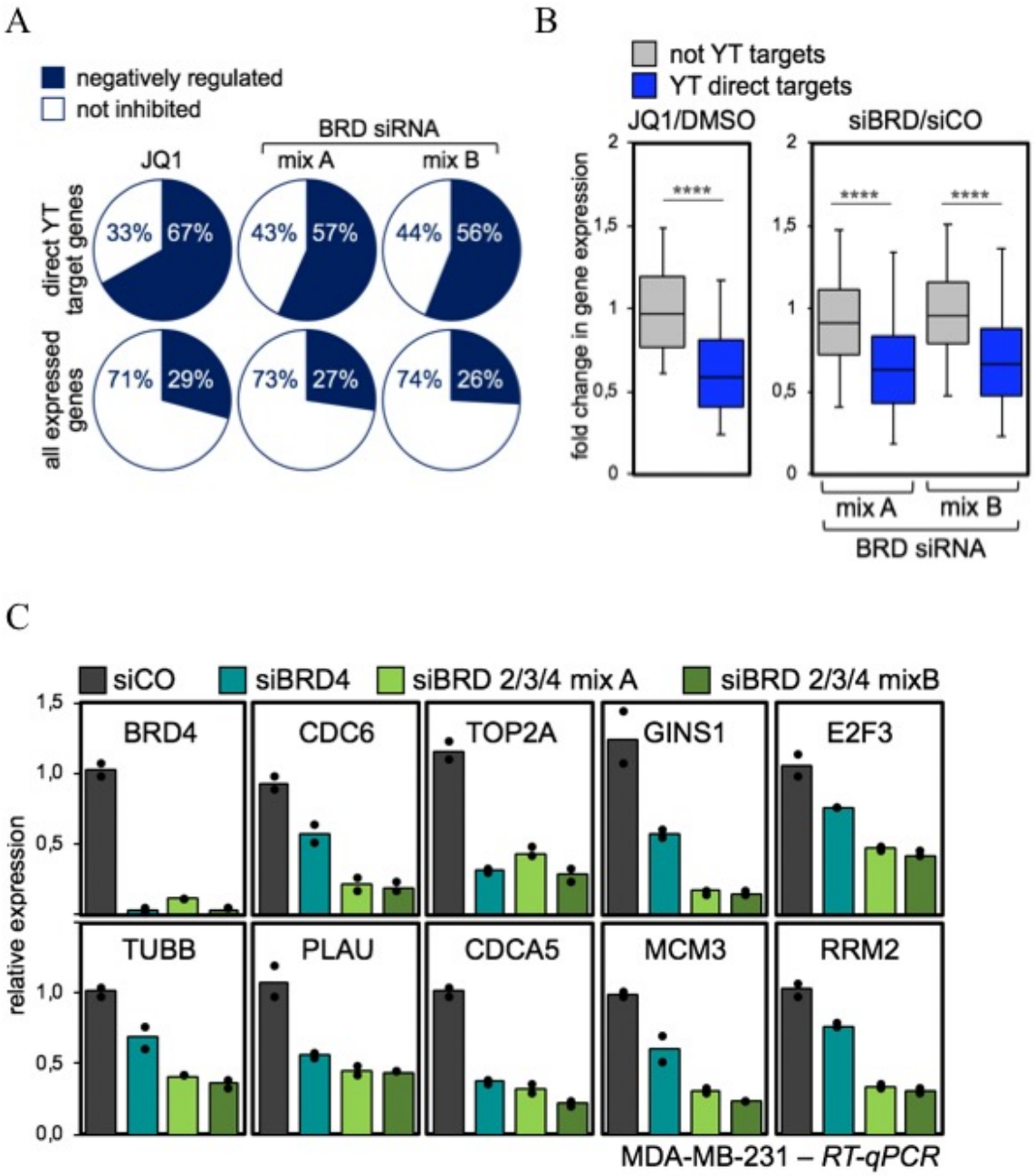
A
negatively regulated
not inhibited
BRD siRNA
JQ1
mix A
mix B
direct YT target genes
all expressed genes
33%
67%
43%
57%
44%
56%
71%
29%
73%
27%
74%
26%
B
not YT targets
YT direct targets
JQ1/DMSO
siBRD/siCO
fold change in gene expression
****
mix A
mix B
BRD siRNA
C
siCO
siBRD4
siBRD 2/3/4 mix A
siBRD 2/3/4 mixB
BRD4
CDC6
TOP2A
GINS1
E2F3
TUBB
PLAU
CDCA5
MCM3
RRM2
relative expression
MDA-MB-231 – RT-qPCR

Figure 5

a. Diagrams showing that the fraction of YAP/TAZ direct targets genes which are inhibited by JQ1 or BRD2/3/4 siRNAs is larger than the fraction of all expressed genes downregulated in the same experimental conditions;
b. Box plots showing fold change in gene expression of high-confidence YAP/TAZ direct targets (n=616) vs. not-YAP/TAZ targets (n=771) upon treatment with JQ1 (left) or depletion of BET proteins (right). The group of not YT targets contains genes not significantly affected by YAP/TAZ depletion (FDR>0.05) in our RNA-seq dataset. **** p<10-10 (one-tailed Mann-Whitney U test);
c. RT-qPCR for a set of YAP/TAZ target genes, showing downregulation upon depletion of BRD4 alone (siBRD4) or BRD2/3/4 (siBRD mix A and B). Data are presented as individual data points + average (bar);

Figure 6

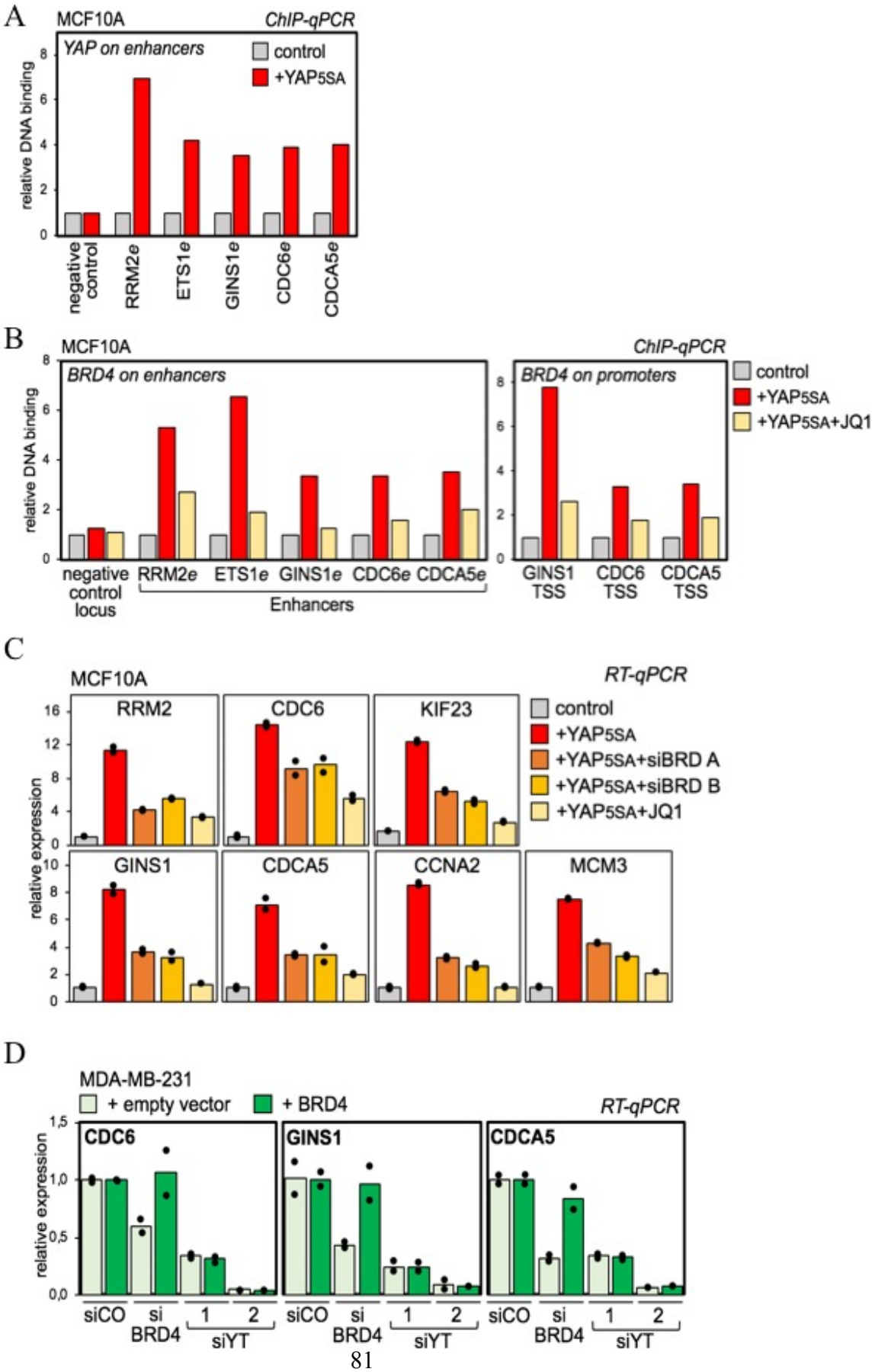
A
MCF10A
ChIP-qPCR
YAP on enhancers
control
+YAP5SA
relative DNA binding
negative control
RRM2e
ETS1e
GINS1e
CDC6e
CDCA5e
B
MCF10A
ChIP-qPCR
BRD4 on enhancers
BRD4 on promoters
control
+YAP5SA
+YAP5SA+JQ1
relative DNA binding
negative control locus
RRM2e
ETS1e
GINS1e
CDC6e
CDCA5e
Enhancers
GINS1 TSS
CDC6 TSS
CDCA5 TSS
C
MCF10A
RT-qPCR
RRM2
CDC6
KIF23
GINS1
CDCA5
CCNA2
MCM3
control
+YAP5SA
+YAP5SA+siBRD A
+YAP5SA+siBRD B
+YAP5SA+JQ1
relative expression
D
MDA-MB-231
+ empty vector
+ BRD4
RT-qPCR
CDC6
GINS1
CDCA5
relative expression
siCO
si BRD4
1
2
siYT

Figure 6

a. ChIP-qPCR verifying YAP binding at enhancers of YAP/TAZ target genes in YAP5SA-overexpressing MCF10A cells. DNA enrichment was calculated as fraction of input and is presented as fold vs. control cells. ChIP with pre-immune IgG displayed background signal and is not shown;
b. ChIP-qPCR showing increased BRD4 binding on enhancers and promoters of YAP/TAZ targets upon YAP5SA overexpression in MCF10A cells, but not in the presence of JQ1 (1μM, 6h). ChIP with pre-immune IgG displayed background signal (which was comparable in all samples). DNA enrichment was calculated as fraction of input and is presented as fold vs. BRD4 binding in control cells;
c. RT-qPCR for representative YAP/TAZ target genes showing upregulation upon YAP5SA overexpression in MCF10A cells, but not in the presence of JQ1 (1μM, 24h) or upon depletion of BRD2/3/4 (siBRD mix A and B). Data are presented as individual data points + average (bar);
d. RT-qPCR showing that sustained expression of human BRD4 does not rescue the expression of YAP/TAZ target genes in MDA-MB-231 cells upon depletion of YAP/TAZ. Exogenous BRD4, instead, can rescue the expression of the same genes after depletion of endogenous BRD4. Data are presented as individual data points + average (bar).

Figure 7

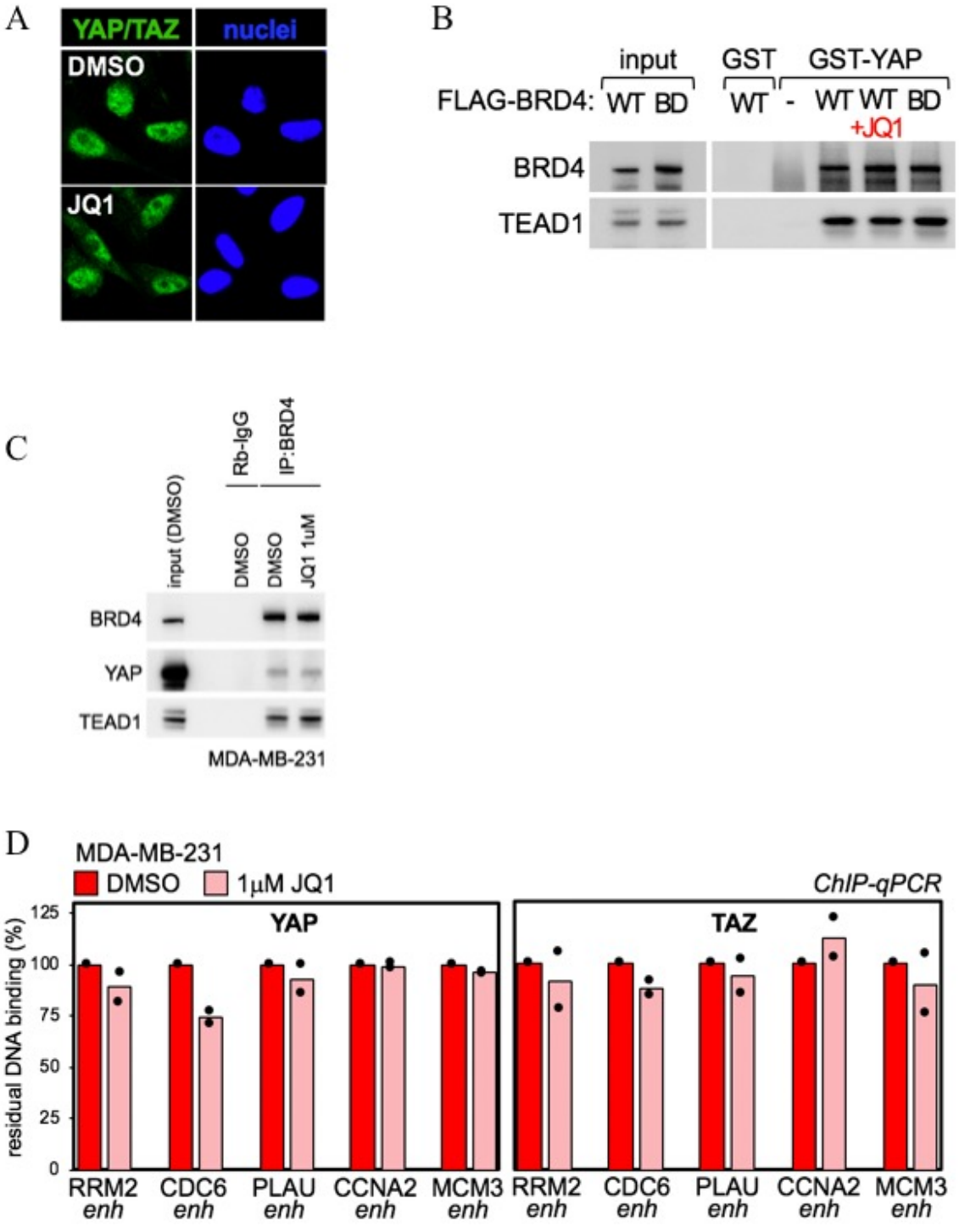
A
YAP/TAZ
nuclei
DMSO
JQ1
B
input
GST
GST-YAP
FLAG-BRD4:
WT BD
WT
-
WT WT BD
+JQ1
BRD4
TEAD1
C
Rb-IgG
IP:BRD4
input (DMSO)
DMSO
DMSO
JQ1 1uM
BRD4
YAP
TEAD1
MDA-MB-231
D
MDA-MB-231
DMSO
1μM JQ1
ChIP-qPCR
YAP
TAZ
residual DNA binding (%)
125
100
75
50
25
0
RRM2 enh
CDC6 enh
PLAU enh
CCNA2 enh
MCM3 enh
RRM2 enh
CDC6 enh
PLAU enh
CCNA2 enh
MCM3 enh

Figure 7

a. Representative confocal images for YAP/TAZ Immunofluorescence (IF) staining in MDA-MB-231 cells upon treatment with JQ1 (1μM, 24h). Nuclei were counterstained with DAPI. Scale bar is 20 μm.
b. GST pull-down assay showing that GST-YAP interacts with FLAG-BRD4 (in nuclear extracts of HEK293T cells) even in the presence of JQ1 or upon mutation of BRD4 bromodomains. Similar results were obtained with GST-TAZ (data not shown). WT=wild type; BD=BD-mutant;
c. YAP and TEAD1 co-immunoprecipitation with BRD4 in MDA-MB-231 cells also in presence of JQ1;
d. ChIP-qPCR showing that YAP and TAZ binding at enhancers is not affected by JQ1 in MDA-MB-231 cells. ChIP with pre-immune IgG displayed only background signal. DNA enrichment was calculated as fraction of input and is presented as % of YAP or TAZ binding in control cells (DMSO);

Figure 8

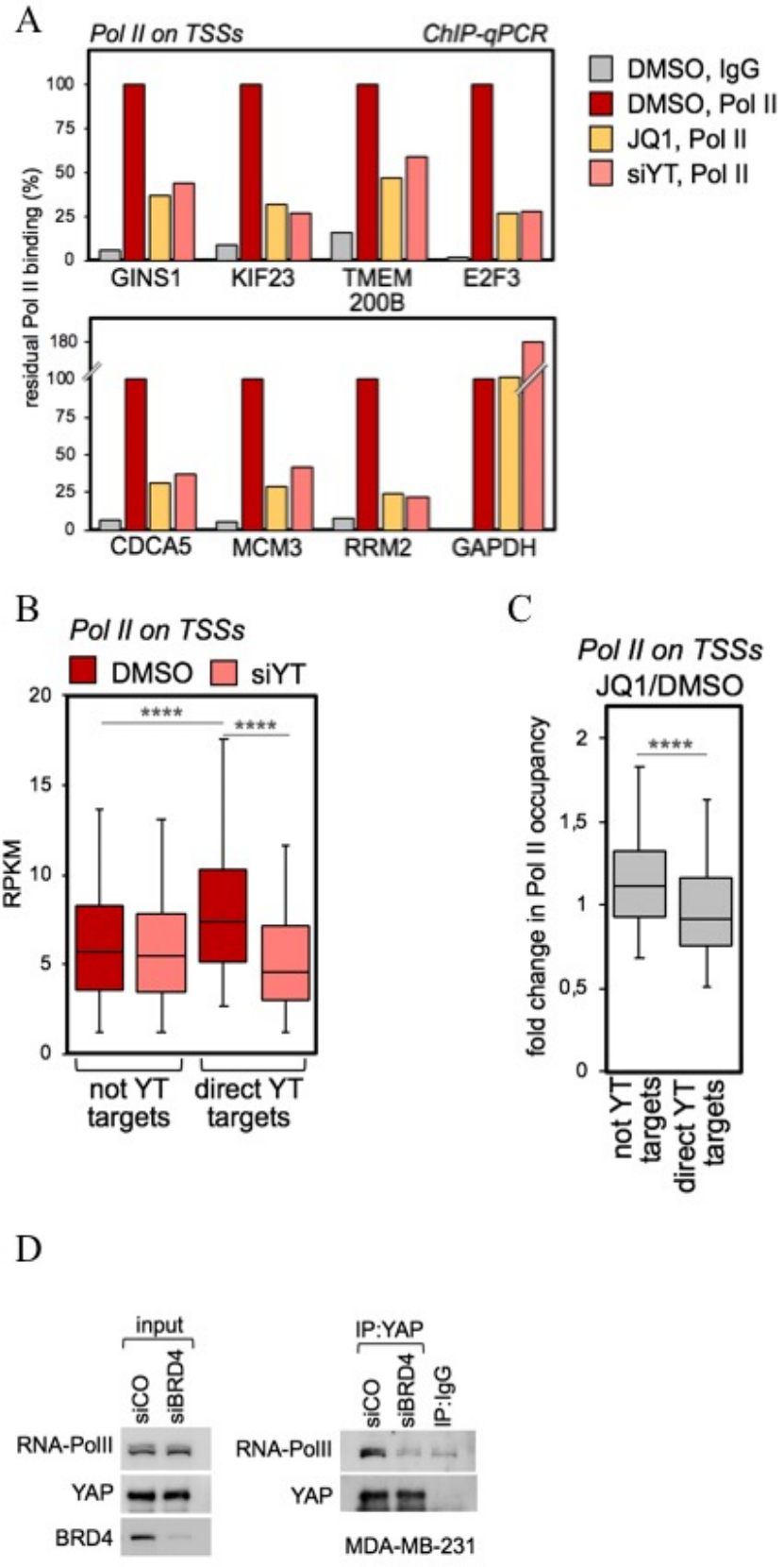
A
Pol II on TSSs
ChIP-qPCR
DMSO, IgG
DMSO, Pol II
JQ1, Pol II
siYT, Pol II
residual Pol II binding (%)
GINS1
KIF23
TMEM 200B
E2F3
CDCA5
MCM3
RRM2
GAPDH
B
Pol II on TSSs
DMSO
siYT
RPKM
****
****
not YT targets
direct YT targets
C
Pol II on TSSs
JQ1/DMSO
fold change in Pol II occupancy
****
not YT targets
direct YT targets
D
input
IP:YAP
siCO
siBRD4
IP:IgG
RNA-PolII
YAP
BRD4
MDA-MB-231

Figure 8

a. ChIP-qPCR showing decreased RNA-Pol II binding to promoters of established YAP/TAZ targets in MDA-MB-231 cells treated with JQ1 (1μM, 24h), or transfected with YAP/TAZ siRNAs (48h). GAPDH promoter represents a non-YAP/TAZ target. ChIP with pre-immune IgG displayed background signal (which was comparable in all samples). DNA enrichment was calculated as fraction of input and is presented as % of RNA-Pol II binding in control cells (DMSO);
b. Box plot showing the distribution of RNA-Pol II ChIP-seq signal (expressed as normalized read density, RPKM) comparing promoters of genes not activated by YAP/TAZ with YAP/TAZ target genes in control (DMSO) or YAP/TAZ depleted cells. **** p<10-10 (one-tailed Mann-Whitney U test);
c. Box plots showing the fold change in RNA-Pol II occupancy on the TSS in JQ1-treated cells vs. control cells (DMSO), comparing promoters of genes not activated by YAP/TAZ with promoters of YAP/TAZ target genes. **** p<10-10 (one-tailed Mann-Whitney U test);
d. Western blot showing RNA-PolII in immunocomplexes of endogenous YAP in MDA-MB-231 nuclear extracts. The interaction is weaker upon depletion of BRD4.

Figure 9

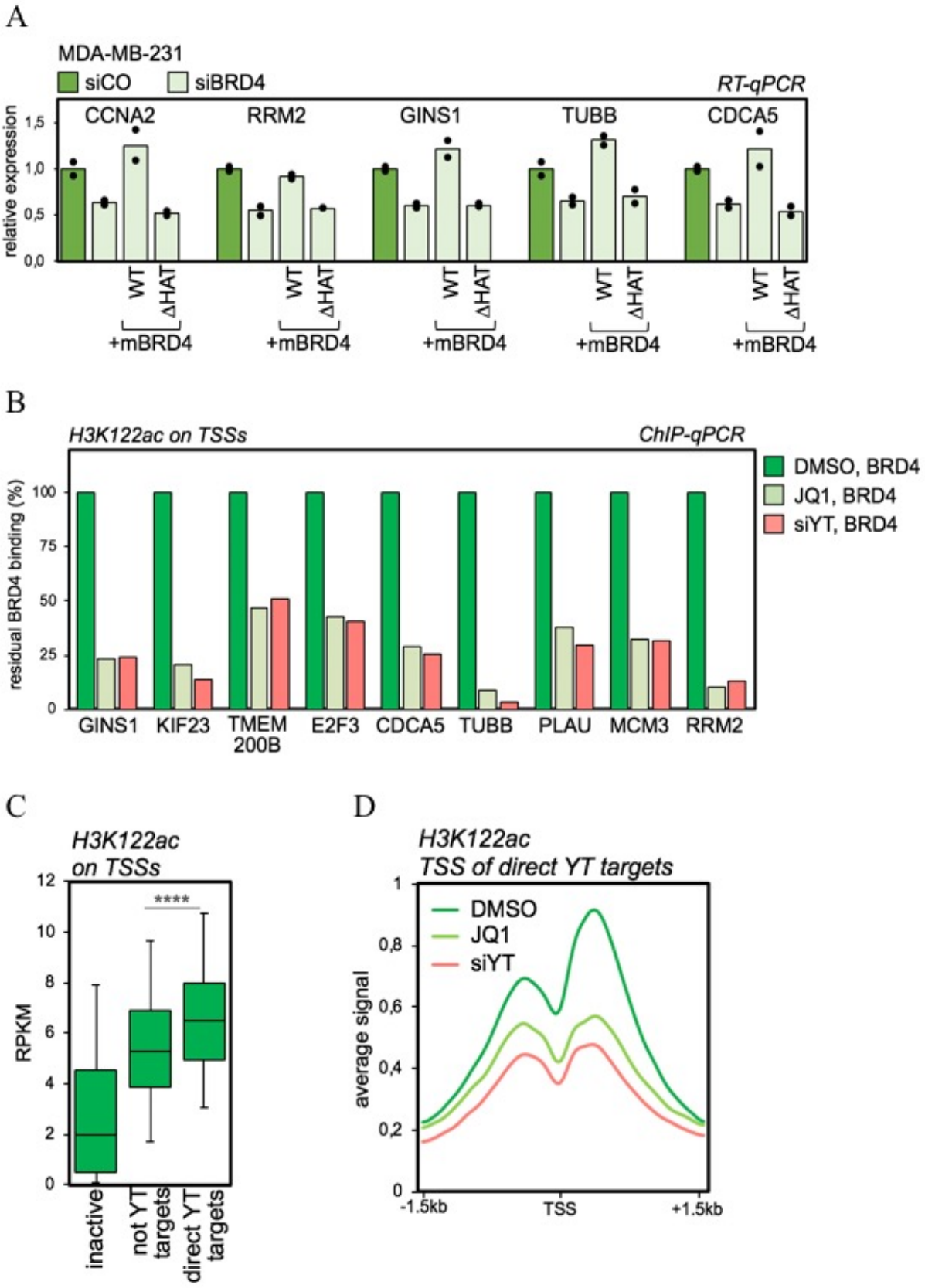
A
MDA-MB-231
siCO
siBRD4
RT-qPCR
relative expression
CCNA2
RRM2
GINS1
TUBB
CDCA5
WT
ΔHAT
+mBRD4
B
H3K122ac on TSSs
ChIP-qPCR
residual BRD4 binding (%)
DMSO, BRD4
JQ1, BRD4
siYT, BRD4
GINS1
KIF23
TMEM 200B
E2F3
CDCA5
TUBB
PLAU
MCM3
RRM2
C
H3K122ac on TSSs
RPKM
****
inactive
not YT targets
direct YT targets
D
H3K122ac TSS of direct YT targets
average signal
DMSO
JQ1
siYT
-1.5kb
TSS
+1.5kb

Figure 9

a. RT-qPCR showing that sustained expression of mouse BRD4 deficient in HAT activity (ΔHAT) does not rescue the expression of a set of YAP/TAZ target genes in MDA-MB-231 cells depleted of endogenous BRD4 (siBRD4). Exogenous wild-type mouse BRD4 (WT), instead, can rescue the expression of the same genes. Data are presented as individual data points + average (bar);
b. ChIP-qPCR showing H3K122ac levels on the promoters of established YAP/TAZ targets in MDA-MB-231 cells, treated with DMSO or JQ1 (1μM, 24h), or transfected with YAP/TAZ siRNAs (48h). DNA enrichment was calculated as fraction of input and is presented as % H3K122ac level in control cells (DMSO).
c. Box plot of H3K122ac ChIP-seq signal (RPKM) on TSS showing an enrichment on YAP/TAZ target genes in comparison with inactive promoters and not-YAP/TAZ targets. **** p<10-10 (one-tailed Mann-Whitney U test);
d. Average ChIP-seq profile of H3K122ac on the promoters of YAP/TAZ target genes in MDA-MB-231 cells, in control cells (DMSO), JQ1 (1μM, 24h) treated cells or after the depletion of YAP/TAZ, in a window of ±1.5 kb centered on TSS.

Figure 10

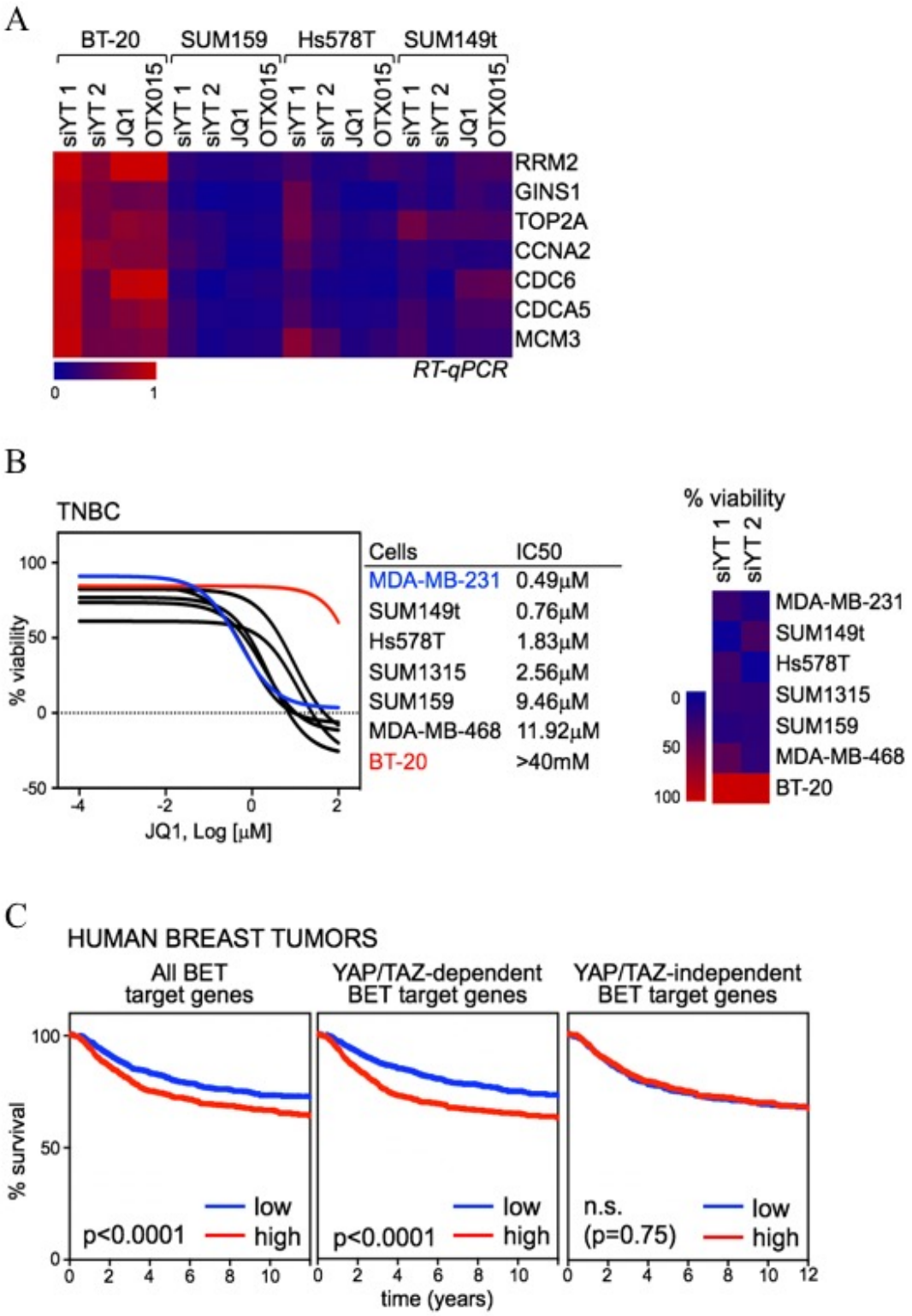
A
BT-20
SUM159
Hs578T
SUM149t
siYT 1
siYT 2
JQ1
OTX015
RRM2
GINS1
TOP2A
CCNA2
CDC6
CDCA5
MCM3
RT-qPCR
0
1
B
TNBC
% viability
JQ1, Log [μM]
Cells
IC50
MDA-MB-231 0.49μM
SUM149t 0.76μM
Hs578T 1.83μM
SUM1315 2.56μM
SUM159 9.46μM
MDA-MB-468 11.92μM
BT-20 >40mM
% viability
siYT 1
siYT 2
MDA-MB-231
SUM149t
Hs578T
SUM1315
SUM159
MDA-MB-468
BT-20
C
HUMAN BREAST TUMORS
All BET target genes
YAP/TAZ-dependent BET target genes
YAP/TAZ-independent BET target genes
% survival
p<0.0001
p<0.0001
n.s.
(p=0.75)
low
high
time (years)

Figure 10

a. Heat map showing the regulation of YAP/TAZ target genes in triple negative breast cancer cells after YAP/TAZ depletion (siYT1, siYT2) or treatment with BET inhibitors (1μM, 24h). Expression values are normalized to cells transfected with control siRNA and to GAPDH.
b. Left: viability curves of different TNBC cells treated with increasing doses of JQ1 (1nM to 100μM) and corresponding IC50. Data are mean of 8 replicates. Right: Heat map showing the % reduction in viability of the same TNBC cell lines. Cells sensitive to JQ1 are also affected by YAP/TAZ depletion, whereas the proliferation of BT20 cells is unaffected by both conditions;
c. Kaplan–Meier graph representing the probability of metastasis-free survival in breast cancer patients, stratified according to high or low expression of all BET target genes. Survival curves have prognostic value only when patients are stratified according to the signature of common YAP/TAZ/BET targets, but not when patients are stratified according to the expression of BET-only targets (Log-rank Mantel Cox Test).

Figure 11

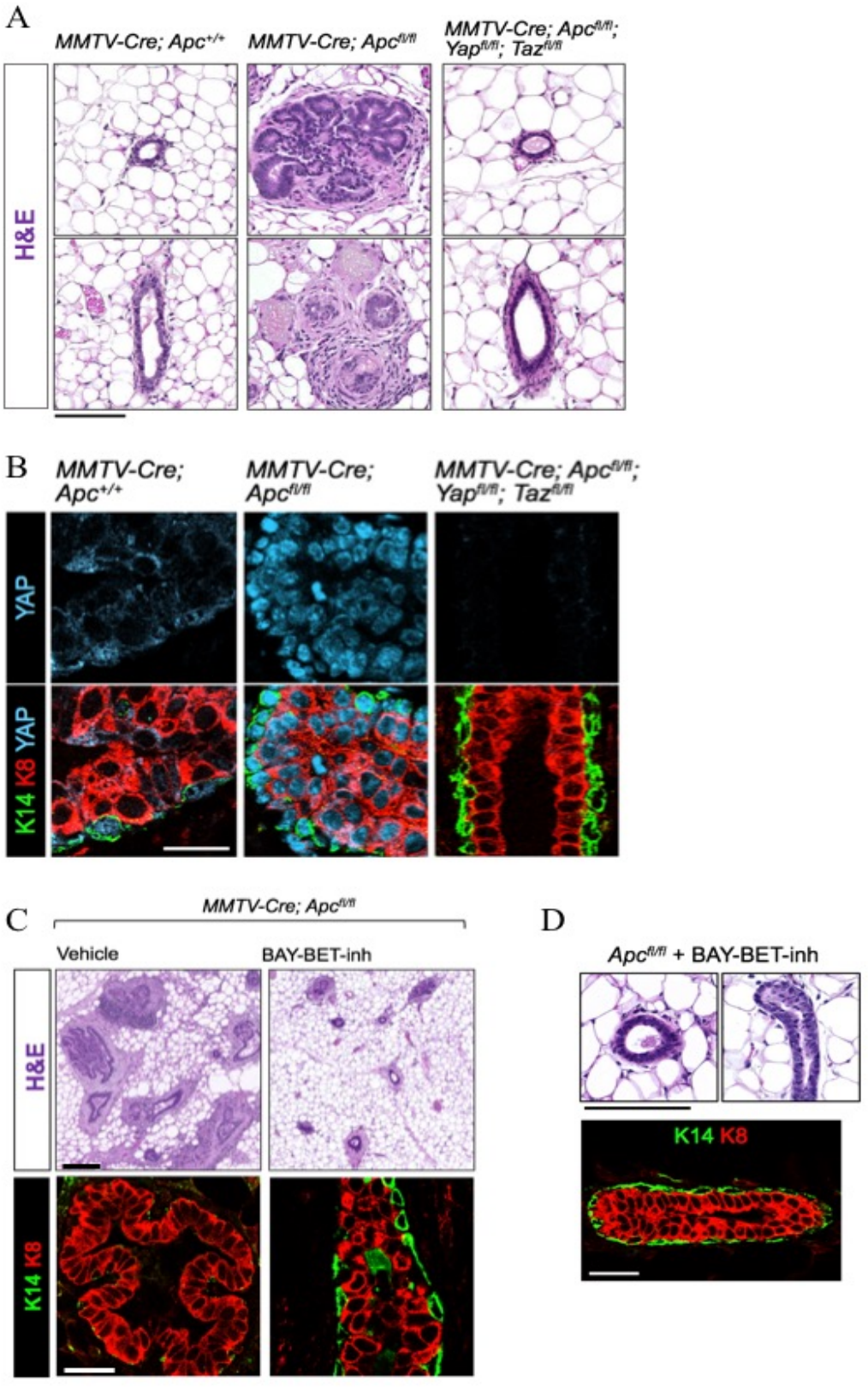
A
MMTV-Cre; Apc+/+
MMTV-Cre; Apcfl/fl
MMTV-Cre; Apcfl/fl; Yapfl/fl; Tazfl/fl
H&E
B
MMTV-Cre; Apc+/+
MMTV-Cre; Apcfl/fl
MMTV-Cre; Apcfl/fl; Yapfl/fl; Tazfl/fl
YAP
K14 K8 YAP
C
MMTV-Cre; Apcfl/fl
Vehicle
BAY-BET-inh
H&E
K14 K8
D
Apcfl/fl + BAY-BET-inh
K14 K8

Figure 11

a. Representative hematoxylin and eosin (H&E) staining of sections of mammary glands from MMTV-Cre;$Apc^{+/+}$, MMTV-Cre;$Apc^{fl/fl}$, or MMTV-Cre;$Apc^{fl/fl}$;$Yap^{fl/fl}$;$Taz^{fl/fl}$ mice. Scale bar is 0.1 mm;
b. Representative immunofluorescence (IF) pictures of mammary glands from the indicated mice, showing YAP accumulation and K14 discontinuities in MMTV-Cre;$Apc^{fl/fl}$. Ducts of MMTV-Cre;$Apc^{fl/fl}$;$Yap^{fl/fl}$;$Taz^{fl/fl}$ mice display a normal morphology. Scale bar is 25 μm;
c. Up: Representative H&E staining of mammary glands sections from MMTV-Cre;$Apc^{fl/fl}$ mice, treated with vehicle (n=3) or BAY-BET inhibitor (n=3) for 6 weeks. BET inhibitor restores normal mammary morphology. All scale bars are 0.1mm. Low: Representative IF pictures of mammary glands from MMTV-Cre;$Apc^{fl/fl}$ mice, treated with vehicle or BAY-BET inhibitor for 6 weeks, showing that treatment with BET inhibitor restores normal distribution of K8 and K14 in the mammary ducts. Scale bars are 25 μm.
d. Up: representative H&E staining of sections of mammary glands from $Apc^{fl/fl}$ mice, treated with BAY-BET inhibitor, showing that mammary ducts maintain a normal morphology. Scale bar is 0.1mm. Low: representative immunofluorescence (IF) pictures of mammary glands from $Apc^{fl/fl}$ mice treated with BAY-BET inhibitor, showing normal distribution of K8 and K14 in the mammary ducts. Scale bar is 25 μm.

Figure 12

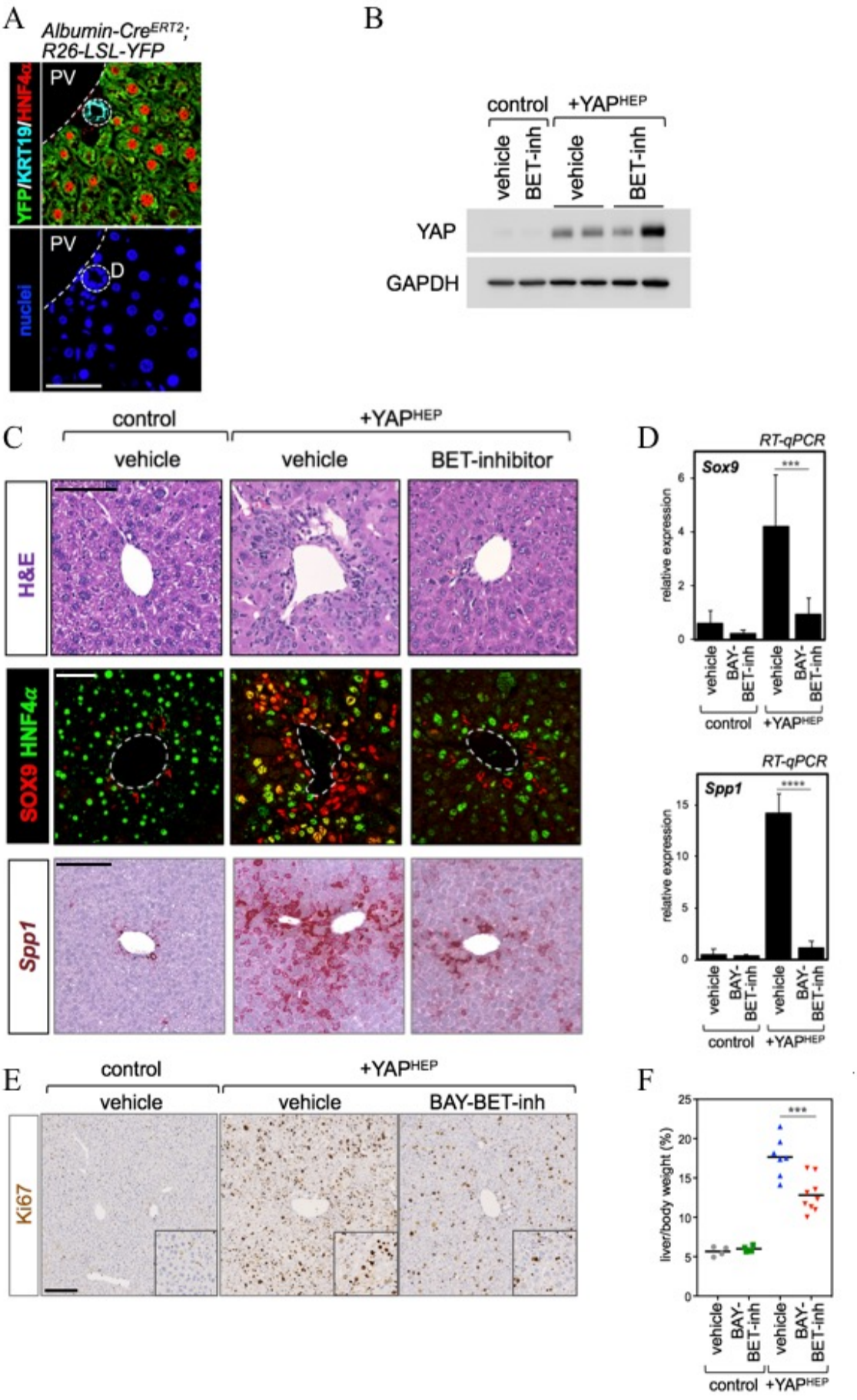
A
Albumin-Cre^ERT2; R26-LSL-YFP
YFP/KRT19/HNF4α
PV
nuclei
D
B
control
+YAP^HEP
vehicle
BET-inh
YAP
GAPDH
C
control
+YAP^HEP
vehicle
BET-inhibitor
H&E
SOX9 HNF4α
Spp1
D
RT-qPCR
Sox9
relative expression
BAY-BET-inh
E
BAY-BET-inh
Ki67
F
liver/body weight (%)

Figure 12

a. Representative IF showing that AlbuminCreERT2 drives the excision of the LSL cassette upstream of the YFP reporter specifically in hepatocytes (HNF4α). PV=portal vein; D=bile duct. Scale bar is 50 mm;
b. Western blot showing the expression of YAPS127A in liver extracts of +YAP^{HEP} mice compared to control mice. All mice received doxycycline; treatment with BET inhibitor does not impair YAPS127A expression;
c. Upper panels: representative hematoxylin and eosin (H&E) staining of liver sections from control mouse livers or livers overexpressing YAPS127A (+YAP^{HEP}), treated with vehicle or BAY-BET-inhibitor. Scale bars are 100μm. Middle panels: representative immunofluorescence (IF) for SOX9 and HNF4α in liver sections of the above listed mice. Scale bar is 50μm. Lower panels: RNA in situ hybridization on liver tissues for Osteopontin (Spp1), in the above listed mice. The induction of this oval-cell marker upon YAP expression is suppressed by concomitant treatment with BAY-BET-inhibitor. Scale bar is 200μm;
d. RT-qPCR showing Sox9 and Spp1 regulation in mouse liver by transgenic YAP overexpression (+YAP^{HEP}) and treatment with BET inhibitor. *** p=0.00025, unpaired t test, two-tailed. **** p=0.000001, unpaired t test, two-tailed;
e. Immunohistochemistry of Ki67 in liver sections from the indicated mice. Ki67+ cells were markedly reduced in mice receiving BAY-BET-inhibitor. Scale bar is 100μm;
f. Graph showing liver/body weight ratio in control mice + vehicle (n=4), or + BAY-BET-inh (n=4), +YAP^{HEP} mice + vehicle (n=7), or + BAY-BET-inh (n=9). BAY-BET- inhibitor impairs liver overgrowth induced by YAP expression. Unpaired t test, two-tailed, p=0.00098.

Figure 13

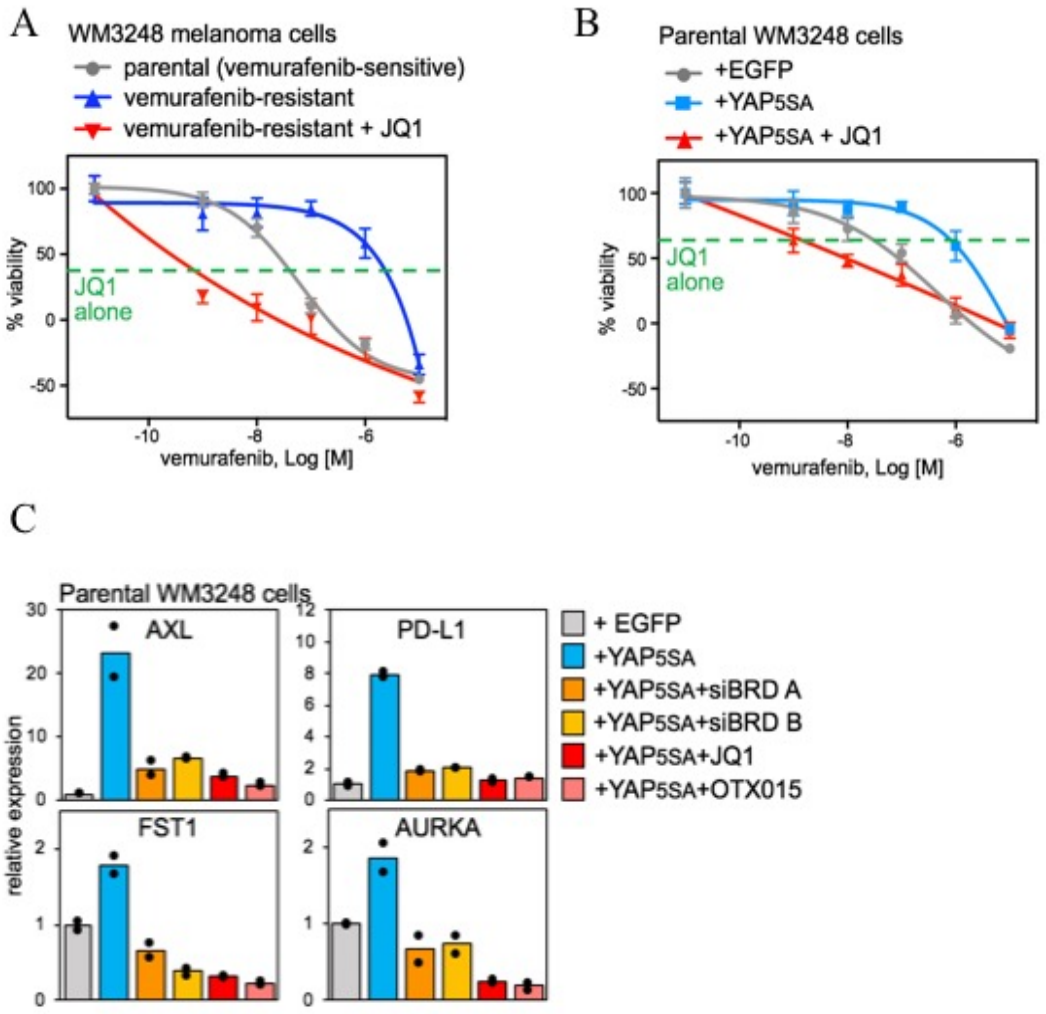
A
WM3248 melanoma cells
parental (vemurafenib-sensitive)
vemurafenib-resistant
vemurafenib-resistant + JQ1
% viability
JQ1
alone
vemurafenib, Log [M]
B
Parental WM3248 cells
+EGFP
+YAP5SA
+YAP5SA + JQ1
% viability
JQ1
alone
vemurafenib, Log [M]
C
Parental WM3248 cells
AXL
PD-L1
FST1
AURKA
relative expression
+ EGFP
+YAP5SA
+YAP5SA+siBRD A
+YAP5SA+siBRD B
+YAP5SA+JQ1
+YAP5SA+OTX015

Figure 13

a. Viability curves of parental (vemurafenib-sensitive) WM3248 and vemurafenib-resistant WM3248 cells, treated with increasing doses of vemurafenib (1nM to 10μM) with or without JQ1(1μM). The green line shows the effect of JQ1 alone (1μM). Data are mean + SD of 8 replicates.
b. Viability curves of parental WM3248 cells (per se vemurafenib-sensitive) transduced with EGFP or YAP5SA, treated with increasing doses of vemurafenib (1nM to 10μM) with or without JQ1(1μM). The green line shows the effect of JQ1 alone (1μM). Data are mean + SD of 8 replicates;
c. RT-qPCR for YAP/TAZ target genes showing upregulation upon YAP5SA overexpression in WM3248 cells and downregulation upon treatment with BET inhibitors (1μM, 24h) or depletion of BRD2/3/4 (siBRD mix A and B). Data are presented as individual data points + average (bar).

Thanks to professor Stefano Piccolo and to my colleagues Francesca, Giusy and Erika for making me a more self-confident person and for giving me the opportunity to work in a cutting-edge laboratory.

Thanks to all the lab for being more friends than just colleagues.